7-11-2013

Investigation of internal damping in carbon fiber and steel cables

Yuanzhong Qiu

Yuanzhong Qiu
Candidate

Civil Engineering
Department

This dissertation is approved, and it is acceptable in quality and form for publication:

Approved by the Dissertation Committee:

Dr. Arup Maji , Chairperson

Dr. Walter Gerstle

Dr. Percy Ng

Dr. Ashok Ghosh

INVESTIGATION OF INTERNAL DAMPING IN CARBON FIBER AND STEEL CABLES

BY

YUANZHONG QIU

B.S., Civil Engineering, Nanchang University, 2006

M. Eng., Civil Engineering, Shanghai University, 2009

DISSERTATION

Submitted in Partial Fulfillment of the

Requirements for the Degree of

DOCTOR OF PHILOSOPHY

Engineering

The University of New Mexico

Albuquerque, New Mexico

May, 2013

DEDICATION

This dissertation describes research performed at the University of New Mexico, Civil Engineering Department between October 2009 and September 2012. It is the result of my own work under the guidance of my advisor Dr. Arup. Maji, and does not include any work done in collaboration, except where stated.

Yuanzhong Qiu

May, 2013

ACKNOWLEDGMENTS

I heartily acknowledge Dr. Arup Maji, my advisor and dissertation chair, for giving me the opportunity to work with him, and for his patience, technical guidance and encouragement throughout the years of research. His guidance and professional style will remain with me as I continue my career.

I also thank my committee members, Dr. Walter Gerstle, Dr. Percy Ng and Dr. Ashok Ghosh, for their valuable assistance in this study. I really appreciate their time and effort in being part of my committee.

Special thanks go to my host family, Wujin Zheng and Hali Ching, for their help and support in many ways. To my roommate, Mekdim Teshome, thank you for the many years of friendship and encouragement.

To my family, thank you for the advice, encouragement, support and love throughout my life.

INVESTIGATION OF INTERNAL DAMPING IN CARBON FIBER AND STEEL CABLES

By

YUANZHONG QIU

B.S., Civil Engineering, Nanchang University, 2006

M. Eng., Civil Engineering, Shanghai University, 2009

DOCTOR OF PHILOSOPHY

Engineering

ABSTRACT

The characterization of cable damping is important for the stability and performance of structures deployed in space using cables. However, literature available for the analysis of carbon fiber cable damping and its effect on dynamical behavior of deployable space structure is scarce. The objective of this work is to examine the variation of cable damping involving different cable properties and the ambient environments through several carefully instrumented tests. An analytical model to predict damping based on internal forces and variable cable geometry is developed and compared with those of tests.

An experimental set-up for the measurement of cable damping is described. Cables in different lengths (0.2032m, 0.3048m and 0.5080m), constructions (20.71turns/m, 41.42tutns/m and 62.13turns/m), temperatures (20℃ and 4℃) and air

pressures (normal and vacuum) are tested under five different tensile forces (111.25N, 222.50N, 333.75N, 445.00N and 578.50N). In addition, the effect of sensor mass, the support and test apparatus on damping are investigated. The damping is identified by the 'half-power bandwidth' method and the 'logarithmic decrement' method. The results indicate that, typically, damping decreases as the length, tension and the number of turns of the tested cable increases. Also, temperature and air pressure contribute to the variation of damping.

To explore the use of finite elements method (FEM) to simulate cable vibration and damping, the COMBIN14 and MASS21 elements in ANSYS13.0 are used. The finite element simulation results agree well with the test results on vibration frequency and time history response. This demonstrates that the selected elements are capable of modeling the dynamic response of cables using the Rayleigh damping constants.

Using simplified mechanistic assumptions, an analytical approach is proposed to model cable damping. The proposed method and related issues are discussed considering numerical examples. It is shown that this method can predict the damping variation trend as observed in the tests of carbon fiber cables.

TABLE OF CONTENTS

DEDICATION ..... **iii**

ACKNOWLEDGMENTS ..... **iv**

ABSTRACT ..... **v**

TABLE OF CONTENTS ..... **vii**

LIST OF FIGURES ..... **x**

LIST OF TABLES ..... **xv**

NOMENCLATURE ..... **xvi**

1 INTRODUCTION **1**
1.1 Motivation 1
1.2 Objective and Scope 5
1.3 Outline of the Dissertation 5

2 LITERATURE REVIEW **7**
2.1 Theoretical Investigation of Cable Damping 7
2.1.1 Masing Model 9
2.1.2 Thin Rod Model 10
2.1.3 Semi-continuous Model 13
2.1.4 Other Models 15
2.2 Experiments on Cable Vibration 18
2.3 Cable Damping in Aerospace Structures 28
2.4 Composite Material Cable Damping 33
2.5 Summary 36

3 EXPERIMENTAL IDENTIFICATION OF CABLE DAMPING **40**
3.1 Introduction 40
3.2 Experimental Setup 41

3.3 Test Procedures and Data Processing 46
3.3.1 Test Procedures 46
3.3.2 Data Processing 47
3.4 Tests Conducted 50
3.4.1 Effect of Cable Tension 51
3.4.1.1 Carbon Fiber Cables Tested at Room Temperature 52
3.4.1.2 Carbon Fiber Cables Tested at a Temperature of 4℃ 58
3.4.1.3 Carbon Fiber Cables Tested in a Vacuum Chamber 63
3.4.1.4 Stainless Steel Cable Tested at Room Temperature 68
3.4.1.5 Evaluation of Rayleigh Damping Constants 69
3.4.2 Effect of Cable Length 73
3.4.2.1 Carbon Fiber Cables Tested at Room Temperature 73
3.4.2.2 Carbon Fiber Cables Tested at a Temperature of 4℃ 75
3.4.2.3 Carbon Fiber Cables Tested in a Vacuum Chamber 77
3.4.3 Effect of Cable Lay Angle 79
3.4.3.1 Carbon Fiber Cables Tested at Room Temperature 79
3.4.3.2 Carbon Fiber Cables Tested at a Temperature of 4℃ 82
3.4.3.3 Carbon Fiber Cables Tested in a Vacuum Chamber 84
3.4.4 Effect of Air Pressure 86
3.4.5 Effect of Support and Test Apparatus 95
3.4.6 Effect of Temperature 98
3.4.7 Effect of Sensor Mass 104
3.5 Conclusions 109

4 FINITE ELEMENT SIMULATION OF CABLE VIBRATION 111
4.1 Review of Literature in FEM Analysis of Cables 111
4.2 Finite Element Analysis of Cable Vibration 113
4.2.1 Modal Analysis 114
4.2.2 Transient Dynamic Analysis 118
4. 3 Conclusions 122

5 ANALYTICAL MODEL OF CABLE VIBRATION DAMPING 123

5.1 Introduction 123
5. 2 Description of Cable Geometry 125
5. 3 Relevant Assumptions 126
5. 4 Axial Strain of Helical wires 127
5.4.1 Axial Strain due to Elongation 128
5.4.2 Axial Strain due to Rotation 131
5. 5 Modeling Contact and Friction Forces 134
5. 5.1 Radius of Deformed Helical Wires Centerline 134
5. 5.2 Interwire Contact and Friction 135
5. 5.2.1 Contact Normal Load per Unit Length 136
5. 6 Determination of Vibration Damping 139
5. 7 Results and Discussion 144
5. 8 Conclusions 151

6 SUMMARY AND CONCLUSIONS 153
6.1 Summary of the Contributions Made 153
6.2 Suggestions for Future Work 154

REFERENCES 156

LIST OF FIGURES

Figure 1.1.1 NuSTAR (NASA) 2

Figure 1.1.2 AstroMesh deployable satellite reflector (Northrop Grumman Corporation) 2

Figure 2.1.1.1 Masing damping model (Gutzer et al., 1995) 10

Figure 2.1.4.1 Schematic diagram of the model of cable system (Yamaguchi et al., 2001) 17

Figure 2.1.4.2 Cross-section of damping treated structural cable (a) typical prefabricated PWS cable (b) damping treated cable (Yamaguchi and Adhikari, 1994) 18

Figure 2.2.1 Complete view of the static hysteresis test set-up (Yu, 1952) 19

Figure 2.2.2 General view of the free decay test set-up (Yu, 1952) 20

Figure 2.2.3 Cable-structure system experimental set-up (Achkire and Preumont, 1996) 22

Figure 2.2.4 Schematic view of the testing system for overhead line cables (Barbieri, et al., 2004) 23

Figure 2.2.5 Diagram of cable damping concept (Thomas, 1981) 25

Figure 2.2.6 Experimental setup of a cantilever cable (Zhu and Meguid, 2007) 26

Figure 2.2.7 Experimental set-up (Casciati et al., 2008) 27

Figure 2.2.8 Analytical models of cable and support (Yamaguchi and Fujino, 1988) 28

Figure 2.3.1 Pantographic deployable structure (a) fully deployed configuration (b) joint detail (Tan and Pellegrino, 2008) 30

Figure 2.3.2 AFRL's Deployable Optical Telescope (Coombs et al., 2008) 32

Figure 2.3.3 DOT mirror petal cable paths and surrounding structure nomenclature (Coombs et al., 2008) 32

Figure 2.4.1 Schematic of test apparatus (El-Kady, et al., 2000) 34

Figure 2.4.2 Experimental setup for resonant frequency measurement at different temperatures (Wei and Kukureka, 2000) 35

Figure 3.2.1 Experimental setup 41

Figure 3.2.2 Tension applying fixture 42

Figure 3.2.3 Details of the clamp 42

Figure 3.2.4 Connection between cable, accelerometers and the dynamic signal acquisition module 43

Figure 3.2.5 Cable ferrule and stop set 43

Figure 3.2.6 Connection between cable and load cell 43
Figure 3.2.7 PCB 352A73 accelerometer 44
Figure 3.2.8 NI USB 9234 dynamic signal acquisition module 45
Figure 3.2.9 Load Cell 45
Figure 3.3.1.1 IM-7 fiber tows 46
Figure 3.3.2.1 Half-power bandwidth method 48
Figure 3.3.2.2 Logarithmic decrement method 48
Figure 3.4.1.1 Stainless steel cable and cross section 52
Figure 3.4.1.2 Recorded time-history responses for a 0.3048m, 20.71turns/m carbon fiber cable at room temperature and 333.75N pretension (a) at 1/5 of cable length (b) at 3/4 of cable length 53
Figure 3.4.1.3 Spectral of signals for a 0.3048m, 20.71turns/m carbon fiber cable at room temperature and 333.75N pretension (a) at 1/5 of cable length (b) at 3/4 of cable length 54
Figure 3.4.1.4 Damping versus tension for cables at room temperature (a) 20.71turns/m (b) 41.42turns/m (c) 62.13turns/m cables 56
Figure 3.4.1.5 Vibration frequency versus tension for cables at room temperature (a) 20.71turns/m (b) 41.42turns/m (c) 62.13turns/m cable 57
Figure 3.4.1.6 Recorded time-history responses for a 0.3048m, 20.71turns/m carbon fiber cable at a temperature of 4℃ and 333.75N pretension (a) at 1/5 of cable length (b) at 3/ 4 of cable length 59
Figure 3.4.1.7 Spectral of signals for a 0.3048m, 20.71turns/m carbon fiber cable at a temperature of 4℃ and 333.75N pretension (a) at 1/5 of cable length (b) at 3/ 4 of cable length 60
Figure 3.4.1.8 Damping versus tension for cables at a temperature of 4 ℃ (a) 20.71turns/m (b) 41.42turns/m (c) 62.13turns/m cables 61
Figure 3.4.1.9 Vibration frequency versus tension for cables at a temperature of 4 ℃ (a) 20.71turns/m (b) 41.42 turns/m (c) 62.13turns/m cables 62
Figure 3.4.1.10 Recorded time-history responses for a 0.3048m, 20.71turns/m carbon fiber cable in vacuum chamber with 333.75N pretension (a) at 1/5 of cable length (b) at 3/4 of cable length 64
Figure 3.4.11 Spectral of signals for a 0.3048m, 20.71turns/m carbon fiber cable in vacuum chamber with 333.75N pretension (a) at 1/5 of cable length (b) at 3/4 of cable length 65

Figure 3.4.1.12 Damping versus tension for cables in a vacuum chamber (a) 20.71turns/m (b) 41.42turns/m (c) 62.13turns/m cables....66
Figure 3.4.1.13 Vibration frequency versus tension for cables in vacuum chamber (a) 20.71turns/m (b) 41.42turns/m (c) 62.13turns/m cables....67
Figure 3.4.1.14 Variation of damping with applied tension....69
Figure 3.4.1.15 Relation curves of alpha with tension....72
Figure 3.4.1.16 Relation curves of beta with tension....72
Figure 3.4.2.1 Cable damping versus length for cables at room temperature (a) 20.71turns/m (b) 41.42turns/m (c) 62.13turns/m cables....74
Figure 3.4.2.2 Cable damping versus length for cables at 4℃ (a) 20.71turns/m (b) 41.42turns/m (c) 62.13turns/m cables....76
Figure 3.4.2.3 Cable damping versus length for cables in a vacuum chamber (a) 20.71turns/m (b) 41.42turns/m (c) 62.13turns/m cables....78
Figure 3.4.3.1 Cable damping versus cable construction for cables at room temperature (a) 0.2032m (b) 0.3048m (c) 0.5080m cables....81
Figure 3.4.3.2 Cable damping versus cable construction for cables at a temperature of 4℃ (a) 0.2032m (b) 0.3048m (c) 0.5080m cables....83
Figure 3.4.3.3 Cable damping versus cable construction for cables in a vacuum chamber (a) 0.2032m (b) 0.3048m (c) 0.5080m cables....85
Figure 3.4.4.1 Pressure gauge....87
Figure 3.4.4.2 Air pumper....87
Figure 3.4.4.3 Vacuum chamber....88
Figure 3.4.4.4 Connection between pressure gauge and chamber....88
Figure 3.4.4.5 Fishing line....88
Figure 3.4.4.6 Foam tape....89
Figure 3.4.4.7 Comparison of damping for 0.2032m carbon fiber cables in air and in vacuum (a) 20.71turns/m (b) 41.42turns/m (c) 62.13turns/m cables....92

Figure 3.4.4.8 Comparison of damping for 0.3048m carbon fiber cables in air and in vacuum (a) 20.71turns/m (b) 41.42turns/m (c) 62.13turns/m cables 93
Figure 3.4.4.9 Comparison of damping for 0.5080m carbon fiber cables in air and in vacuum (a) 20.71turns/m (b) 41.42turns/m (c) 62.13turns/m cables 94
Figure 3.4.5.1 Details of the stiffened support 95
Figure 3.4.5.2 Details of the stiffened frame corners 96
Figure 3.4.5.3 Comparison of damping for cable tested with stiffened and unstiffened setup 97
Figure 3.4.5.4 Vibration frequency with tension 98
Figure 3.4.6.1 Control system of the freezer room 99
Figure 3.4.6.2 Comparison of damping for 0.2032m cables at different temperature (a) 20.71turns/m (b) 41.42turns/m (c) 62.13turns/m cables 101
Figure 3.4.6.3 Comparison of damping for 0.3048m cables at different temperature (a) 20.71turns/m (b) 41.42turns/m (c) 62.13turns/m cables 102
Figure 3.4.6.4 Comparison of damping for 0.5080 cables at different temperature (a) 20.71turns/m (b) 41.42turns/m (c) 62.13turns/m cables 103
Figure 3.4.7.1 Comparison of damping for 0.3048m cables with one accelerometer and two accelerometers (a) 20.71 turns/m (b) 41.42 turns/m (c) 62.13 turns/m cables 106
Figure 3.4.7.2 Comparison of vibration frequency for 0.3048m cables with one accelerometer and two accelerometers (a) 20.71 turns/m (b) 41.42 turns/m (c) 62.13 turns/m cables 107
Figure 3.4.7.3 Damping for a 41.42 turns/m, 0.3048m carbon fiber cable under different conditions 108

Figure 4.2.1 COMBIN14 Spring-Damper (ANSYS help) 114
Figure 4.2.2 MASS21 Structural Mass (ANSYS help) 114
Figure 4.2.3 Finite element representation of a carbon fiber cable 115
Figure 4.2.1.1 Vibration frequency from different methods (0.3048m, 20.71 turns/m carbon fiber cable) 117
Figure 4.2.1.2 Vibration frequency from different methods (0.5080m, 20.71 turns/m carbon fiber cable) 117
Figure 4.2.1.3 Vibration frequency from different methods (0.2032m, 20.71 turns/m carbon fiber cable) 118
Figure 4.2.2.1 Finite element representation of a cable 118

Figure 4.2.2.2 Comparison of time history response (a) FEM result of node at 1/5 of cable length (b) experimental result of node at 1/5 of cable length 120
Figure 4.2.2.3 Comparison of time history response (a) FEM result of node at 3/4 of cable length (b) experimental result of node at 3/4 of cable length 121

Figure 5.2.1 Cable geometry 126
Figure 5.4.1.1 Developed view of helical wire centerline 129
Figure 5.5.2.1 Distributed loads on a helical wire 137
Figure 5.5.2.2 Contact force in cable 139
Figure 5.6.1 Analysis flow chart 143
Figure 5.7.1 Comparison of cable damping (a) 20.71 turns/m (b) 41.42 turns/m, (c) 62.13turns/m cables 145
Figure 5.7.2 Cable damping versus cable construction (a) 0.2032m (b) 0.3048m (c) 0.5080m cables 147
Figure 5.7.3 Cable damping versus length (a) 20.71 turns/m (b) 41.42turns/m (c) 62.13turns/m cables 148
Figure 5.7.4 Comparison of damping (with and without consideration of change of lay angle) (a) 20.71 turns/m, 0.2032m (b) 20.71turns/m, 0.3048m (c) 20.71turns/m, 0.5080m cables 150
Figure 5.7.5 Cable damping versus Poisson's ratio (20.71 turns/m, 0.2032m carbon fiber cable) 151

LIST OF TABLES

Table 3.3.1.1 Damping of a 0.5080m, 62.13 turns/m carbon fiber cable with 445.00N pretension 49

Table 3.4.1.1 Properties of 0.3048m carbon fiber cables 52

Table 3.4.1.2 Cable damping at room temperature 55

Table 3.4.1.3 Cable vibration frequency at room temperature 55

Table 3.4.1.4 Cable damping at a temperature of 4℃ 58

Table 3.4.1.5 Cable vibration frequency at a temperature of 4℃.....58

Table 3.4.1.6 Cable vibration frequency in a vacuum (-20 In. Hg) chamber 63

Table 3.4.1.7 Cable damping in a vacuum chamber (-20 in. Hg).....64

Table 3.4.1.8 Alpha and beta for the tested 0.3048m cables 71

Table 3.4.4.1 Damping in vacuum chamber (0.3048m, 20.71turns/m with 333.75N pretension).....89

Table 3.4.4.2 Comparison of damping (0.2032m carbon fiber cables) 90

Table 3.4.4.3 Comparison of damping (0.3408m carbon fiber cables) 90

Table 3.4.4.4 Comparison of damping (0.5080m carbon fiber cables) 90

Table 3.4.5.1 Vibration damping comparison 96

Table 3.4.5.2 Vibration frequency comparison 97

Table 3.4.6.1 Comparison of damping for 0.2032m cables at different temperatures.....100

Table.3.4.6.2 Comparison of damping for 0.3408m cables at different temperatures.....100

Table.3.4.6.3 Comparison of damping for 0.5080m cables at different temperatures.....100

Table 3.4.7.1 Comparison of damping for cables with one and two accelerometers 105

Table 3.4.7.2 Comparison of vibration frequency for cables with one and two accelerometers 105

Table 3.4.7.3 Damping of a 41.42 turns/m, 0.3048m carbon fiber cable tested under different conditions 108

Table 4.2.1.1 Vibration frequency from different methods (0.2032m, 20.71 turns/m carbon fiber cable)..116

Table 4.2.1.2 Vibration frequency from different methods (0.3048m, 20.71 turns/m carbon fiber cable)..116

Table 4.2.1.3 Vibration frequency from different methods (0.5080m 20.71 turns/m carbon fiber cable)...116

Table 5.7.1 Cable properties.....144

Table 5.7.2 Theoretical analysis results of cable vibration damping.....144

NOMENCLATURE

The following symbols are used in this dissertation:

Chapter 3 and 4:

ω_n, ω_1, ω_2	frequencies corresponding to response peak and $1/\sqrt{2}$ of the response peak
ζ	modal damping ratio
δ	the logarithmic decrement
n	number of vibration cycles
ζ_1, ζ_2	the first and the second modal damping ratio
x_1, x_{n+1}	the vibration amplitudes at n cycles apart
[C]	damping matrix
[M]	mass matrix
[K]	stiffness matrix
α, β	the Rayleigh damping constants
F	the impulse force applied at the center of the cable
H	cable pretension
l	cable length
m	mass per unit length of the cable

Chapter 5:

R_c, R_w	radius of the cable core and helical wires
P, P_1	pitch length of helical wires
α, α_1	lay angle of the undeformed and deformed helical wires

ε_t	total strain of helical wires along tangent direction
ε_t^A	the tangent strain of helical wires due to elongation
ε_t^R	the tangent strain of helical wires due to rotation
$L,\ L_1$	initial and deformed length of the cable structure
S, S_1	initial and deformed length of the helical wires
θ, θ_1	initial and final angle that a helical wire sweeps out
V, V_1	volume of the undeformed and deformed cable structure
R_h, R_{h1}	radius of the undeformed and deformed helical wire centerline
ΔS	change of helical wire length
$\Delta\alpha$	change of cable lay angle
ε_c	the axial strain in the cable core wire.
ν	Poisson's ratio
CF	compaction factor
$\theta_z = \theta_1 - \theta$	the relative rotation of the structure
δ_a	mutual approach of wires
μ	friction coefficient
γ_z	ratio of the deformed and undeformed cable structure length
γ_t	ratio of the deformed and undeformed helical wire length
P_{nch}	the contact normal force between cable core and helical wires
P_{nhh}	the contact normal force between helical wires
a_{hh}, a_{ch}	contact half width
E	Young's modulus
E_t	transverse modulus

β	contact angle
m	number of helical wires in a layer
Q, Q_1	the tangential distributed force
W, W_1	the tangential distributed force along helical wires
H	tangential force along helical wires
η	loss factor
ΔU	the energy dissipation per cycle
U	the stored energy
a_n, a_{n+1}	two successive vibration amplitudes
δ	logarithmic decrement
ξ	cable modal damping ratio
Δ_1	relative movement
S_{6T}	tonsorial shear strain between cable wires associated with wire axial strain
U_ε	stored strain energy
y	vibration profile
b	vibration amplitude
U_T	stored energy due to tension

Chapter 1

Introduction

This chapter first describes the motivation of this research for the experimental and analytical investigation of carbon fiber and steel cable damping, and then summarizes the objective and scope of the research. At the end of this chapter, the organization of this dissertation is presented.

1.1 Motivation

Cables, as assemblages of wires have been widely used as tension members in many modern flexible structures, ranging from suspension bridges, electrical and signal transmission systems to deployable space structures. As examples for cable application in space structures, Fig. 1.1.1 shows the nuclear spectroscopic telescope array (NuSTAR) launched by NASA in June, 2012. The NuSTAR telescope extends to achieve a 10-meter focal length after being launched into orbit in order to improve the sensitivity of the optics. A deployable satellite reflector from Northrop Grumman Corporation is shown in Fig. 1.1.2. It will be used to help NASA's Jet Propulsion Laboratory (JPL) map soil moisture and the freezing and thawing cycles globally with unprecedented accuracy, resolution and coverage, which aims to understand the health of the Earth's ecology.

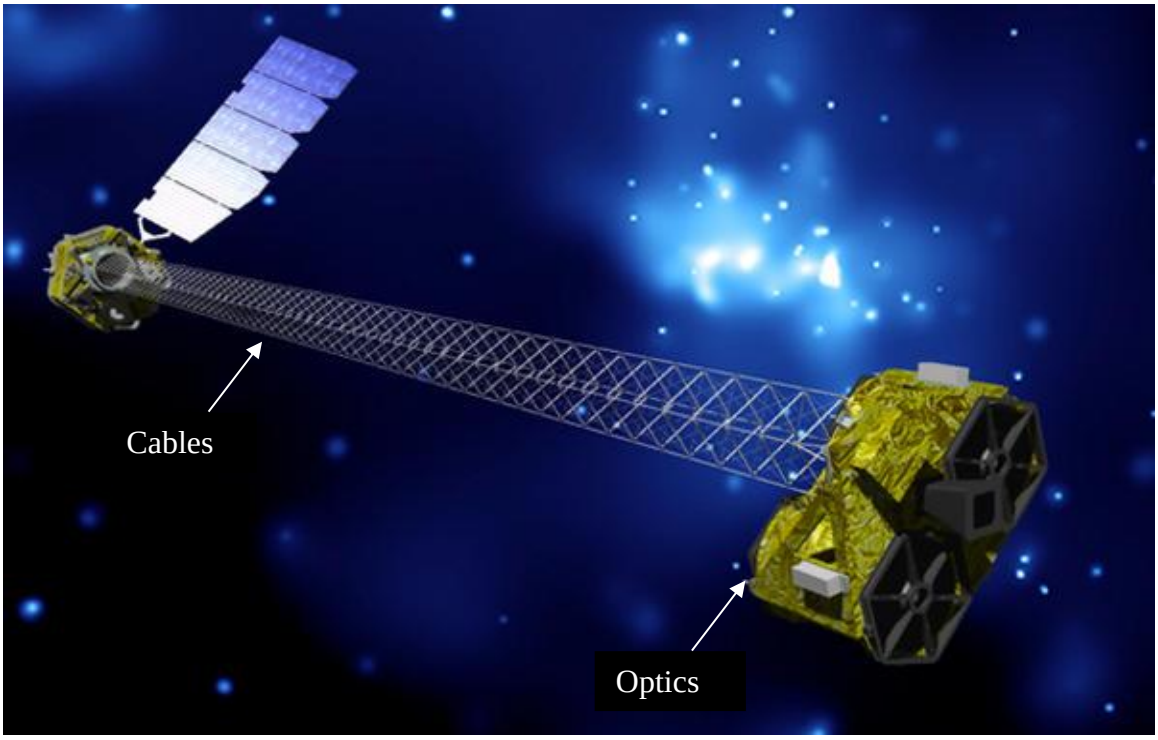

Figure 1.1.1 NuSTAR (NASA)

Figure 1.1.2 AstroMesh deployable satellite reflector (Northrop Grumman Corporation)

For deployable masts, deployable antennas and other aerospace structures, vibration can be caused by launch loads, deployment, and micro-lurch (small accelerations due to various forces) etc. Quite often these small vibrations are not desirable and may cause malfunctions of the sensor systems. The interest lies in reducing the vibration by dissipation of vibration energy or damping. Although characterization of cable damping in a vibrating structure has long been an active area of research in structural dynamics, the demands of modern engineering have led to a steady increase of interest in recent years. Investigations of cable damping have a significant role in vibration suppression in space structures under an environment devoid of atmospheric damping. The recent developments in the fields of space structures have provided impetus towards developing procedures for dealing with cable damping in the context of structural dynamics. Beside these, in the last few decades, carbon fiber cable has become an appropriate option for aerospace structures because of its light weight and high strength. The sophistication of modern design methods together with the development of improved composite structural materials instilled a trend towards lighter and larger space structures.

At the same time, there is also a constant demand for larger optics, which needs to be deployed in orbit and has a dimensional stability much smaller than the wavelength of light in order to obtain high quality images and other information with minimum noise and vibration level. The increasing demand requires that the cables to play a more appreciable role in the dynamics of space structures.

Unfortunately, these highly flexible and lightweight cables possess low damping and are susceptible to vibration, especially in the space environment devoid of atmospheric

damping. Besides, the knowledge of carbon fiber cable dynamic behavior is very scarce. Therefore, measuring cable damping and understanding its mechanisms are particularly significant for structures deployed in space where the internal damping is critical for structural stability. An extensive ground based test is essential to provide some fundamental dynamic properties of carbon fiber cables in space structural applications.

The demands of lighter space structures and more sensitive space structures are conflicting and the problem cannot be solved without proper understanding of energy dissipation or damping behavior. In spite of a large amount of research on the investigation of damping characterization of steel cable and transmission line conductor, understanding of cable damping mechanisms is quite primitive, and it is a field which still holds quite a bit of intrigue in the engineering community. This is because the modeling of damping is very complex, and it is not in general clear which variables are relevant to the damping values. Moreover, it seems that in a realistic situation there exist many sources of energy dissipation: the structural joints, the material, and the fluid damping etc. Here the difficulty lies in understanding the damping mechanisms and providing a model to be used in predicting transient responses, decay times or other characteristics in design and analysis where the structural performance is affected by energy dissipation.

1.2 Objective and Scope

The overall objective of this work is to study the variation of damping involving different cable parameters and environments, and to develop an analytical model for understanding damping mechanisms and predicting damping of cables in space applications.

This work covers the tests of carbon fiber cables under different length (0.2032m, 0.3048m and 0.5080m), tension (111.25N, 222.50N, 333.75N, 444.50N and 578.50N), configuration (20.71turns/m, 41.42turns/m and 62.13turns/m), temperature (20℃ and 4℃) and air pressure (normal and vacuum). Finite element simulation of carbon fiber cable vibration is provided for comparing and establishing a relationship with experiments. A model for predicting damping is developed based on internal forces, fiber deformation and internal cable geometry under simplified but physically realistic assumptions.

1.3 Outline of the Dissertation

Motivated by the existing problems and gaps identified in Section 1.1, a systematic study on determination and analysis of carbon fiber cable and steel cable damping has been carried out in this dissertation. The dissertation is divided into six chapters.

In Chapter 2, a brief review of literature on currently available experimental and analytical studies on damping properties of stainless steel cables and composite cables, the effects of cable damping on dynamic behavior of cable structures and techniques for vibration suppression is presented. Based on this literature review, some open problems have been identified which are summarized in Chapter 2.

In Chapter 3, an experimental setup for measuring cable damping is provided, and several tests of carbon fiber cables and a stainless steel cable under different conditions are reported. The test variables included the cable length, tension, configuration, along with the ambient temperature (20℃ and 4℃) and air pressure (normal and vacuum). In addition, the effect of sensor mass, support and test apparatus on cable damping are investigated. From the tests, some important conclusions are derived which are discussed and analyzed in this dissertation.

In Chapter 4, attention is specially focused on the simulation of cable vibration using the finite element method (FEM) for comparing and establishing the relationship with the experiments. A simple and appropriate simulation of cable damping is suggested.

Chapter 5 is aimed at using the conclusions from tests to validate a theoretical model proposed to analyze the cable vibration damping. The expression of damping is derived under certain simplified but physically realistic assumptions. The proposed method and several related issues are discussed by considering numerical examples.

Finally, Chapter 6 presents the conclusions emerging from the studies taken up in this dissertation and makes a few suggestions for further research.

Chapter 2

Literature Review

In this chapter, previous experimental and analytical studies to understand damping characterization and damping mechanism of stainless steel cables and composite cables are reviewed. Also, many attempts to suppress vibrations of cable and cable structure are described. From the literature review, several important conclusions are derived to guide this research on the experimental and analytical investigation of carbon fiber and steel cable damping. Additional literature review specific to the issues addressed in our research have been provided in the relevant sections in later chapters.

2.1 Theoretical Investigation of Cable Damping

The vibrating taut string or cable was one of the first physical systems to which the analytical tools of mechanical and mathematics were applied. The problem of cable dynamics and the characterization of cable damping still attract a great deal of attention from the scientific community leading to a rich technical literature. This is due to the wide application of cables in engineering field and to their tendency to vibrate. Vibrations can result in cable or connection failures due to fatigue (Cluni et al., 2007). Consequently, how much energy can be dissipated by cables is of importance when considering dynamic behavior of structures with cables.

In many of the earlier theoretical analyses, several simplifying assumptions have been made to obtain analytical or closed form solutions. One of the assumptions is about the interwire friction. Friction takes place at the interfaces of cable helical wires and is hard to model. For simplification, most of the researchers analyzed two extreme cases: either a no-slip friction model or a full-slip friction model. An attempt to relate the internal friction to the damping properties of a cable was made by Vinogradov and Atatekin (1986). A cantilever cable deformed under a transverse load applied at the free end was investigated, the interwire slip was assumed to occur due to the twisting of helical wires. Although it is clear that the interaction between the wires is the cause of energy losses, a precise mechanism of interwire friction and interwire slippage in a deformed cable remains unknown. Therefore, it is necessary to obtain a full understanding of the interwire friction and interwire slippage within the cable to achieve realistic prediction of cable damping.

Another important assumption is about the internal wire contact. Based on the wire diameter and helix angle, there are three possible types of contact: (a). Wire-wire contact, in which wires in the same layer are in contact, and no contact with adjacent layers; (b). Core-wire contact, in which the wires in the same layer do not touch each other, and are in contact only with the cable core; (c). Mixed (wire-wire and core-wire) contact, in which both wire-wire and core-wire contact occur. In the previous models, one contact mode is commonly selected as the primary contact to simplify the solution.

Depending on the type of cable geometry, the modes of loading and the contact behavior, several theoretical models have been proposed to date which may be classified as: the

'Masing' model, in which the interwire friction was considered using the 'JENKIN' element; the 'thin rod' model, which takes bending and torsional stiffness of the individual wires into account; and the 'semi-continuous' model in which each layer of helical wires is modeled as an equivalent 'thin cylinder' or 'thick cylinder'.

2.1.1 Masing Model

The 'Masing' model was first proposed by Masing (1923) to model the energy dissipated per cycle in metals, and it was then used by Gutzer et al., (1995) for the investigation of self-damped stranded steel cables. In this model, the cable was treated as a collection of discrete and continuous systems of bonded wire layers, as shown in Fig. 2.1.1.1. Each of the layers consists of one or more 'JENKIN' elements. The 'JENKIN' element consists of a spring with stiffness c_i and associated with a dry friction element described by its maximum friction force H_i. An inner variable 'y' has to be introduced for every 'JENKIN' element, to describe the relative position of the friction element. For a complete knowledge of the system state the inner variables have to be known, or information has to be given on deformation history. The damping parameters of the system were identified using the slowly varying amplitude and phase method.

Sauter and Hagedorn (2002) further developed a hybrid approach by using the distributed 'Masing' model together with the beam theory to model a stock-bridge damper cable. This model accounts for the interwire friction force by selecting an appropriate number of 'JENKIN' elements. They also performed experiments on a cantilever self-damped cable to measure the 'Masing' components by measuring the cable response to a cyclical end load.

In summary, the ‘Masing’ model provides a good way to simulate the interwire friction, however, the ‘Masing’ components are difficult to obtain.

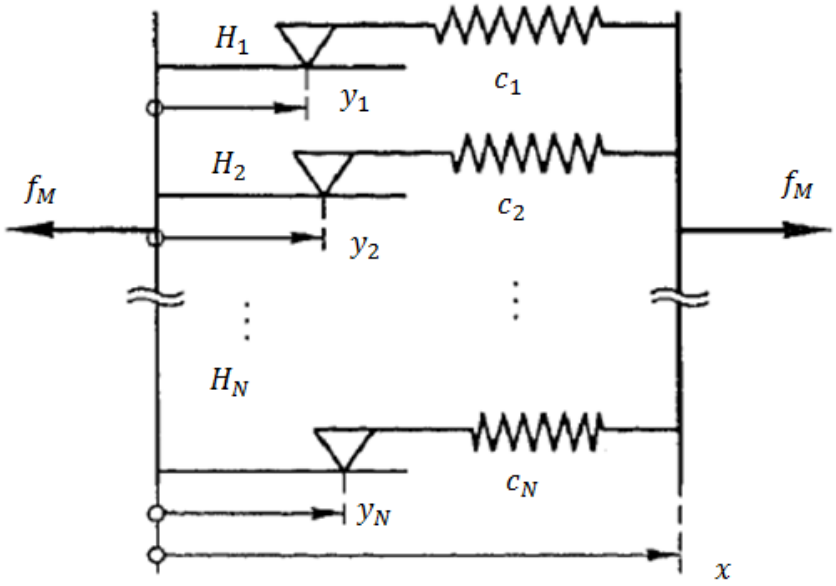

Figure 2.1.1.1 Masing damping model (Gutzer et al., 1995)

2.1.2 Thin Rod Model

The ‘thin rod’ model was first proposed by Owada (1952), who used the Kirchhoff’s equation of equilibrium to calculate axial and torsional stiffness of a simple strand. In the ‘thin rod’ model, the basic element of cable is a single thin rod, the equations are established for individual wire of strand. The wire bending and twisting is added in this model.

Huang and Vinogradov (1991) investigated the effect of frictional force and interwire slip on the mechanical properties of an axially loaded straight cable. The effect of interwire slip was considered on macro-scale properties of the cable. The formula of frictional

energy dissipation over one axial load cycle was derived. The analysis showed that the damping coefficient is inversely proportional to cable pretension. Huang and Vinogradov (1992) also addressed the dynamic behavior of a cable under cyclic tension. To obtain the load-elongation relationship, the total elongation of the cable was assumed to be comprised by two parts, one from the slipped section, and the other from the section without interwire slippage, where the process of cable elongation was accompanied by micro-slippage of the cable. The analytical results demonstrated that cable axial stiffness is slightly increased when tension increases, and that damping is inversely proportional to cable pretension. However, the analysis might underestimate the cable elongation caused by vibration.

For a cable subjected to uniform bending, Huang and Vinogradov (1994) showed that losses caused by dry friction occur due to twisting and bending of individual wire, and the energy dissipation is linearly proportional to bending curvature. Huang and Vinogradov (1996a, 1996b) analyzed the damping of a cable under a quasi-static cyclic loading, the cable was modeled as an equivalent rod with amplitude dependent damping, and the interwire dry friction was considered. The formula for equivalent damping coefficient was obtained and showed that the energy losses are proportional to the cube of the axial tension, and inversely proportional to the interwire friction forces. In this paper, the authors concluded that the damping in cables is caused mainly by dry friction between wires, while a small amount of energy is dissipated through individual wires.

Other researchers also have conducted extensive research on cable interwire behavior and energy dissipation using the ‘thin rod’ model. Huang (1978) and LeClair (1989) included

the interwire friction interaction in their models and analyzed single layered spiral strands, Lanteigne (1985) investigated the problem of interlayer slippage in a multi-layered strand. Ramsey (1990) has attempted to include interwire friction in multi-layered strands undergoing axial loading using the 'thin rod' model. Sathikh et al., (1989a) showed that the axial slip is more appropriate than twist slip. In another paper, Sathikh (1989b) derived a more accurate expression for the minimum interwire frictional resistance and applied this to cable vibration. Utilizing these researches, Sathikh (1989c) studied the interwire friction effects on the transverse vibration of helically stranded taut cable with hinged ends. Numerical analysis indicated that the wire's axial slip force is more predominant than the wire's twist slip force. However, only friction between wires and cable core was taken into account while the friction between wires was neglected. This research was extended to obtain a general 'thin rod' model for the pre-slip bending response by Sathikh et al., (2000).

Raoof and Huang (1991a) proposed a theoretical formulation for obtaining upper bounds to single layer helical strand damping under cyclic bending to a constant radius of curvature. Parametric studies show that the traditional coulomb friction model tends to grossly overestimate cable damping for large radius of curvature. And the present model suggests that for certain ranges of helix angle, increasing helix angle leads to decrease in cable damping.

More complex analytical model is based on curved beam theory assumptions. Within the framework of curved beam theory, Labrosse and Conway (2000a, 2000b) investigated the frictional damping properties of axially loaded simple straight metallic cables. In this

approach, the wires were modeled as curved beams, and the changes in curvature and twist of the wires were assumed to be negligible. In the analysis, cable core-wire contact and a linearized pivoting friction were considered. The numerical results indicated that a larger lay angle lead to a lower damping, and the energy dissipated by pivoting friction is very small and negligible compared to other sources of dissipation. Marcel et al., (2010) studied the influence of cable rigidity on free vibration modes of a suspended overhead transmission line conductor. The 'Euler-Bernoulli beam' model with viscous, hysteretic or dry internal friction damping was considered in the analysis. The authors found that the influence of hysteretic and dry friction damping on high damping modes can be neglected. Zhu and Meguid (2007) investigated the flexural damping of slack wire cable by modeling cable as curved beam.

In summary, by using the 'thin rod' model, the frictional forces can be considered as the external forces acting on the wires, however, the bending is considered in this model, and it is not appropriate for a tensioned cable.

2.1.3 Semi-continuous Model

Homogenization is a well-known method in solid mechanics, and can be used for the continuum modeling of a discrete system composed of many identical repetitive elements. In this 'semi-continuous' model, each layer of wires in a strand is mathematically represented by an orthotropic circular cylinder has 'averaged' mechanical properties.

One of the ‘semi-continuous’ model is the ‘orthotropic sheet theory’, which was first developed by Hobbs and Raoof (1982) for the modeling cables and was extended by Raoof and his associates over the past three decades. In this model, the individual layer of wires was modeled as an equivalent cylindrical thin orthotropic sheet, instead of the rod or curved beam used in the ‘thin rod’ model, each sheet has the ‘averaged’ elastic properties, and the whole cable is treated as a discrete of concentric orthotropic cylinders.

Using the ‘orthotropic sheet theory’, Hobbs and Raoof (1984) investigated the frictional energy dissipation in multilayered spiral strands. The test results showed that damping is slightly dependent on cable axial load due to the non-linear nature of the contact. It was shown that the configuration of cable influences damping significantly. In addition, the authors found that the lay angle is a key geometric parameter that affects cable characteristics, and damping can be enhanced by decreasing the lay angle. This has also been demonstrated in another paper (Raoof, 1996). The damping properties of axially preloaded multilayered spiral strands under lateral vibration were investigated by Raoof (1991b), and Raoof and Huang (1993a). An equivalent hysteretic damping per unit length of cable (assumed to depend only on cable construction and cable vibration modes) was used to derive the differential equation of cable lateral vibration. A formula for the determination of damping on the basis of energy dissipation theory was derived. According to the results, the overall structural damping of cable decreases significantly with increasing cable length and with increasing tension. Raoof and Huang (1991b) investigated the damping mechanism of axially preloaded multi-layered sheathed spiral strand in underwater applications. The results demonstrated that the damping ratio decreases with the mean axial strain and the length of cable. The damping ratio also

varied with the cable construction. Raoof and Davies (2006) conducted theoretical parametric studies on the axial and torsional energy loss of axially preloaded spiral strands. They pointed that the axial damping may be significantly enhanced by slight decrement of lay angle, but the torsional damping will be reduced.

Another 'semi-continuous' model was developed by Blouin and Cardou (1989), and later extended by Jolicoeur and Cardou (1994), and Cardou and Jolicoeur (1997). In this model, the layer wires are replaced with a cylinder of orthotropic, transversely isotropic material. The only major difference between the 'orthotropic sheet theory' (thin cylinder) and the orthotropic cylinder (thick cylinder) model is that the first one is considered for two-dimensional and the second one is for three-dimensional calculations.

In these studies, a great deal of attention has been paid to the inter-wire contact phenomena and friction. In all, the proposed 'orthotropic sheets theory' gives a good prediction of cable characteristics, the accuracy increases as the number of layers increases. However, it is based on the homogenization of the cable layers into orthotropic cylindrical sheets and it is not appropriate for a cable with one core and 6 helical wires (1+6 structure).

2.1.4 Other Models

Claren and Diana (1969a) presented the analytical and experimental study on a transmission line cable. According to their results, damping of a taut cable is independent of tension, which is contrary to the general experience. To further understand cable damping behavior, effect of wire slippage on the damping of axially loaded cable was

also explored by Claren and Diana (1969b). The results indicated a nonlinear relationship between the slippage coefficients versus tension. In addition, the average hysteretic damping coefficient was inversely proportional to the square of the slippage factor.

Zhong (2003) proposed a frictional bending model, where the cable was modeled as a one dimensional continuum with varying flexural rigidity, to estimate damping due to internal friction. This study showed that the variation of cable flexural rigidity results in damped vibration. Knapp and Liu (2005), Liu and Knapp (2005) proposed an analytical approach for self-damped cables, where a flexural rigidity-curvature relationship, instead of an external damping term was included in the governing equation of motion. The results showed that the variation of cable flexural rigidity with helical wire slip causes friction energy dissipation in the cable. Also, the effect of variations in core radius due to pressure from the helical layers was investigated.

All of the aforementioned investigations focus on the damping of a single cable with small diameter. However, only the knowledge of the dynamic characteristics of individual cables is not sufficient for the prediction of dynamic characteristics of a structural system, and the interaction between the structural components should be considered. Yamaguchi et al., (2001) investigated a cable system (Fig. 2.1.4.1) with two parallel sagged cables connected by a single secondary cable, whose weight and rigidity is much smaller than that of the main cables. Equations of motion for the cable system were derived using a modal synthesis method with sub-structural formulation. Free and forced vibrations of the cable system were analyzed. The results showed that the

secondary cable has a great contribution to the structural damping and can cause greater damping in the case of coupled motion of the main cables and the secondary.

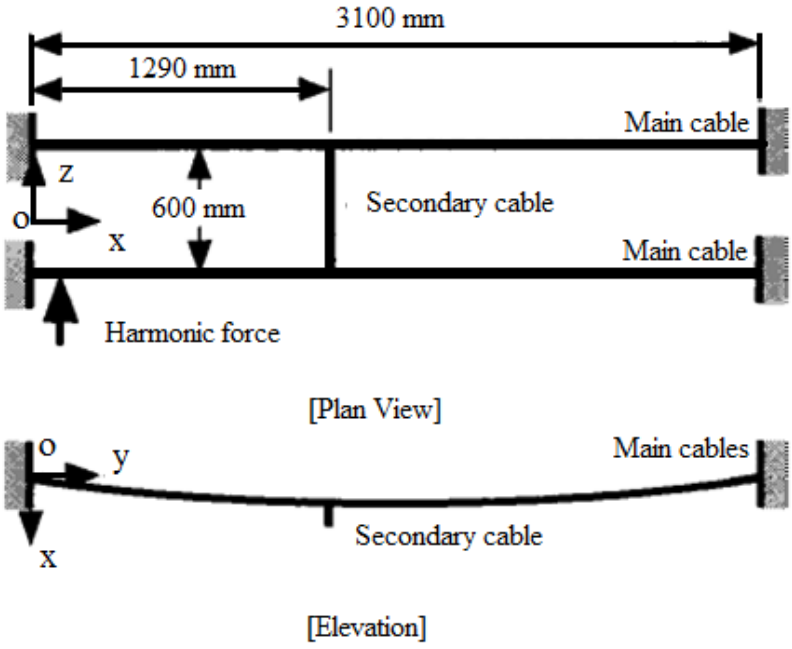

Figure 2.1.4.1 Schematic diagram of the model of cable system (Yamaguchi et al., 2001)

Research on cable damping demonstrated that a cable exhibits low damping, which in itself is not enough to alleviate cable vibration. Thus, a method to enhance cable damping by adding a visco-elastic layer was proposed (Yamaguchi and Adhikari, 1994). Fig. 2.1.4.2 shows the cross-section of the original cable and the damping treated cable in which the author explored the axial and bending loss factor. In this analysis, the 'Ross-Ungar-Kerwin' theory of damping treatment in plates/beams has been extended to a structural cable, and the complex modulus for a visco-elastic material was introduced to compute the axial loss factor. Also, in the analysis, it was assumed that introduction of a visco-elastic layer does not alter the strand configuration, and only the additional damping due to the material was considered. Moreover, the damping due to the outer

cover was assumed to be negligible. However, according to Raoof (1984), construction of the cable has a significant effect on cable damping; therefore, the assumption that the introduction of a viscoelastic material will not change the configuration of cable might lead to an incorrect damping value for the new cable.

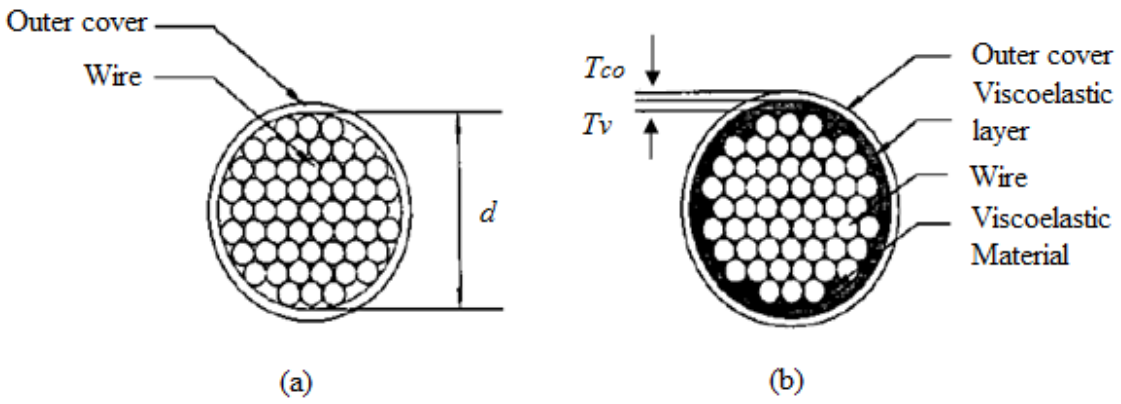

Figure 2.1.4.2 Cross-section of damping treated structural cable (a) typical prefabricated PWS cable (b) damping treated cable (Yamaguchi and Adhikari, 1994)

Wu et al., (2003) investigated the non-linear vibration of loosening cables, where the cable loosening was considered by equating the total horizontal tension force in the cable to be zero. The governing differential equation of motion considering flexural rigidity and damping was derived.

2.2 Experiments on Cable Vibration

Many researchers have performed laboratory and field vibration tests on cables, in attempts to understand the damping behavior of cables and the dependence of cable damping on tension, length, vibration amplitude, temperature, cable construction and wear history.

Yu (1949, 1952) conducted the dynamic decay test and the static hysteresis test on seven-wire and single-wire cables subjected to pure bending. Fig. 2.2.1 and Fig. 2.2.2 show the experimental mock-up for the analogous static and the dynamic tests, respectively.

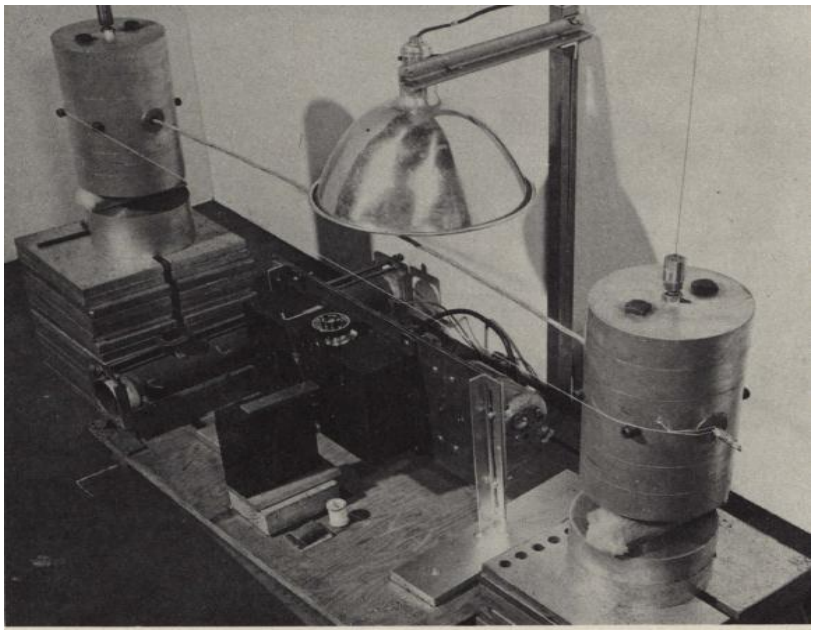

Figure 2.2.1 Complete view of the static hysteresis test set-up (Yu, 1952)

The results showed that the inter-strand dry friction is the major source of internal damping. In addition, cable damping varies with length, number of cable wires, vibration amplitude and cable pretension. Increment of length reduces cable damping capacity, greater number of wires leads to higher damping value, the energy dissipated is a linear function of vibration amplitude, the pre-stressing of stranded cable below the yield point has no effect on cable damping, while pre-stressing over yield point considerably reduces damping capacity. The effect of cable pre-stressing on damping is different from the result presented by Raoof and Huang (1993b), who concluded that a higher tension

causes a lower damping. The disparity might because of the different loading condition and cable configuration.

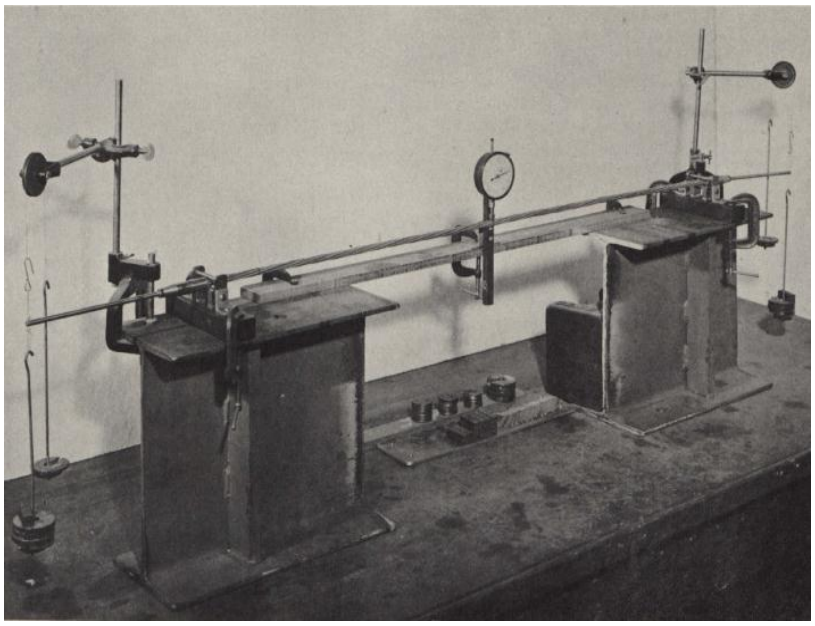

Figure 2.2.2 General view of the free decay test set-up (Yu, 1952)

Hard and Holben (1967) tested the self-damping of tensioned transmission line conductors using vibration decay technique. The damping was evaluated using the 'logarithmic decrement' method. They found that cable length has no significant influence on damping within reasonable limits, and that the effect of tension on damping is significant. A marked decrease in damping was observed initially as tension increases, followed by a less significant change when the load increases.

Claren and Diana (1969a) used the forced vibration method to get the energy dissipated per cycle of a tensioned transmission line conductor by measuring the energy input per cycle while keeping the vibration amplitude constant. From the results, they concluded

that the energy could be dissipated without macroscopic slippage of the strands, but by the deformation of microscopic inter-strand asperities.

Seppa (1971) measured self-damping of tensioned cables using the forced vibration method. The results showed that the energy dissipated is inversely proportional to tension. It is surprising that his result presented a strong dependence of energy dissipation on frequency, which contrasts the basic theory that the Coulomb damping is frequency independent.

Ramberg et al., (1977) measured the logarithmic decrement of slack and taut marine cables in air and in water. They also found that the logarithmic decrement ratio decreases as cable tension increases. In their tests, pinned cable terminations were used and they argued that this minimized the support losses. However, no experimental support was provided.

Interwire friction was identified as the primary source of energy dissipation by Vanderveldt et al., (1973). Ropes with centrally attached mass with different constructions were tested. Experimental results showed that transverse vibration damping decreases as the cable axial load increases. The author also cited Yu's (1952) work, and added that no simple model taking into account transverse damping behavior can be assumed.

Murkowski (1988) tested the internal damping of a mine hoist cable under non-planar transverse vibration. The results showed that the time rate of change of curvature is the major parameter influencing cable internal damping mechanism.

Achkire and Preumont (1996, 1998) described a non-contact measurement technique for the transverse vibration of small cables and strings using collocated actuator-sensor pairs, as shown in Fig. 2.2.3. The performance of an active tendon for the control of a cable-structure system was investigated. The result showed that active damping of 1.8% was achieved for cables with small sag.

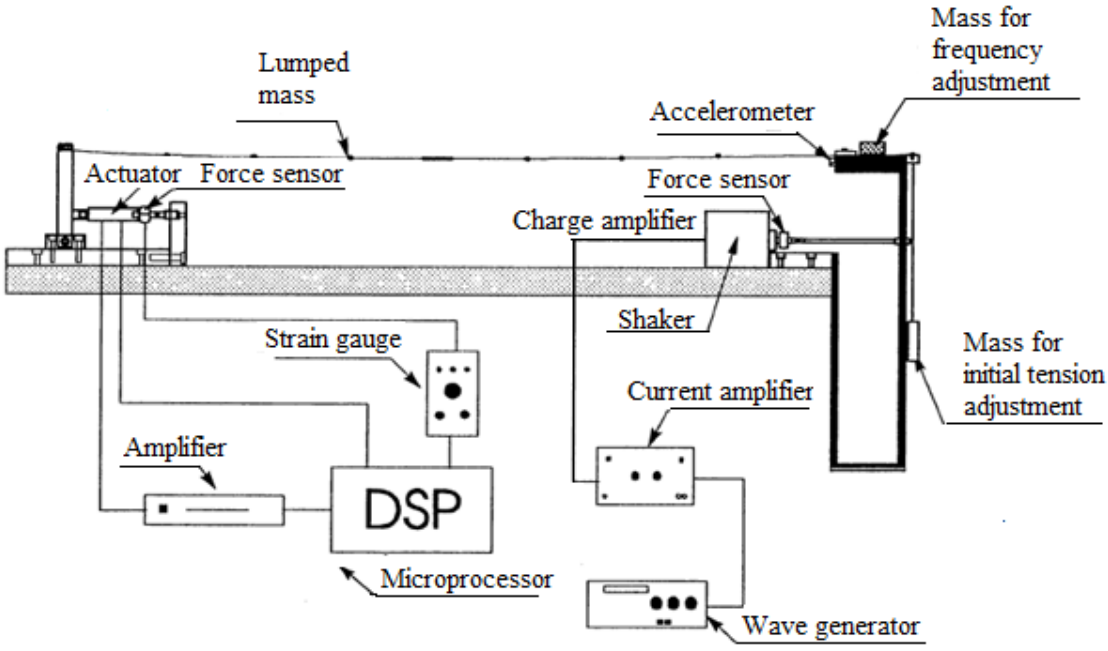

Figure 2.2.3 Cable-structure system experimental set-up (Achkire and Preumont, 1996)

Zheng et al., (2003) tested an inclined cable scaled down from a 143m-long prototype cable in an actual cable structure. The internal damping properties of in-plane and out-of-plane vibration under different tension forces were investigated. The results demonstrated that the modal damping ratios of the out-of plane vibration and the first in-plane vibration decrease as tension increases.

Novak et al., (2004) and Barbieri et.al (2004) proposed a non-contact vibration testing set-up for transmission line cables, as shown in Fig. 2.2.4. A damping identification procedure for the system using non-contact sensors was presented. Subsequently, Barbieri et al., (2004a, 2004b) identified the damping of a transmission line cable system subjected to axial load using the aforementioned procedure. Four different methods were employed to adjust the damping matrix. The results showed a good agreement between the experimental values and the estimated values from the four methods. Besides, the results indicated that damping decreases length and tension increases. This linear dynamic analysis of transmission line cables was later extended to nonlinear analysis (Renato et al., 2008).

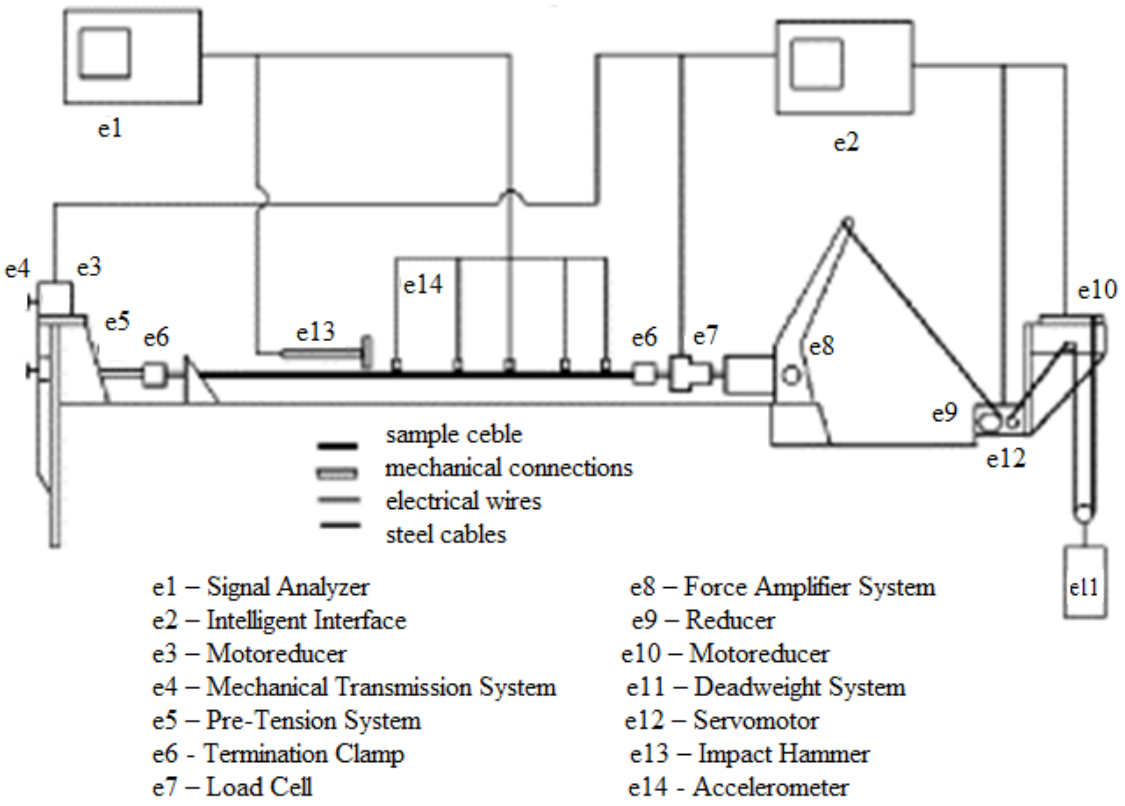

Figure 2.2.4 Schematic view of the testing system for overhead line cables (Barbieri, et al., 2004)

For cable-stayed bridges or suspended bridges, it is common to add dampers to suppress cable vibration. In order to study the damping enhancement effect of adding oil dampers, Xu et al., (1998, 1999) tested scaled model cables with and without oil dampers for a cable-stayed bridge. The test results showed that a higher tension causes a lower damping. Ko et al., (2002) and Duan et al., (2003) presented field vibration tests of a long steel stay cable with and without magneto-rheological (MR) dampers. The in-plane equivalent modal damping of different cable vibration modes was identified using the vibration decay response. Damping was simulated as the combined Rayleigh and frequency independent damping, and shows a satisfactory agreement with the experimental results. For a cable without MR dampers, the modal damping ratio is independent of vibration amplitude within the tested range. Kim and Jeong (2005) also investigated the effects of tension and vibration amplitude on cable damping. The resonant vibration testing results demonstrated that cable damping might be linearly proportional to the vibration amplitude, and decreases as tension increases.

Thomas (1981) discussed the damping design technique of wind turbine guy cables and demonstrated the feasibility of the design with tests. The proposed damping technique used a damper to dissipate energy by coulomb friction, which is simply a pair of weights that are suspended from the cable and slide on two inclined surfaces whenever the cable moves (Fig. 2.2.5). The test results from the 17-meter Research Turbine at Sandia National Laboratories demonstrated that the damping technique works to alleviate the resonant vibration of the cables, and a higher tension in the cable leads to a lower damping ratio.

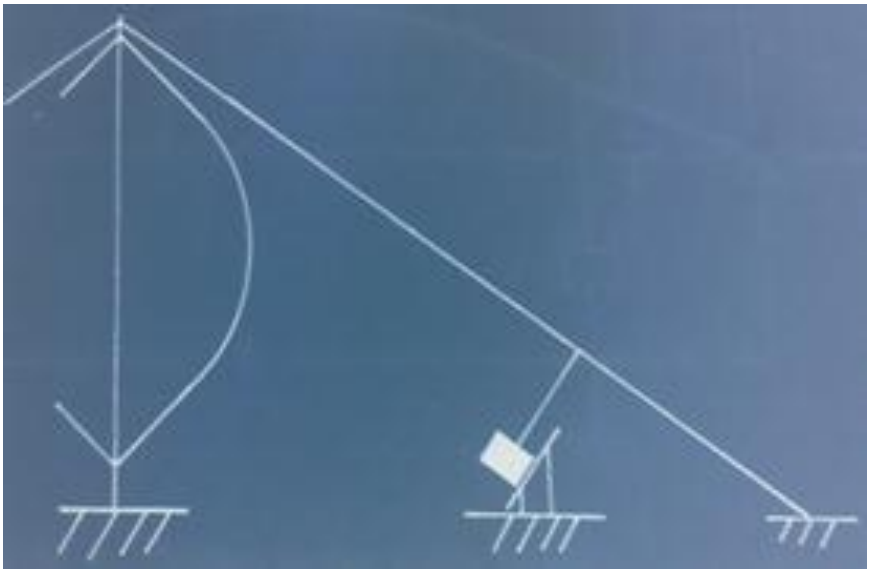

Figure 2.2.5 Diagram of cable damping concept (Thomas, 1981)

Zhu and Meguid (2007) conducted free vibration tests of a cantilevered steel wire cable using the experimental setup shown in Fig. 2.2.6, where the vibration was captured by the high speed camera and the flexural damping were obtained by analyzing photogrammetry data. The cable demonstrated a high flexural damping at zero tension and its damping was measured to be as high as 37.7% of the critical damping. Comparison of the experimental and the numerical results indicated that the Rayleigh damping is suitable to model the flexural damping of slacking wire cable. Besides, the results denoted that the flexural hysteresis influences dynamic behavior of slacking wire cable significantly.

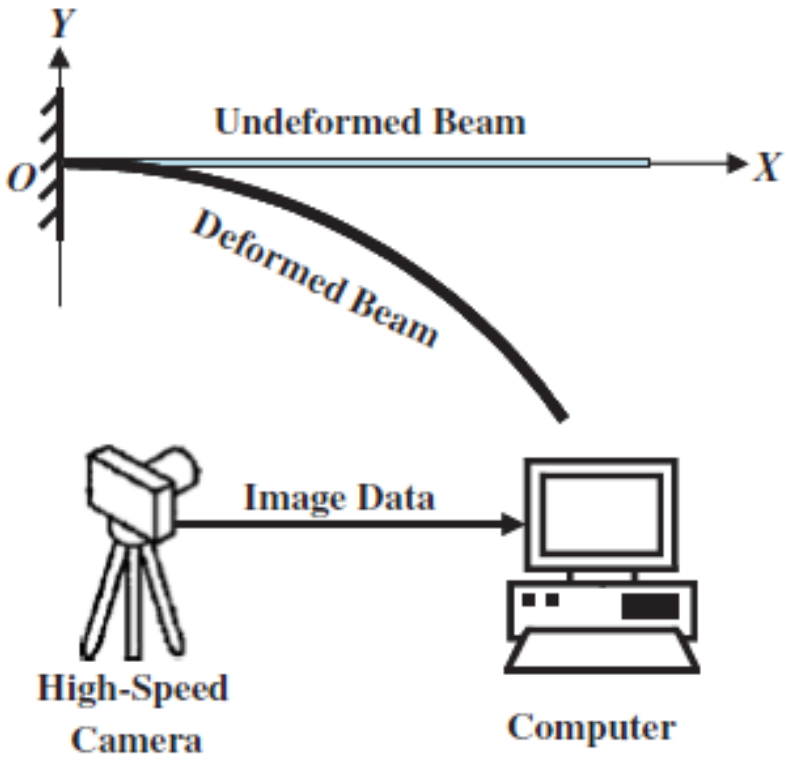

Figure 2.2.6 Experimental setup of a cantilever cable (Zhu and Meguid, 2007)

Casciati et al., (2008) investigated the effect of cable vibration mitigation using shape memory alloy (SMA). A set of laboratory tests on a suspended steel cable and several 'steel cable-SMA wires' systems were conducted using the experimental setup shown in Fig. 2.2.7. The results showed that the application of pre-stressed SMA wire increases the fundamental frequency and the damping coefficient. The enhancement of damping capacity depends on the number of the SMA wire wrapped. However, the mechanism of damping augmentation is not clear; it could be due to energy dissipation by the friction between cable and the added SMA wires, or internal dissipation in the SMA itself.

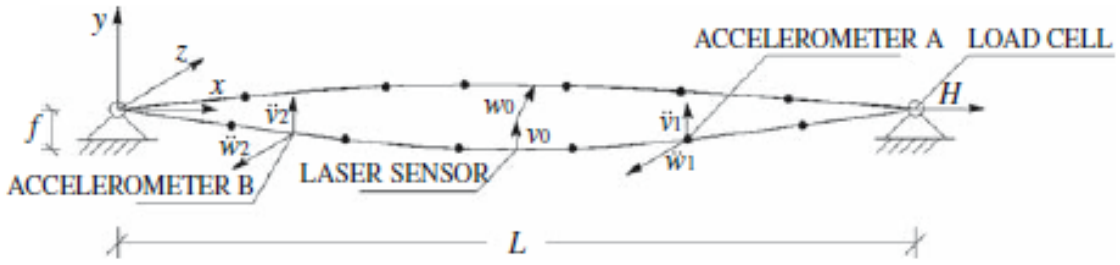

Figure 2.2.7 Experimental set-up (Casciati et al., 2008)

Yamaguchi (1987) measured the flexural oscillation modal damping of a 7-wire stranded suspension cable. The effects of sag-to-span ratio, span length, and initial tensile force on cable modal damping were discussed. The results demonstrated that there exists a critical value for the damping and pretension relationship: damping decreases with increasing pretension when the initial tension is less than the critical value; however, when the initial tension exceeds the critical value, the damping remains constant. In addition, the damping was found to be inversely proportional to cable length. The effect of pretension on damping in this paper is different to that given by Yu (1949, 1952).

To investigate how the support flexibility influence cable damping, Yamaguchi (1988) conducted a series of tests on the flexural oscillation of suspended cables. The cable support was modeled as a spring-mass system with three equivalent springs and one equivalent mass (Fig. 2.2.8), however, the damping of cable support was not explicitly considered. The results indicated that the additional dynamic strain is dependent on the support flexibility, and the damping is proportional to the square of the dynamic strain. In addition, the dependence of damping on support flexibility has a close relationship with the cable sag-ratio and vibration modes. The authors pointed out that the energy dissipation from support is one of the major sources of damping.

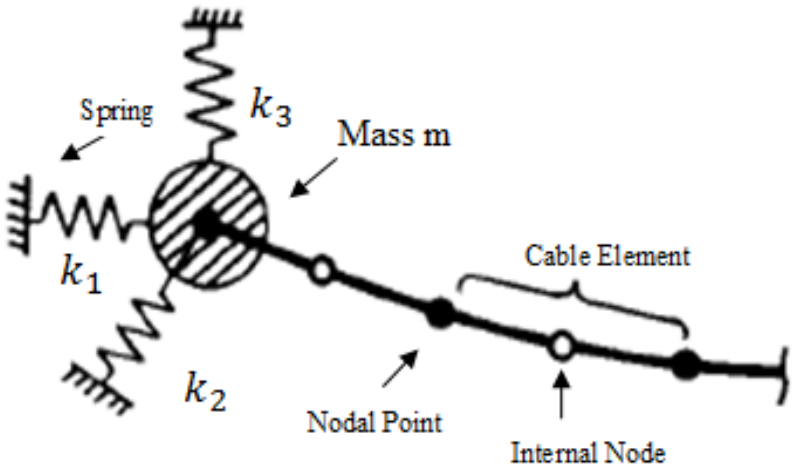

Figure 2.2.8 Analytical models of cable and support (Yamaguchi and Fujino, 1988)

Raoof (1990) tested newly manufactured and well used cables to investigate the variation of damping with service history. The results showed that the used cable has a lower damping than a newly manufactured cable.

Experiments on a stiff cantilever cable having a concentrated mass at the free end were conducted by Pivovarov and Vinogradov (1985) to investigate the influence of various damping mechanisms in a cable under flexure. The results showed that at least two types of damping mechanism exist in cyclically bending cables, the friction type damping dominates at low frequency and viscous damping dominates at high frequencies.

2.3 Cable Damping in Aerospace Structures

Large trusses connected by tension cables are used to design large aerospace structures. It has the advantages of being deployed and easily reconfigurable by changing the static tension in the cables. Aerospace engineers have developed many structures which rely on

cable elements for crucial functions. In some deployable structures, passive cables are applied to terminate the deployment and to increase the stiffness of the fully-deployed structure, and the active cables are designed to control the deployment process and apply a pre-stress in the fully deployed structure (Kwan et al., 1993). Moreover, vibration control techniques are expected to play an increasing role in maintaining stability and sensitivity of sensor systems. Thus, a good estimation of cable damping is significant since it directly influences the stability of sensitivity of the structure.

Tan and Pellegrino (2008) investigated nonlinear vibration of a cable-stiffened deployable pantographic structure, as shown in Fig. 2.3.1, which is fully pre-stressed at the end of deployment. The modal identification test results indicated that damping of the passive cables is inversely proportional to pretension. In addition, the research showed that an increment of the active cable tension caused a decrement of the modal damping of the system.

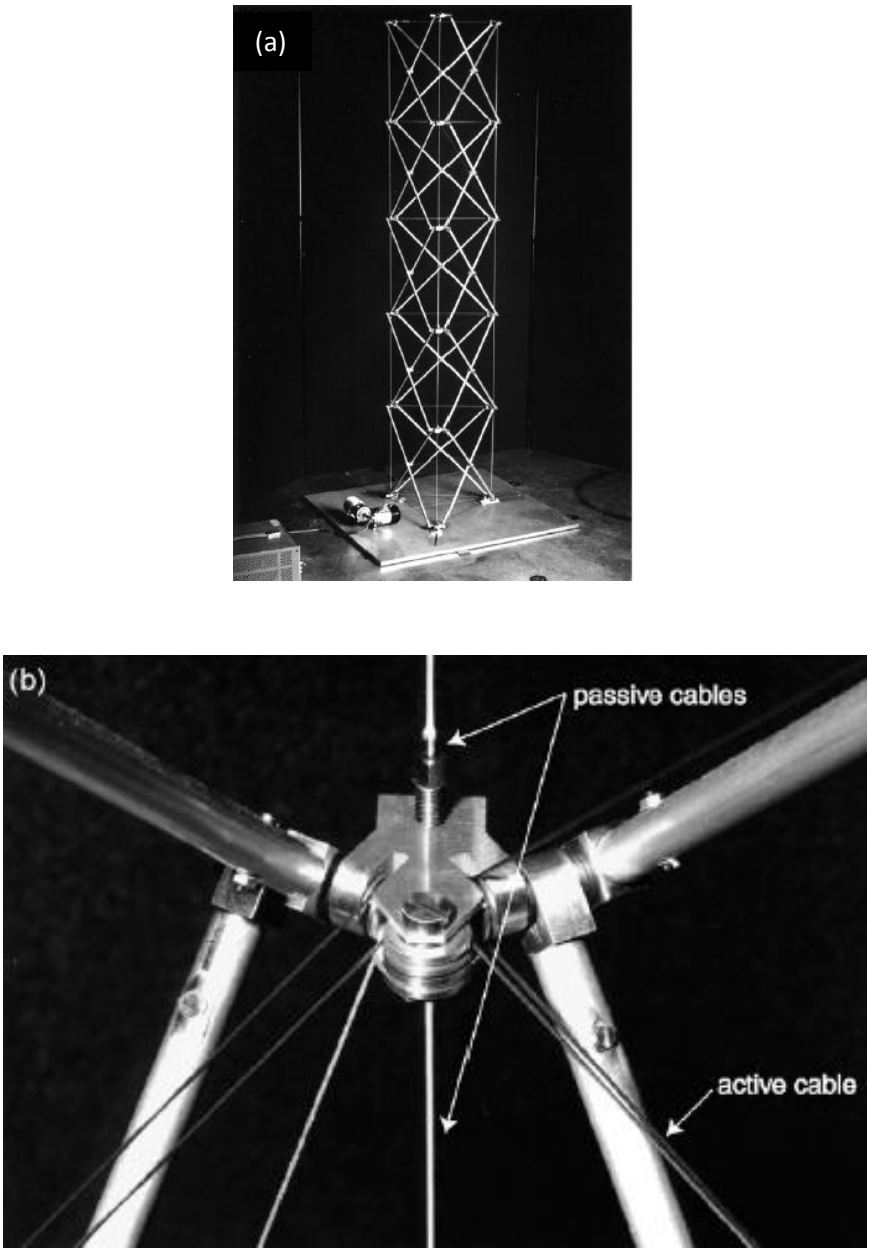

Figure 2.3.1 Pantographic deployable structure (a) fully deployed configuration (b) joint detail (Tan and Pellegrino, 2008)

For a space structure, one of the major uncertainties in damping prediction is the level of damping that would be seen in the absence of the air damping mechanism. Aiming to throw some light on this problem, He and Powell (1990) investigated the damping of a

long taunted tether connecting two spacecraft by modeling it as a visco-elastic continuum without bending stiffness. The longitudinal and the lateral vibration damping were investigated. Three different damping models, structural damping, internal viscous damping and external viscous damping were used to simulate the damping of the tether. The results showed that the longitudinal vibration was primarily affected by the material damping, and the damping ratio cannot be modeled using the three damping models. In addition, the authors concluded that the air friction on the tether skin and the aerodynamic drag on the end mass contributed less than 1% to the overall damping of the optical fiber cable.

Power and signal cables are used as non-structural cables in space structures, and the effect of these cables on damping is not understood either. Robertson et al., (2007) and Babuska et al., (2010) described research on these cables. Simple cable and beam tests were conducted in order to determine their influence on space structures. The results indicated that even a small number of cables may have a significant dynamic effect, and that a large fraction of added cable mass increased the damping.

Coombs et al., (2008) investigated the effect of cables on a space structure. The Air Force Research Laboratory‘s Deployable Optical Telescope (DOT) were tested with different cable configurations, as shown in Fig. 2.3.2 and Fig. 2.3.3. The results showed that changes to the structural dynamics were dependent on the cable to base structure mass ratio. Small mass ratio on the order of 0.5% leads no appreciable modal changes, and a mass ratio on the order of 3% resulted in a doubling of damping at specific modes, but no change in the natural frequencies.

Figure 2.3.2 AFRL's Deployable Optical Telescope (Coombs et al., 2008)

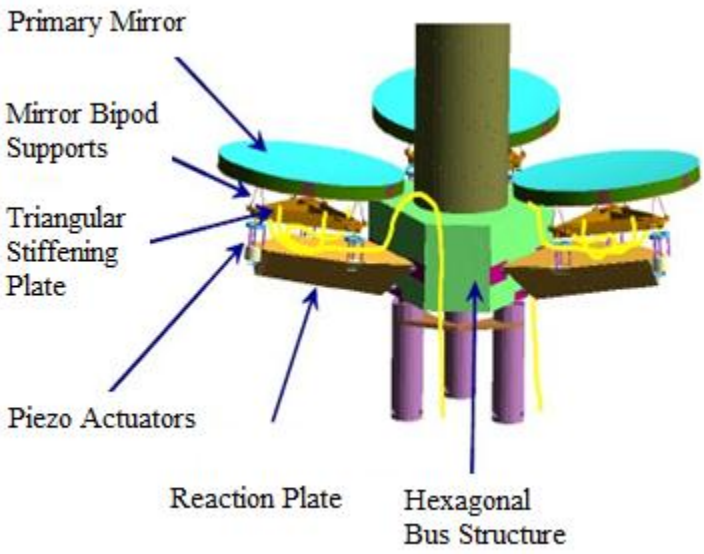

Figure 2.3.3 DOT mirror petal cable paths and surrounding structure nomenclature (Coombs et al., 2008)

2.4 Composite Material Cable Damping

In common usage, a composite material is defined as a combination of two or more materials on a macroscopically homogeneous level (e.g., fibers of one stiff material embedded uniformly, but with directionality, in a matrix or another). In Recent years, composite cables have been widely used in stayed-cable bridges, space structures and other engineering fields due to the advantage of lightweight, high strength, corrosion and fatigue resistance. However, reliable information on damping properties and damping mechanism of composite cable is very scarce.

El-Kady et al., (2000) presented the experimental and analytical studies on the loss factor of carbon fiber reinforced plastic (CFRP) and pre-stressing steel tendons using the test apparatus schematic shown in Fig. 2.4.1. The cable was excited by a hydraulic shaker on the double cantilever system. The 'half-power bandwidth' method and the 'resonant dwell' technique were adopted to determine damping. The authors stated that the effect of bonding material leads to a higher loss factor at the lowest modes for CFRP strands than for steel cables, but for the higher modes, the loss factor is unchanged. In addition, cable damping decreases as length increases. Though the results revealed the different effect of bonding material on cable damping, the authors did not provide any exploration on the reason for the difference.

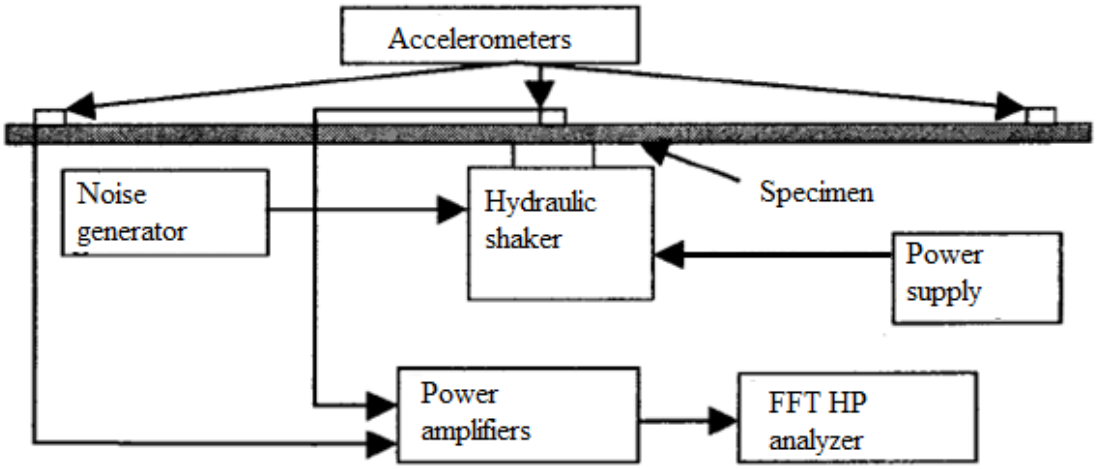

Figure 2.4.1 Schematic of test apparatus (El-Kady, et al., 2000)

Wei and Kukureka (2000) employed the resonance technique to evaluate damping and elastic properties of optical fiber cables. The 'half-power bandwidth' method and the 'logarithmic decrement' method were used to obtain cable damping. The results demonstrated that damping first decreases as length increases, and then remains constant. However, no theoretical or numerical results were provided to validate the experimental results.

Using the resonance technique and the experimental setup shown in Fig. 2.4.2, Wei and Kukureka (2003) tested the damping properties of pultruded composite rods and telecommunication optical fiber cables at various temperatures (-22 to 266 °F , at a heating rate of 1.8 °F/min). The loss factor of tested cables was defined as the ratio of the loss modulus to the storage modulus.

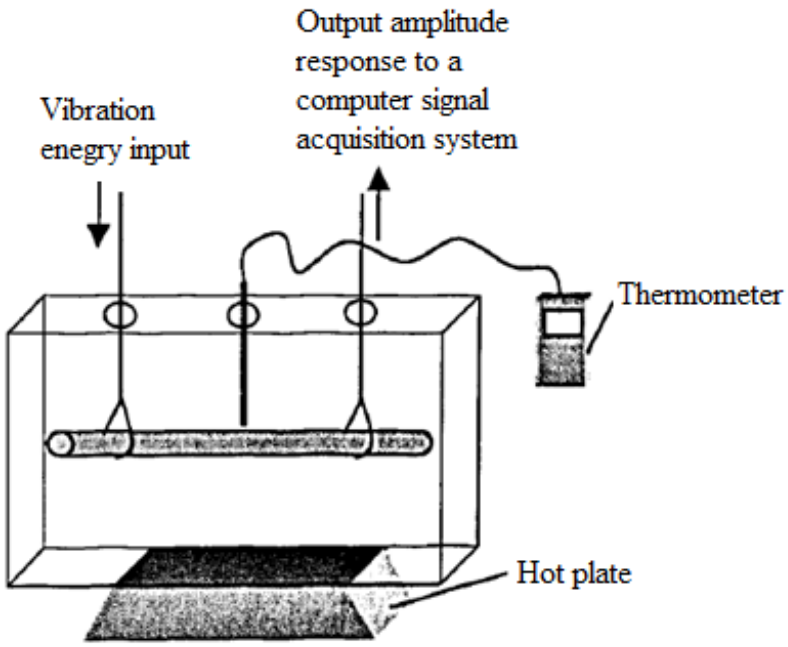

Figure 2.4.2 Experimental setup for resonant frequency measurement at different temperatures (Wei and Kukureka, 2000)

Xie et al., (2008, 2010) conducted free vibration tests on carbon fiber reinforced plastics (CFRP) cables, steel cables, CFRP wires and steel wires. The results showed that damping is amplitude dependent: higher vibration amplitude leads to higher damping. Moreover, the author concluded that the tension force has little influence on damping.

Du et al., (2011) investigated the damping properties and damping mechanisms of fiber reinforced vinyl ester composites and fiber reinforced epoxy composites at different temperatures and frequencies. The results indicated that damping of the composite increases with frequency and declines as the ambient temperature increases. When the matrix material is the same, carbon fiber has higher damping than glass fiber material, and when the fiber material is the same, vinyl ester composites present higher damping.

In addition, the results showed that interface sliding is a key contributor to damping for the composite material.

Wang and Wu (2011) presented a theoretical evaluation on modal damping of a hybrid fiber reinforced polymer (FRP) cable with a smart damper. The theoretical equation of damping was derived based on the energy principle.

2.5 Summary

From literature review of the theoretical and experimental investigations of cable damping, the damping effect on space structures and the damping of composite cables, summaries and conclusions are drawn as follows:

a) Several models have been developed to simulate cable damping under axial, bending or torsional loading cases or subjected to the combination of the load cases. One of the model is the 'Masing' model, which is good for the simulation of interwire friction by assuming a 'JENKIN' element that consists of a spring with stiffness c_i and an associated dry friction element described by its maximum friction force H_i. However, obtaining the 'Masing' coefficients is difficult. The 'thin rod' model is another commonly used model, which modeled the cable wire as 'thin rod' or 'curved beam' within the framework of beam theory. The friction force can be considered as external force acting on cable wires, however, bending is considered in this model, and it is not appropriate for tensioned cable. Another model is the 'semi-continuous' model, one commly used 'semi-continuous' model is the 'orthotropic sheets' theory proposed by Raoof (1982), which modeled the cable wire layers as several cylindrical

orthotropic sheets. However, the ‘orthotropic sheets’ theory is based on the homogenization of the cable layers into orthotropic cylindrical sheets and is not appropriate for cables with one core and six helical wires. The ‘thin rod’ model gives much more reliable results than the ‘orthotropic sheets’ theory for seven wire cables. In addition, several other models were proposed to simulate the cable wire slippage and corresponding friction, such as the ‘frictional bending’ model proposed by Zhong (2003). In summary, most of the existing models have ignored friction and interwire contact deformation, and is not adequate to predict the actual cable damping;

b) In the aspect of interwire slippage and interwire friction, most of the research focused on the occurrence of interwire slippage, with the assumption that the interwire friction coefficient and the interwire normal force are constant. In addition, it assumed that the elongation of the cable is composed of two parts (one from the cable section without wire slippage and one with wire slippage), and superposition is applicable for the two parts of cable elongation. However, the assumption of constant interwire friction is not reasonable, especially when the cable interwire slippage happens. The real behavior of the interwire slippage and interwire friction is not clear;

c) For the cable contact behavior, usually the wire-core contact or the wire-wire contact is considered for the analysis. This could underestimate cable damping for cables with soft core and small diameter. Because the coupling core-wire and wire-wire contact behavior could be existed;

d) Material treatment to enhance damping was investigated by Yamaguchi (1994), but the assumption that the added damping material will not change cable construction is not appropriate;

e) Almost all of the investigations of cable damping concentrated on a single cable. However, for the study of cable effects on the dynamic behavior of cable structure, it is important to take into account the cable interaction behavior. The transmission of energy from cable to cable is a crucial problem for the estimation of structural responses;

f) A number of cable parameters that influence damping properties have been investigated theoretically and experimentally, such as the cable pretension load, lay angle, length, cable configuration and service history. The experimental results showed that there is a disparity regarding the influence of cable pretension. One of the conclusions is that the damping decreases as tensile force increases (Raoof and Huang 1993b, Seppa 1971, Ramberg and Griffin 1977 et al.,). The second is that the pretension has little influence on damping (Claren and Diana 1969a), while the third conclusion is that a critical value of pre-stress corresponding to the variation of damping exists (Yu 1949, 1952, Hard and Holben, 1967). The disparity might be the result of energy dissipated through end termination or just the different loading cases of the tests. Tests on cables with different construction indicated that damping decreases as lay angle increases, and there exists a critical value corresponding to the maximum damping. However, the effect of the change of lay angle was not included in the analytical models. One major conclusion about the influence of cable length is that as length increases, damping decreases, but it was also argued by some authors that length contributes little to damping;

g) In order to get an accurate estimation of cable damping, it is important to exclude the damping sources in the tests. For example, the effect of support conditions was

considered by Yamaguchi (1988). To make an accurate measurement of damping, the control of the support motion is quite important;

h) Research of cable damping in space structure focus on the effect of the cable on the dynamic behavior of a cable structure. Modeling the cable structure system include modeling the cable and the host structure. It seems that no reasonable method or mechanism is applicable to estimate the cable damping in space using ground based test data. In addition, there is no formula to estimate the cable damping, and no damping tested in vacuum, and very scare investigation of temperature effect on cable damping;

i) The available investigations of composite material cable damping properties and damping mechanism are very scarce. The existing literature focused on the testing of damping properties under various length, ambient temperature, and different cable constructions of CFRP cables. Though the tests achieved some basic characteristics of composite material cable damping, the damping mechanism is not clarified.

Chapter 3

Experimental Identification of Cable Damping

In this Chapter, first, an experimental setup for testing cable vibration damping is described. Then several tests of carbon fiber cables and a stainless steel cable are reported. From experiments, some important features of cable damping variation are observed and discussed.

3.1 Introduction

From literature review, the problem of cable damping still attracts a great deal of attention from the scientific community leading to extensive experiments on the investigation of damping and vibration mitigation of cable and cable structure. However, the reported tests appear to have concentrated on stainless-steel cables and much less attention has been paid to the carbon fiber cables, especially for those in space structural applications. Moreover, there is no investigation of cable damping in vacuum, and the available study of temperature effect is very scarce. The damping mechanisms of carbon fiber cables remains poorly understood. Therefore, the objective of this chapter is to test several carbon fiber cables and a stainless steel cable in attempts to find out the dependence of damping on tension, length, lay angle/construction, ambient temperature and air pressure. The eventual goal of the tests is to propose a reasonable analytical

model to estimate carbon fiber cable damping, and to enhance the stability and performance of structures by an optimal design of cables.

3.2 Experimental Setup

For the experimental setup, it is possible to vary the applied tension and cable length, and the test apparatus can be easily modified to test cable damping in vacuum. Fig. 3.2.1 shows the full view of the experimental setup. It consists of a tension application and measurement system, a cable clamp system, and a data collection and processing system.

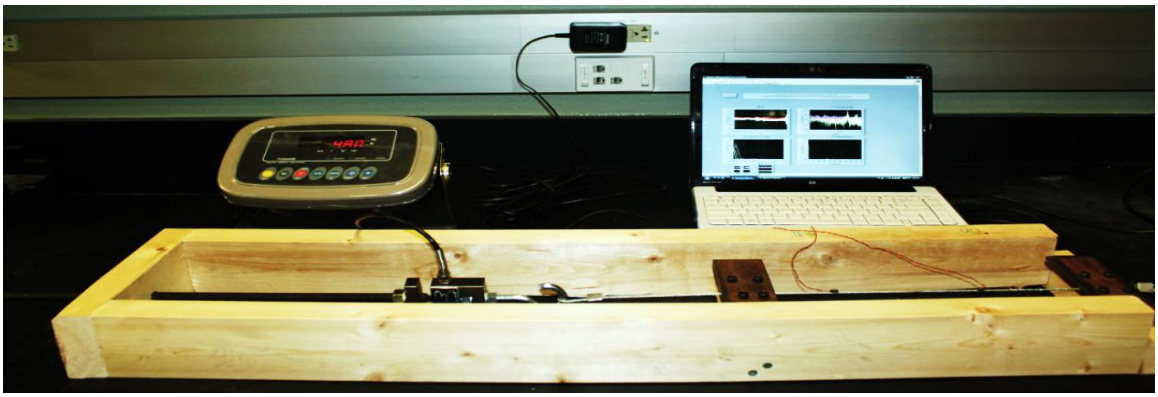

Figure 3.2.1 Experimental setup

Fig. 3.2.2 shows a close-up of the fixture for applying tension. Each cable was first fixed to the clamp at the right end of the wooden frame, which is done by screwing four bolts to tighten the two steel plates that constitute the clamp system shown as Fig. 3.2.3. The left end of the cable was passed through the clamp on the left (Fig. 3.2.4) which is initially not tight. A loop, at the left end of the cable, was formed using a cable ferrule and stop set (shown as Fig. 3.2.5), and was connected to a load cell (Fig. 3.2.6). The load cell with digital meter provided the reading of the tension during the test. The other end

of the load cell was connected to an all thread stainless steel rod, which is used to adjust cable tension by tightening the bolt at the left end of the wooden frame, shown as Fig. 3.2.2. Once the appropriate load was applied, the clamp on the left (Fig. 3.2.4) was tightened to hold the tension during the tests.

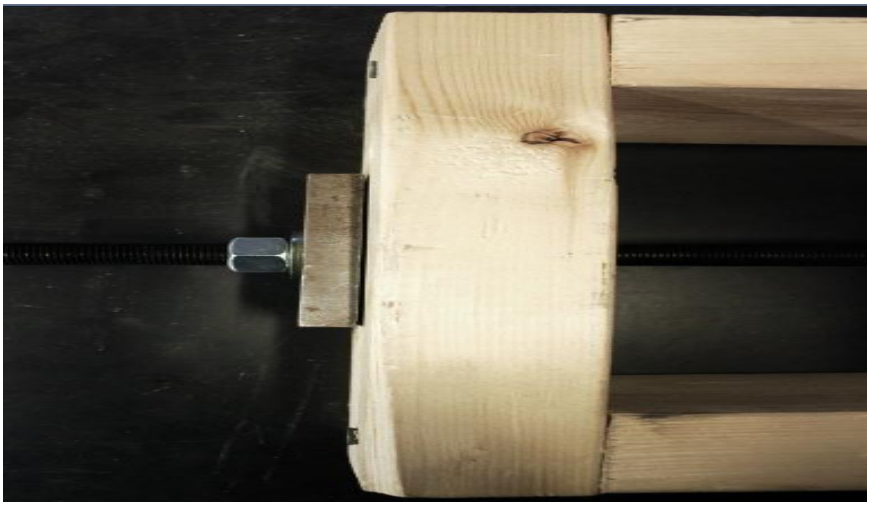

Figure 3.2.2 Tension applying fixture

Figure 3.2.3 Details of the clamp

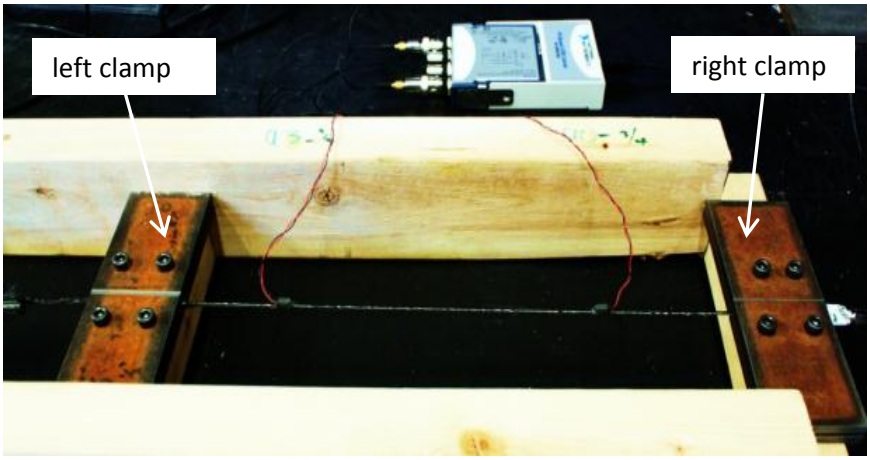

Figure 3.2.4 Connection between cable, accelerometers and the dynamic signal acquisition module

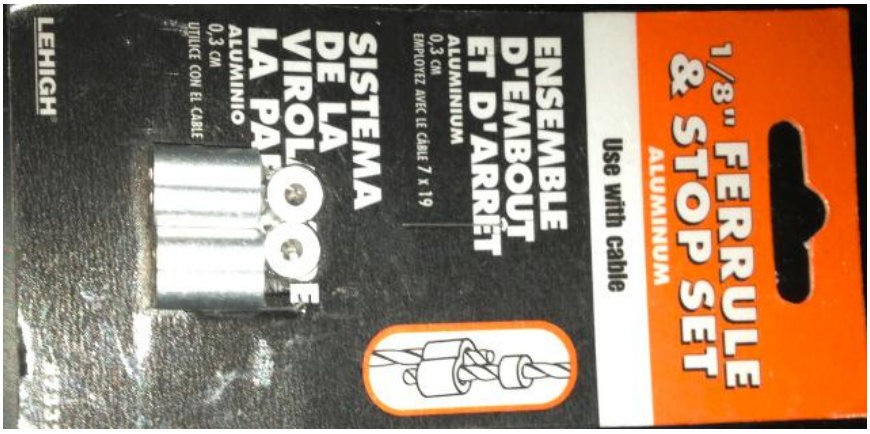

Figure 3.2.5 Cable ferrule and stop set

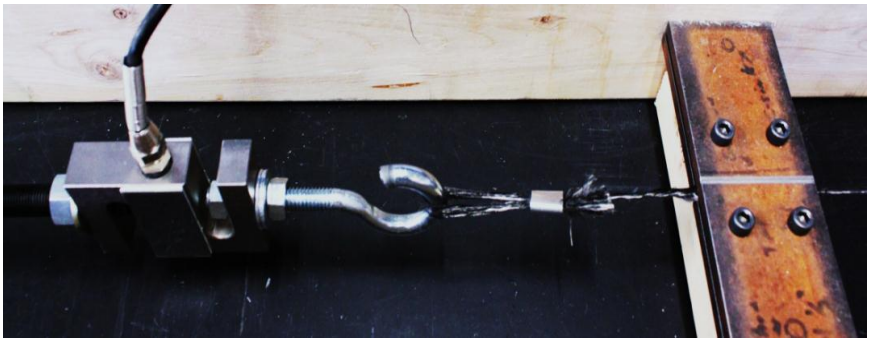

Figure 3.2.6 Connection between cable and load cell

Two accelerometers, type PCB Model 352A73, shown as Fig. 3.2.7 were mounted to the cable using wax at approximately three quarters and one fifth of the cable span (Fig. 3.2.4), respectively. The mass of the accelerometer is 0.3gm, and the size is 2.8mm×8.6mm×4.1mm (Height × Length × Width). These acceleration locations were chosen to such that the first three vibration modes could be detected at either transducer by avoiding the nodal points. In addition, having the two accelerometers located on opposite sides of the cable span aims to minimize the torsion effects caused by small movements of the accelerometers during the cable oscillations.

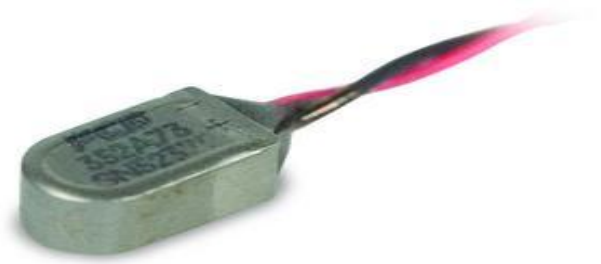

Figure 3.2.7 PCB 352A73 accelerometer

The accelerometers were connected to a NI 9234 dynamic signal acquisition (DSA) module, as shown in Fig. 3.2.8. The NI 9234 DSA module has a built-in antialiasing filter that automatically adjusts to the sampling rate. The DSA module was connected to a laptop, as shown in Fig. 3.2.1.

Figure 3.2.8 NI USB 9234 dynamic signal acquisition module

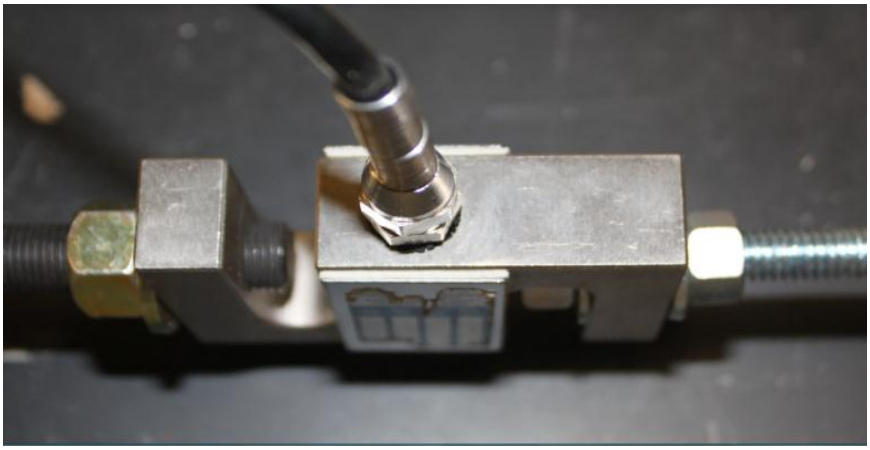

Figure 3.2.9 Load cell

Tests were also conducted in different environmental conditions. Carbon fiber cables of different length and different configuration were tested at room temperature (20°C) and in a temperature controlled room (4°C) at the University of New Mexico. The test setup described above was also sealed to test cables in vacuum condition, with an air pump to sustain vacuum. These modifications to the test mock-up will be described in the appropriate sections later.

3.3 Test Procedures and Data processing

3.3.1 Test Procedures

The tests were conducted with the following procedures:

Step 1: Fabricating a carbon fiber cable

A carbon fiber cable was made by twisting seven IM7 carbon fiber tows (HERCULES INC, type IM7-W-12K), as shown in Fig. 3.3.1.1. First, the strands were fixed at both ends using the cable ferrule and stop set. Then holding the untwisted strands at the left end, and twisting the strands from the right end for a required number of turns in clockwise direction.

Figure 3.3.1.1 IM-7 fiber tows

Step 2: Connecting the cable to the load cell, mounting the accelerometers and applying tension

The left end of the newly manufactured cable was connected to the load cell using the formed loop, as shown in Fig. 3.2.2. Then the accelerometers were mounted to the cable using wax and connected to the dynamic signal acquisition (DSA) module. After clamping the right end of the cable, tension force was applied by slowly tighten the bolt at the left end of the wooden frame.

Step 3: Exciting cable vibration and collecting data for processing

The vibration of the cable was excited by tapping the cable center.

3.3.2 Data Processing

A dynamic signal acquisition (DSA) module with signal conditioning function, type NI USB 9234, was connected to a laptop and accelerometers. It digitizes the incoming signals to the analog output signals. Each signal was buffered, analog pre-filtered, and digital filtered with a cutoff frequency that automatically adjust to the data rate chosen (25k/s). The time histories of signals recorded by the two accelerometers were elaborated to obtain the spectrum via Lab-VIEW 8.6 with the 'Fast Fourier Transform' (FFT). The natural frequency of the cable vibration was obtained by recording the frequencies at where a response peak is observed. The modal damping ratio was determined using the 'half-power bandwidth' method in frequency domain and the 'logarithmic decrement' method in time domain, respectively. Fig. 3.3.2.1 and Fig. 3.3.2.2 give a simple illustration of the two methods. To estimate modal damping ratio using the 'half-power bandwidth' method, the frequency response function (FRF) amplitude of the system is obtained first. Corresponding to each natural frequency, there is a peak in FRF amplitude

(X_{max}). Corresponding to $1/\sqrt{2}$ of the response peak are the two half point. The frequencies corresponding to FRF amplitude peak (X_{max}) and $1/\sqrt{2}$ of the FRF amplitude peak were obtained as: ω_n, ω_1 and ω_2, respectively. Then the modal damping ratio was calculated using Eq. (3-1) (Chopra, 2001):

$$\frac{\omega_2^2-\omega_1^2}{2\omega_n^2} = 2\zeta \tag{3-1}$$

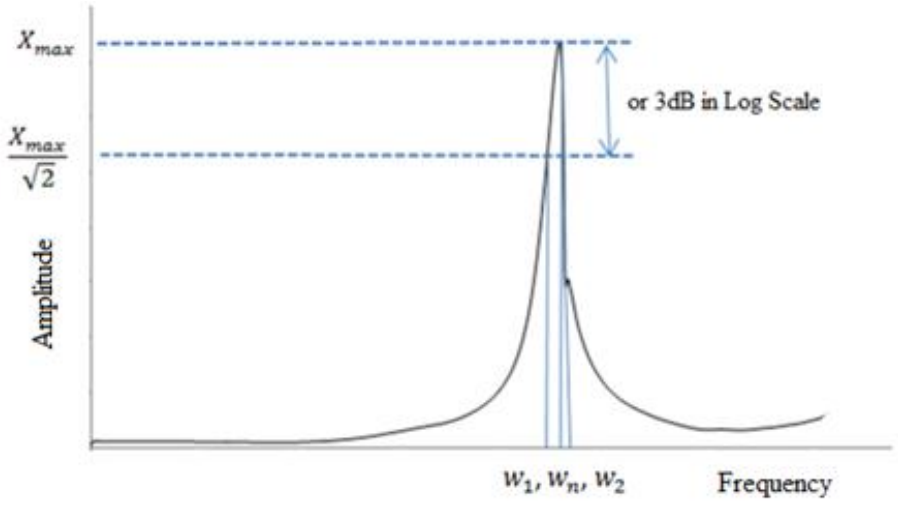

Figure 3.3.2.1 Half-power bandwidth method

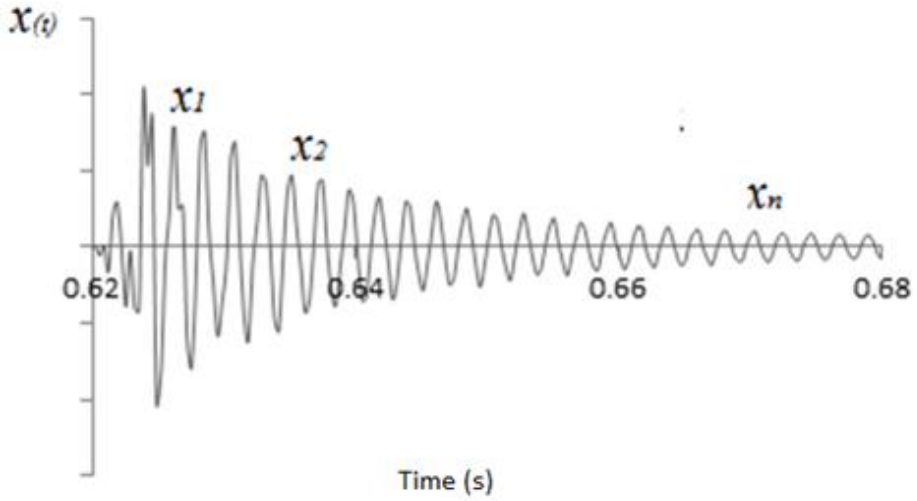

Figure 3.3.2.2 Logarithmic decrement method

To determine damping using the 'logarithmic decrement' method, time history response was recorded by accelerometers, and the modal damping ratio can be determined using Eq. (3-2) and Eq. (3-3) (Chopra, 2001).

$$\delta = \frac{1}{n} ln \left| \frac{x_1}{x_{n+1}} \right| = \frac{2\pi}{\sqrt{1-\zeta^2}} \tag{3-2}$$

$$\zeta = \frac{\delta}{\sqrt{4\pi^2+\delta^2}} \tag{3-3}$$

Where δ is the logarithmic decrement, ζ is the modal damping ratio, and x_1, x_{n+1} are the vibration amplitudes at *n* cycles apart.

For each cable, seven tests were conducted, and fourteen data (from 2 accelerometers × 7 tests) were stored. By using the 'half-power bandwidth method' in frequency domain or the 'logarithmic decrement method' in time domain, 14 damping values were obtained. The damping for the tested cable, for example, a 0.5080m, 62.13 turn/m carbon fiber cable with 445.00N pretension, was obtained by removing the data sets with maximum and minimum damping values (data No.3 and 6 in Table 3.3.3.1), and averaging the remaining ten values.

Table 3.3.1.1 Damping of a 0.5080m, 62.13 turns/m carbon fiber cable with 445.00N pretension

Data No	1	2	3	4	5	6	7
Damping estimated with data recorded by accelerometer at 3/4 of cable length (%)	0.36	0.36	0.36	0.36	0.36	0.35	0.35
Damping estimated with data recorded by accelerometer at 1/5 of cable length (%)	0.35	0.36	0.37	0.36	0.36	0.35	0.35
Damping of the tested cable	0.36						
Variance	3×10^{-5}						

From Table 3.3.1.1, the variance of the modal damping ratio for this cable is 3×10^{-5}, which shows a good repetition of the tests and the result is reliable. The vibration natural frequency was determined in the same way.

3.4 Tests Conducted

A comprehension of damping variation with cable parameters and ambient environment is essential to understand cable damping mechanisms and to design effective vibration control methods. Six different configurations of tests were performed and the results were analyzed and discussed:

a) Stainless steel cable in the length of 0.3048m and in the diameter of 0.003175m under different tensile forces;
b) Carbon fiber cables in the length of 0.2032m, 0.3048m and 0.5080m with three different configurations (20.71turns/m, 41.42turns/m and 62.13 turns/m) under room temperature and room air pressure;
c) Carbon fiber cables in the length of 0.2032m, 0.3048m and 0.5080m with three different configurations (20.71turns/m, 41.42turns/m and 62.13turns/m) at a temperature of 4 ℃;
d) Carbon fiber cables in the length of 0.2032m, 0.3048m and 0.5080m with three different configurations (20.71turns/m, 41.42turns/m and 62.13turns/m) in a vacuum chamber (-20 in. Hg);
e) Carbon fiber cable in the length of 0.3048m with configuration of 41.42turns/m using the stiffened wooden frame (bracing at the corners and cable supports);

f) Carbon fiber cables in the length of 0.3048m with three different configurations (20.71turns/m, 41.42turns/m and 62.13turns/m) with one accelerometer mounted to the cable.

3.4.1 Effect of Cable Tension

The test results of stainless steel cable by Yu (1949, 1952) have shown that the variation of damping depends on cable pre-stressing and yielding. Cable pretension has no effect on damping when cable pre-stressing below the yield point, while pre-stressing over yield point leads to a considerable reduction of damping. The same conclusion was obtained by Hard and Holben (1967) for a transmission line conductor. However, the experimental results by Seppa (1971), Ramberg and Griffin (1977), Raoof (1993b), Xu et al., (1998, 1999), Kim and Jeong (2005), Zheng et al., (2003), and Barbieri et al., (2004a, 2004b) showed that damping decreases as tension increases, while Yamaguchi (1987) concluded that tension has no influence on damping. The disparity could be due to different configuration and loading of the tests. In addition, almost all of these tests were performed with stainless steel cables or transmission line cables. Thus, it is necessary to provide some tests with carbon fiber cables to investigate the effect of tension on damping.

The tests were carried out using the experimental setup shown in Fig. 3.2.1. The tested stainless steel cable is made of several (7 × 7) stainless steel wires, as shown in Fig. 3.4.1.1, and the carbon fiber cable is made by twisting seven IM7 carbon fiber tows (HERCULES INC, type IM7-W-12K). The geometric and the mechanical properties of the 0.3048m carbon fiber cables are summarized in Table 3.4.1.1. To investigate the

effect of the applied tension on damping, cables were loaded with tension force of 111.25N, 222.50N, 333.75N, 445.00N and 578.50N. Results of cables tested within test configurations (a) to (d) were used to analyze the effect of tension on damping.

Figure 3.4.1.1 Stainless steel cable and cross section

Table 3.4.1.1 Properties of 0.3048m carbon fiber cables

Cable construction (turns/m)	Length (m)	Mass per unit length (kg/m)	Young's Modulus (Pa)
20.71	0.3048	0.00427	2.76×10^{11}
41.42	0.3048	0.00432	2.76×10^{11}
62.13	0.3048	0.00446	2.76×10^{11}

3.4.1.1 Carbon Fiber Cables Tested at Room Temperature

The time history responses and the spectrum of the signals at the two measuring points were obtained using the recorded data from the two accelerometers located at three quarters and one fifth of the cable span. Fig. 3.4.1.2 shows the time history responses of a 0.3048m, 20.71 turns/m carbon-fiber cable with 333.75N pretension. From Fig. 3.4.1.2, it is noticed that the vibration decayed in about 0.08 second and 35 cycles. Fig. 3.4.1.3

presents the corresponding frequency domain data, where a vibration natural frequency of 458.67Hz was identified from the frequency corresponding to the response peak.

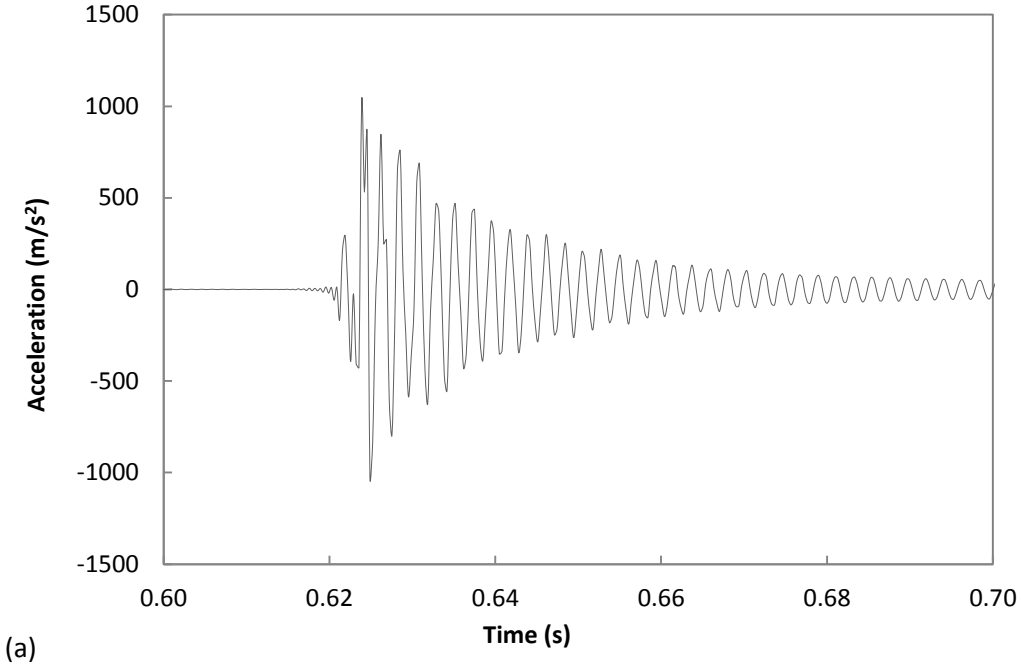

(a)

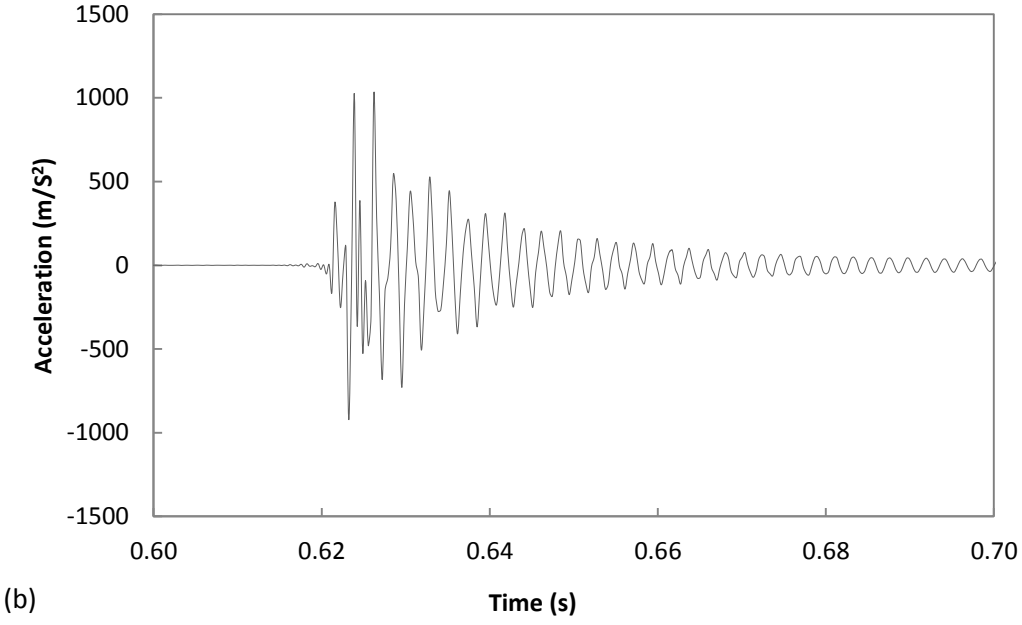

(b)

Figure 3.4.1.2 Recorded time-history responses for a 0.3048m, 20.71turns/m carbon fiber cable at room temperature and 333.75N pretension (a) at 1/5 of cable length (b) at 3/4 of cable length

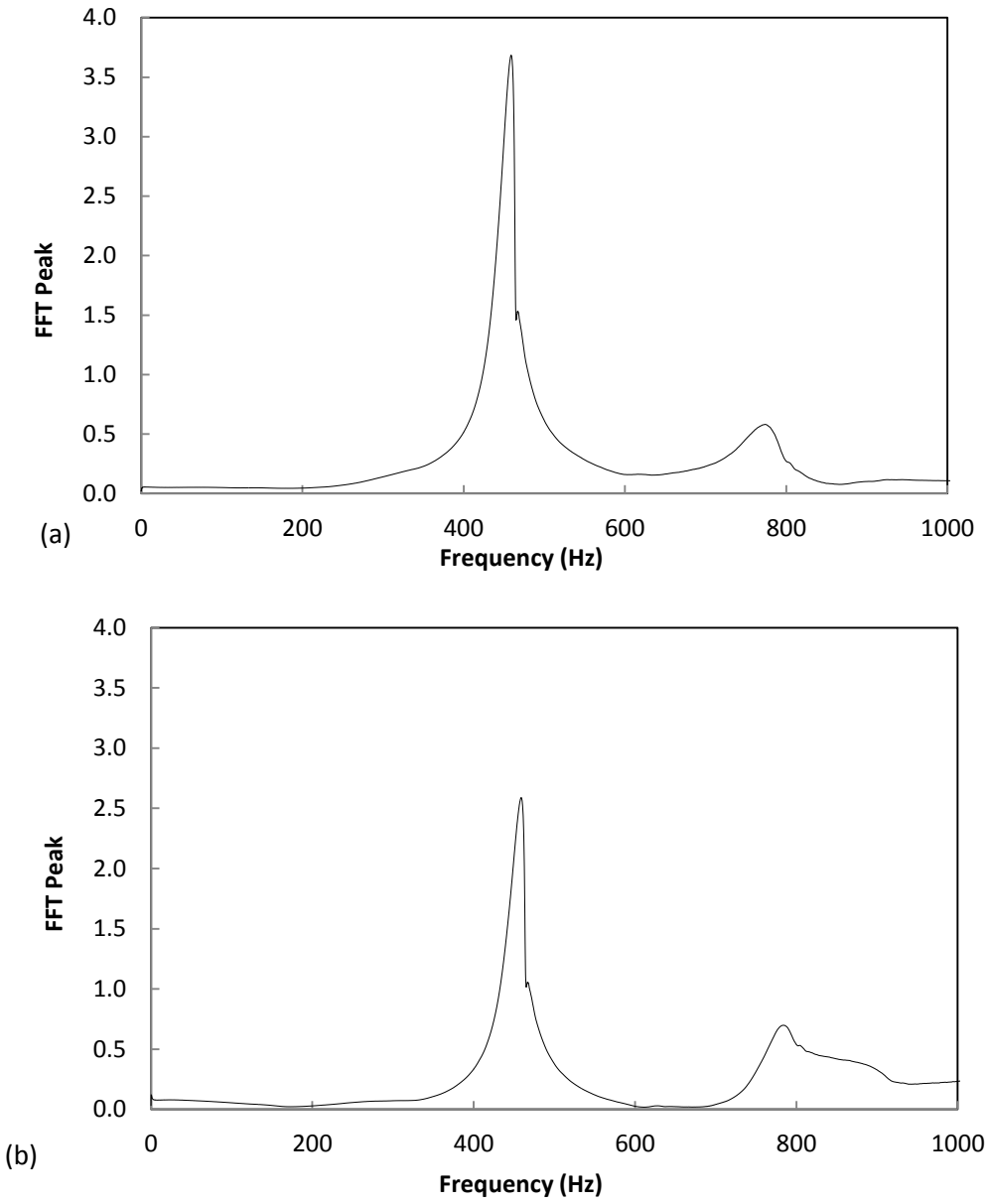

Figure 3.4.1.3 Spectral of signals for a 0.3048m, 20.71turns/m carbon fiber cable at room temperature and 333.75N pretension (a) at 1/5 of cable length (b) at 3/4 of cable length

Table 3.4.1.2 and Table 3.4.1.3 list, respectively, the results of the modal damping ratio and the identified vibration frequencies for cables tested at room temperature. In Fig. 3.4.1.4, the experimental determined modal damping ratios for different length and

construction cables are plotted against tension and Fig. 3.4.1.5 plots the variation of vibration frequency with tension.

Table 3.4.1.2 Cable damping at room temperature

Tension (N)	Damping for 20.71turns/m cables (%)			Damping for 41.42turns/m cables (%)			Damping for 62.13turns/m cables (%)		
	0.2032 m	0.3048 m	0.5080 m	0.2032 m	0.3048 m	0.5080 m	0.2032 m	0.3048 m	0.5080 m
111.25	5.50	2.42	2.22	4.59	2.27	1.54	4.20	1.68	1.14
222.50	3.79	2.11	1.81	3.07	1.80	1.11	2.40	1.24	0.96
333.75	3.18	1.83	1.33	2.53	1.68	0.94	1.73	1.18	0.54
445.00	3.06	1.45	1.14	2.35	1.39	0.69	1.23	0.97	0.50
578.50	2.60	1.40	1.00	2.18	1.36	0.70	1.18	0.90	0.36

Table 3.4.1.3 Cable vibration frequency at room temperature

Tension (N)	Frequency for 20.71turns/m cables (Hz)			Frequency for 41.42turns/m cables (Hz)			Frequency for 62.13turns/m cables (Hz)		
	0.2032 m	0.3048 m	0.5080 m	0.2032 m	0.3048 m	0.5080 m	0.2032 m	0.3048 m	0.5080 m
111.25	365.71	309.87	159.62	360.29	280.96	117.82	352.68	266.82	114.97
222.50	515.79	392.63	225.8 2	492.74	369.02	209.3	474.18	360.33	204.54
333.75	625.85	458.67	263.45	612.20	430.00	262.28	591.53	418.68	261.46
445.00	694.65	517.74	308.86	693.57	500.49	292.50	687.77	485.62	300.93
578.50	797.60	554.68	355.53	788.08	534.65	347.72	767.40	502.50	341.27

The results presented in Fig. 3.4.1.4 show a decrease in the cable damping as tension increases. For the 0.2032m cables, the damping presents a significant decrement when tension is less than about 222.50N, whereas, for cables in the length of 0.3048m and 0.5080m, damping decreases at a slow tempo with the applied tension, and the significant decrement presented in the 0.2032m cables is not observed, which suggests that a short cable could have a greater end effects. From Fig. 3.4.1.5, it is evident that a greater tension leads to a higher vibration frequency, and a longer cable exhibits a lower vibration frequency.

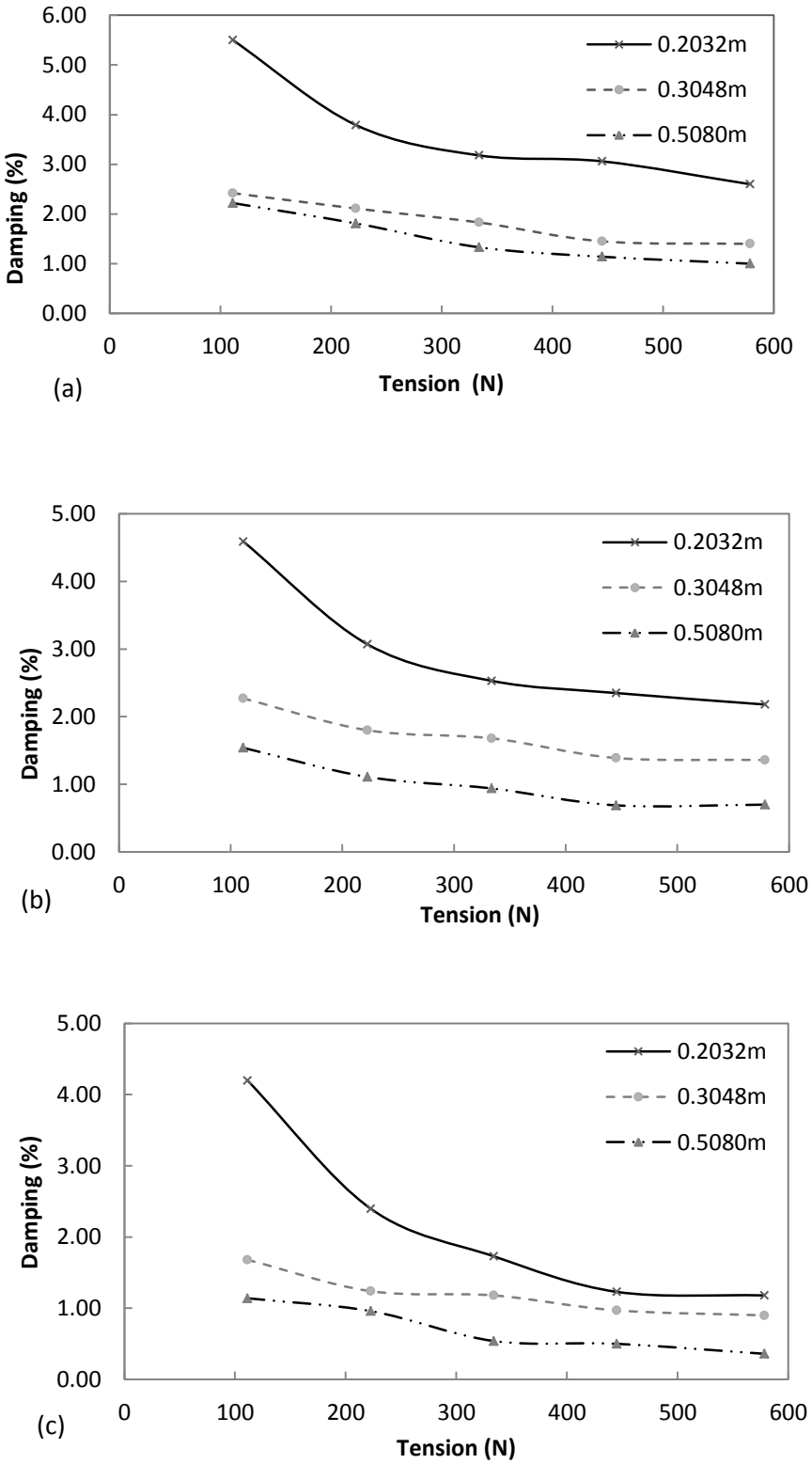

Figure 3.4.1.4 Damping versus tension for cables at room temperature (a) 20.71turns/m (b) 41.42turns/m (c) 62.13turns/m cables

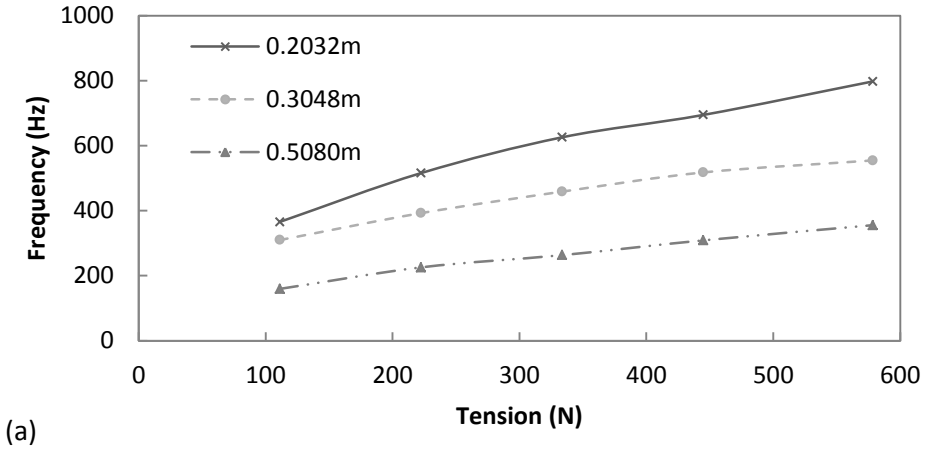

(a)

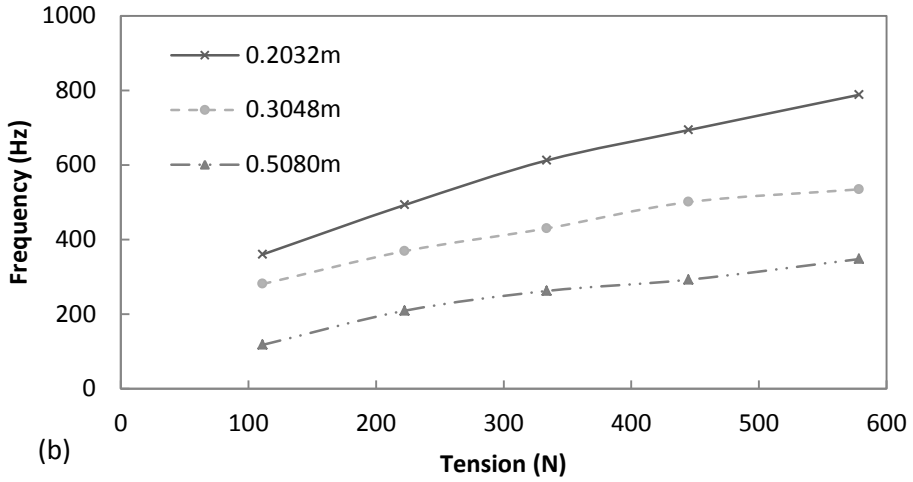

(b)

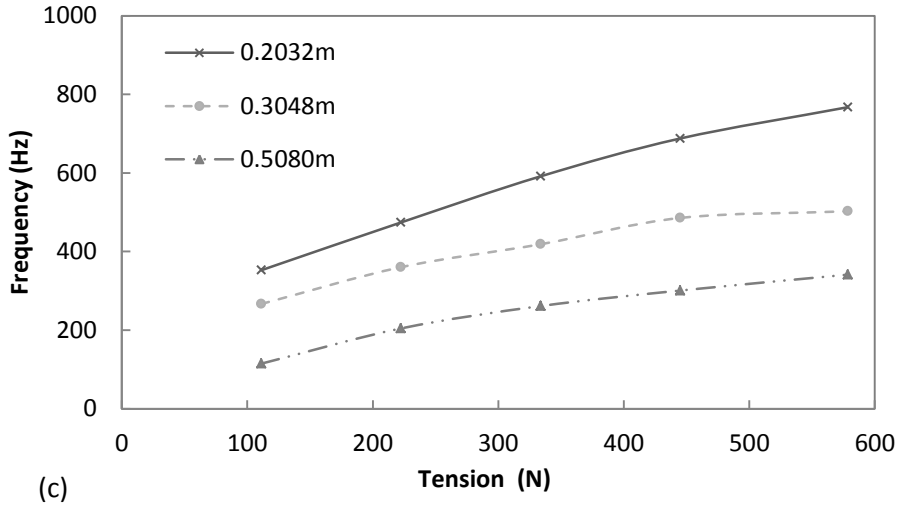

(c)

Figure 3.4.1.5 Vibration frequency versus tension for cables at room temperature (a) 20.71turns/m (b) 41.42turns/m (c) 62.13turns/m cable

3.4.1.2 Carbon Fiber Cables Tested at a Temperature of 4℃

For different length, different configuration carbon fiber cables tested in a cold room with a temperature of 4℃, Table 3.4.1.4 and Table 3.4.1.5 present the modal damping ratios and vibration frequencies, respectively. The time history responses for a 0.3048m, 20.71 turns/m carbon fiber cable tested at a temperature of 4℃ and 333.75N pretension were recorded by the two accelerometers and shown in Fig. 3.4.1.6. Comparing these with the time history responses (Fig. 3.4.1.2) of the cable tested at room temperature, the time responses in Fig. 3.4.1.6 shows a quicker logarithmic rate of decay (in 0.05 second). In other words, a higher damping is presented for cable tested at a temperature of 4℃. The corresponding spectrum data are shown in Fig. 3.4.1.7.

Table 3.4.1.4 Cable damping at a temperature of 4℃

Tension (N)	Damping for 20.71turns/m cables (%)			Damping for 41.42turns/m cables (%)			Damping for 62.13turns/m cables (%)		
	0.2032 m	0.3048 m	0.5080 m	0.2032 m	0.3048 m	0.5080 m	0.2032 m	0.3048 m	0.5080 m
111.25	5.95	3.53	2.58	4.92	2.58	2.35	4.37	1.88	1.58
222.50	4.25	2.70	2.26	3.69	2.25	1.89	2.46	1.55	1.32
333.75	3.57	1.98	1.92	2.74	1.89	1.65	1.72	1.23	1.13
445.00	3.12	1.63	1.51	2.36	1.60	1.38	1.43	1.09	0.95
578.50	2.71	1.55	1.45	1.95	1.46	1.07	1.30	1.03	0.81

Table 3.4.1.5 Cable vibration frequency at a temperature of 4℃

Tension (N)	Frequency for 20.71turns/m cables (Hz)			Frequency for 41.42turns/m cables (Hz)			Frequency for 62.13turns/m cables (Hz)		
	0.2032 m	0.3048 m	0.5080 m	0.2032 m	0.3048 m	0.5080 m	0.2032 m	0.3048 m	0.5080 m
111.25	360.53	267.38	162.64	356.08	262.27	131.68	360.49	242.03	118.04
222.50	516.70	351.89	219.34	526.42	369.34	209.35	501.18	349.19	212.79
333.75	613.04	460.92	283.06	612.85	444.31	262.32	591.01	430.68	266.96
445.00	703.35	523.54	318.79	701.78	518.47	302.10	702.81	505.73	298.65
578.50	796.57	588.25	360.05	783.16	580.32	344.19	796.47	563.62	367.58

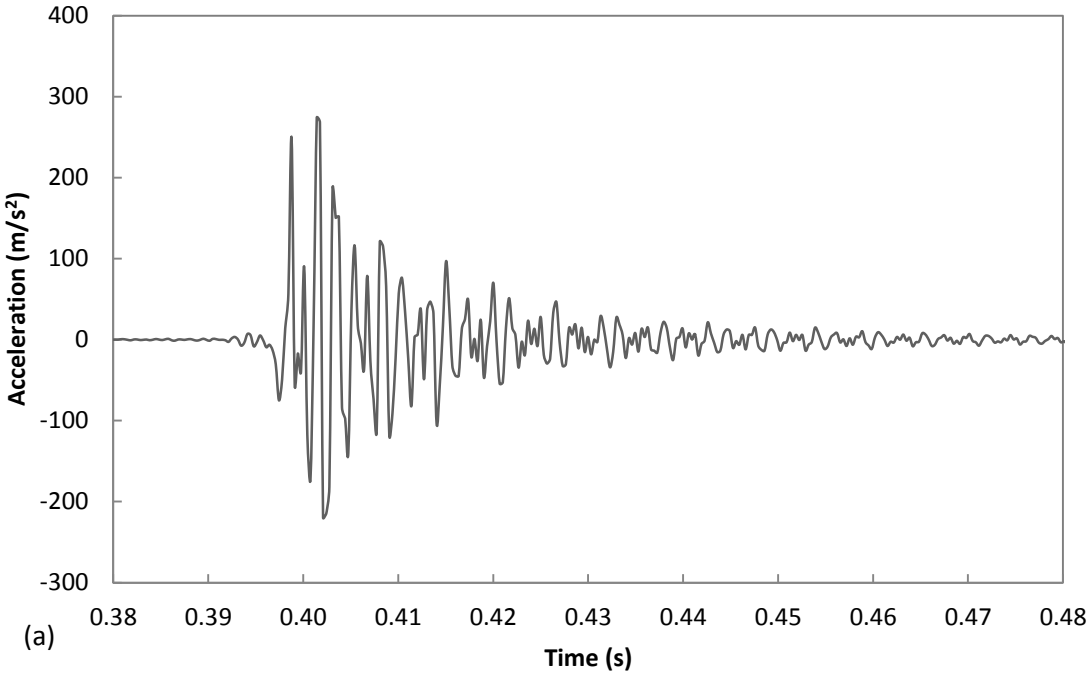

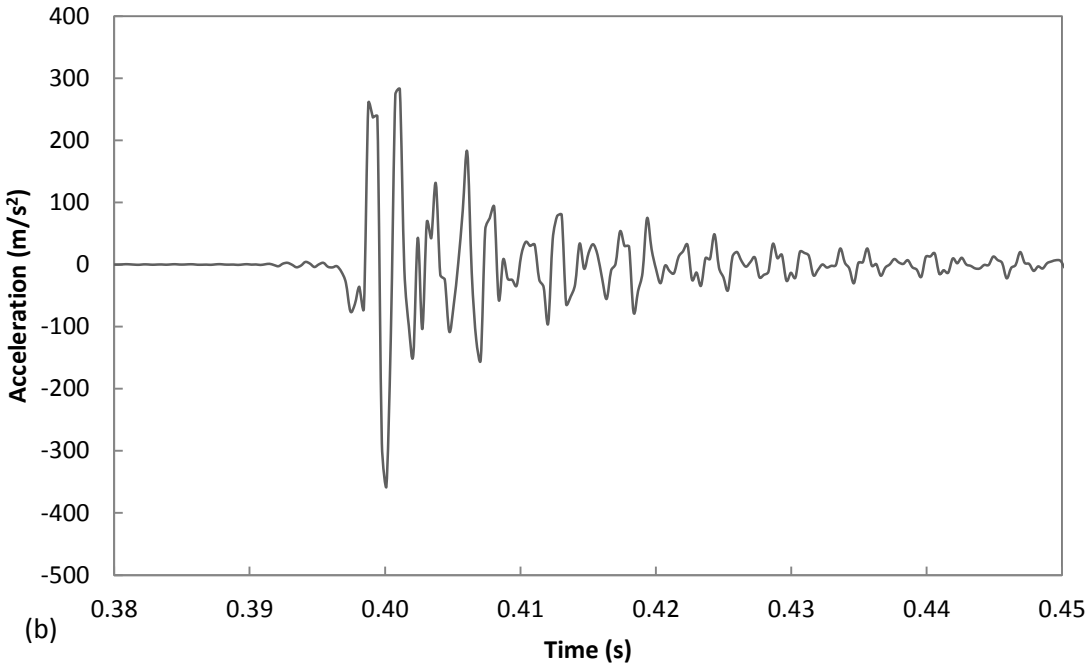

Figure 3.4.1.6 Recorded time-history responses for a 0.3048m, 20.71turns/m carbon fiber cable at a temperature of 4℃ and 333.75N pretension (a) at 1/5 of cable length (b) at 3/ 4 of cable length

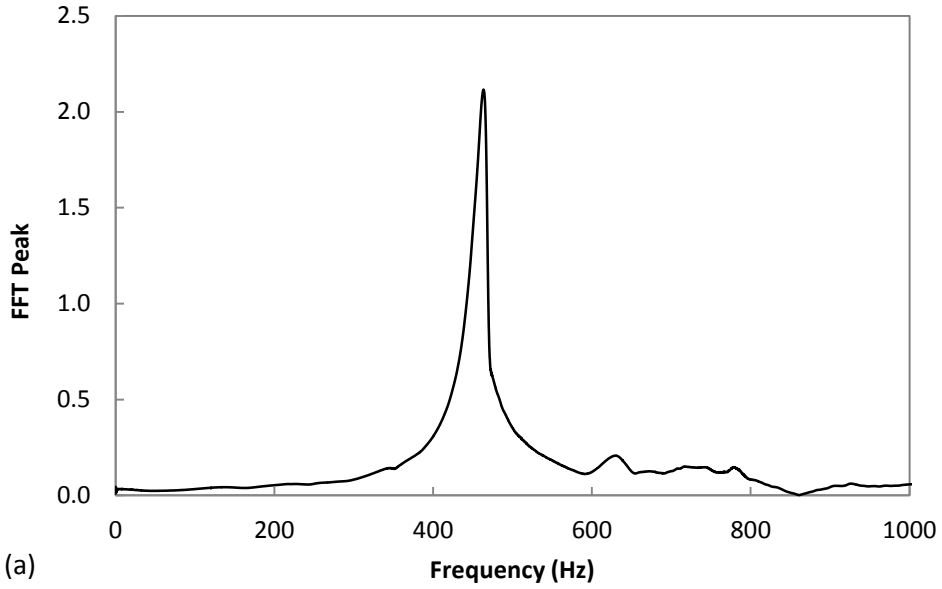

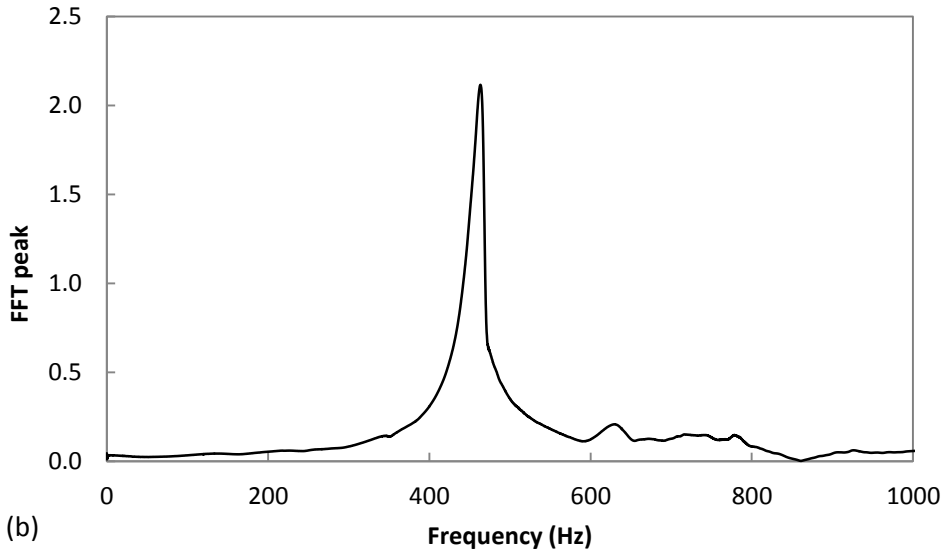

Figure 3.4.1.7 Spectral of signals for a 0.3048m, 20.71turns/m carbon fiber cable at a temperature of 4℃ and 333.75N pretension (a) at 1/5 of cable length (b) at 3/ 4 of cable length

Fig. 3.4.1.8 depicts the vibration damping versus tension for cables tested at a temperature of 4℃ , and Fig. 3.4.1.9 plots the variation of vibration frequency with tension.

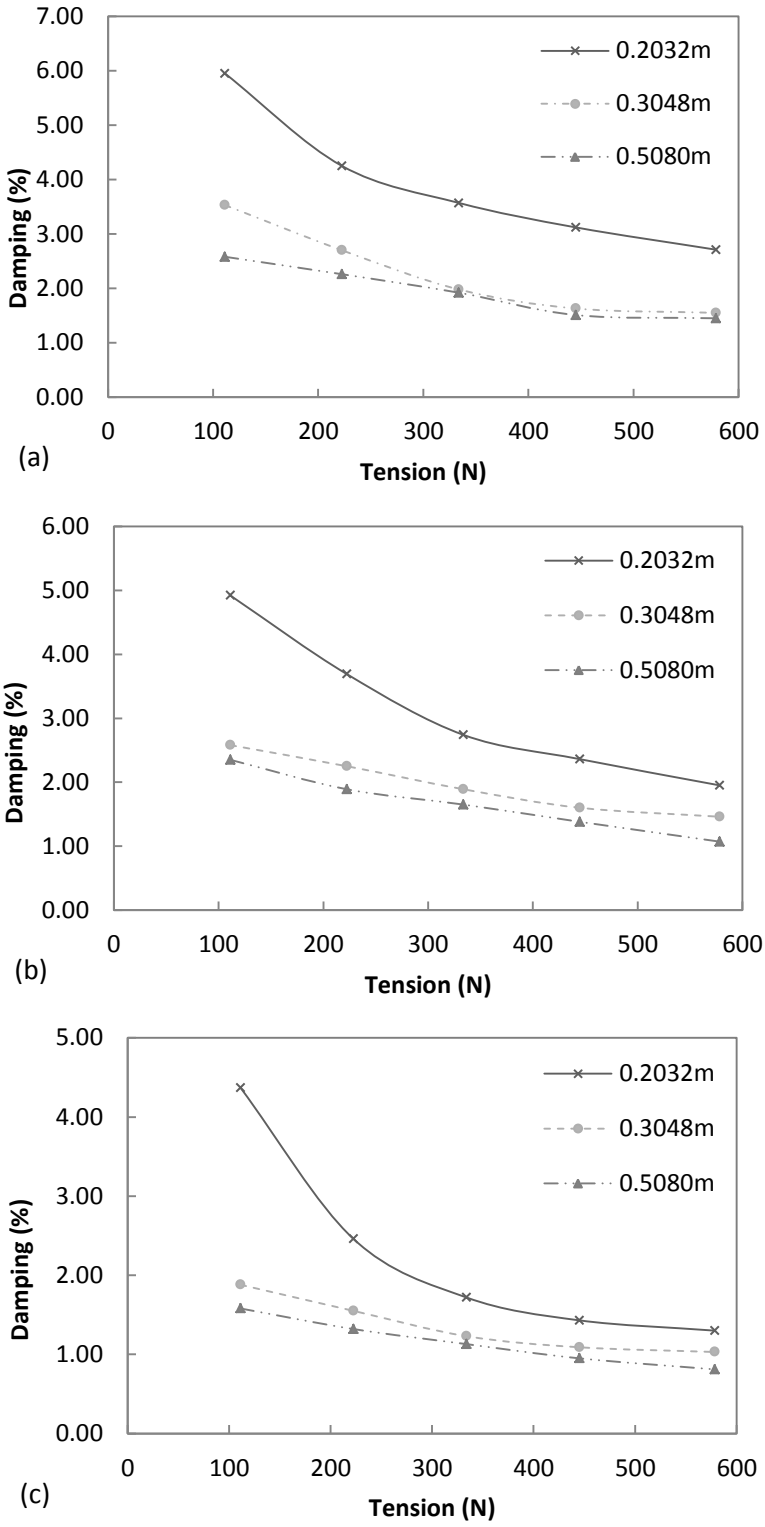

Figure 3.4.1.8 Damping versus tension for cables at a temperature of 4 ℃ (a) 20.71turns/m (b) 41.42turns/m (c) 62.13turns/m cables

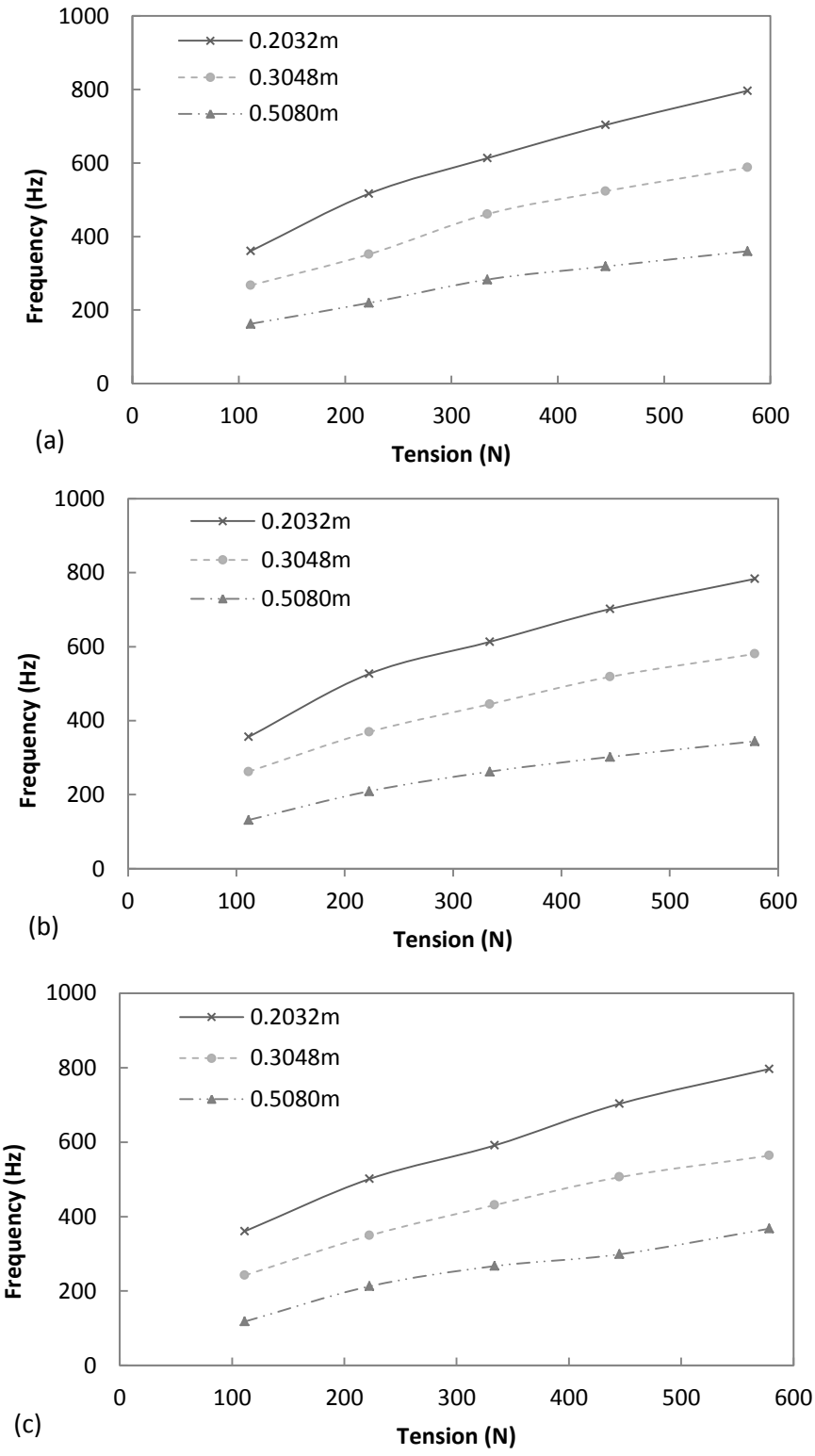

Figure 3.4.1.9 Vibration frequency versus tension for cables at a temperature of 4 ℃ (a) 20.71turns/m (b) 41.42 turns/m (c) 62.13turns/m cables

It is observed from Fig. 3.4.1.8 that cable damping decreases as tension increases. For cables in the length of 0.2032m, the damping shows a fast descendant as tension increases when tension is less than around 222.50N. For cables in the length of 0.3048m and 0.5080m, damping decreases slowly under the applied tension, the significant decrement observed in the 0.2032m cables was not noticed, which suggests that the end effects on damping is greater for shorter cables. Besides, a slower damping decrement rate was noticed for cables at a temperature of 4 ℃ compared with cables at room temperature (20℃). The vibration frequency increases as tension increases and decreases as length increases as indicated in Fig. 3.4.1.9.

3.4.1.3 Carbon Fiber Cables Tested in a Vacuum Chamber

As regards the carbon fiber cables tested at 20℃ in a vacuum chamber, the identified cable vibration frequencies and modal damping ratios are listed in Table 3.4.1.6 and Table 3.4.1.7, respectively. The time history responses of a 20.71 turns/m, 0.3048m carbon fiber cable are presented in Fig. 3.4.1.10. From the figures, the time history responses show a slower decay than the cables in air. The corresponding spectrum signals are shown in Fig. 3.4.1.11, which gives a vibration frequency about 581.37 Hz.

Table 3.4.1.6 Cable vibration frequency in a vacuum (-20 In. Hg) chamber

Tension (N)	Frequency for 20.71turns/m cables (Hz)			Frequency for 41.42turns/m cables (Hz)			Frequency for 62.13turns/m cables (Hz)		
	0.2032 m	0.3048 m	0.5080 m	0.2032 m	0.3048 m	0.5080 m	0.2032 m	0.3048 m	0.5080 m
111.25	351.90	310.35	161.25	323.18	279.29	143.24	321.7	281.76	140.81
222.50	481.72	413.36	214.78	466.96	359.82	226.24	464.29	356.29	210.82
333.75	581.37	471.12	286.02	575.97	420.68	280.82	580.89	424.31	284.33
445.00	705.72	518.26	319.62	660.10	498.45	313.83	657.14	491.28	305.97
578.50	796.83	567.86	357.24	747.26	567.72	357.80	745.16	521.81	353.93

Table 3.4.1.7 Cable damping in a vacuum chamber (-20 in. Hg)

Tension (N)	Damping for 20.71turns/m cables (%)			Damping for 41.42turns/m cables (%)			Damping for 62.13turns/m cables (%)		
	0.2032 m	0.3048 m	0.5080 m	0.2032 m	0.3048 m	0.5080 m	0.2032 m	0.3048 m	0.5080 m
111.25	4.94	2.14	1.87	4.14	2.03	1.34	3.89	1.33	0.88
222.50	3.62	1.94	1.24	2.62	1.51	0.92	1.90	1.08	0.66
333.75	2.95	1.47	0.85	2.06	1.32	0.76	1.43	0.91	0.51
445.00	2.73	1.16	0.65	1.67	1.13	0.60	1.25	0.72	0.45
578.50	2.48	1.06	0.62	1.41	0.99	0.58	1.11	0.67	0.33

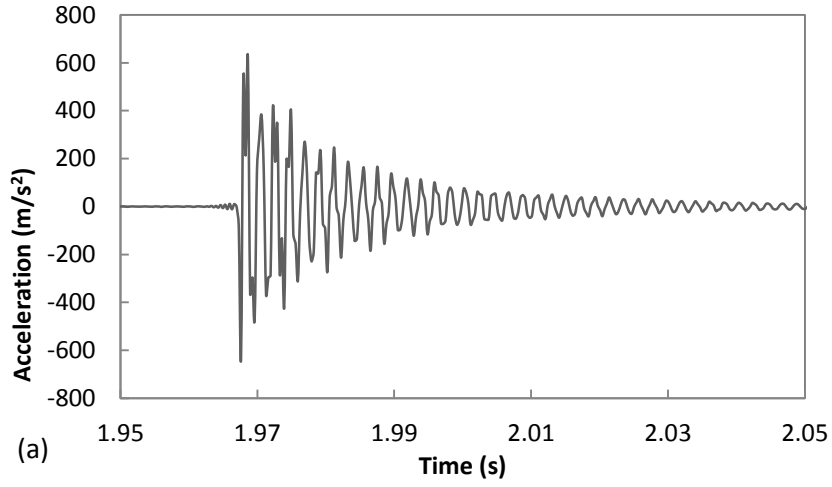

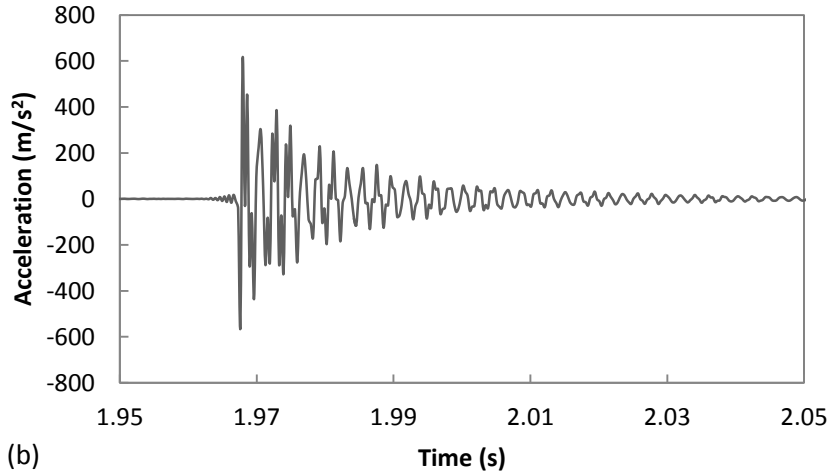

Figure 3.4.1.10 Recorded time-history responses for a 0.3048m, 20.71turns/m carbon fiber cable in vacuum chamber with 333.75N pretension (a) at 1/5 of cable length (b) at 3/4 of cable length

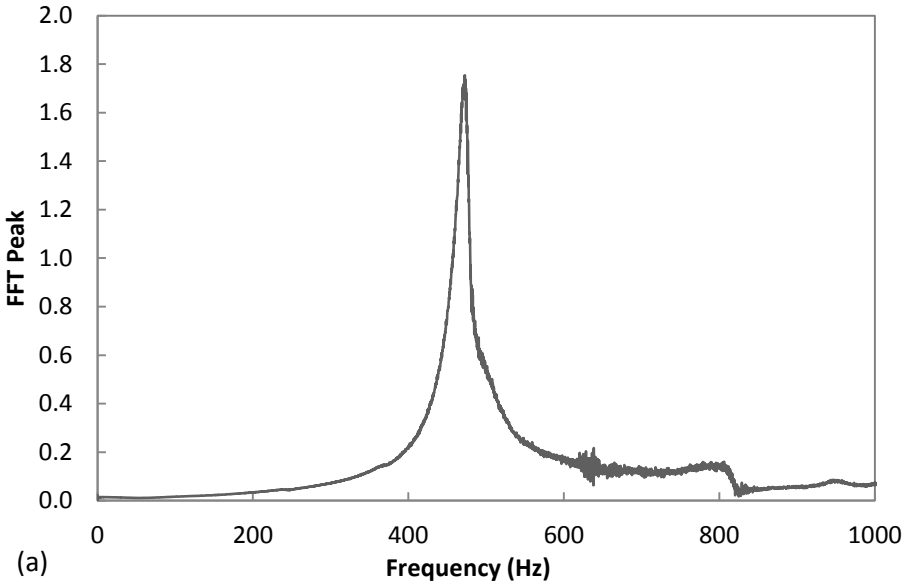

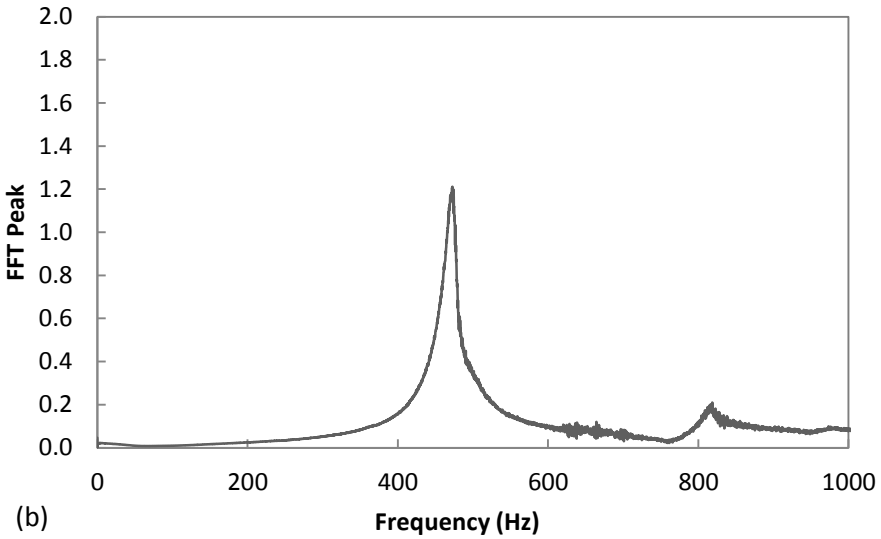

Figure 3.4.11 Spectral of signals for a 0.3048m, 20.71turns/m carbon fiber cable in vacuum chamber with 333.75N pretension (a) at 1/5 of cable length (b) at 3/4 of cable length

The results presented in Table 3.4.1.6 and Table 3.4.1.7 are plotted in Fig. 3.4.1.12 and Fig. 3.4.1.13, respectively, where shows the trend of modal damping ratio and vibration frequency with the various tension forces.

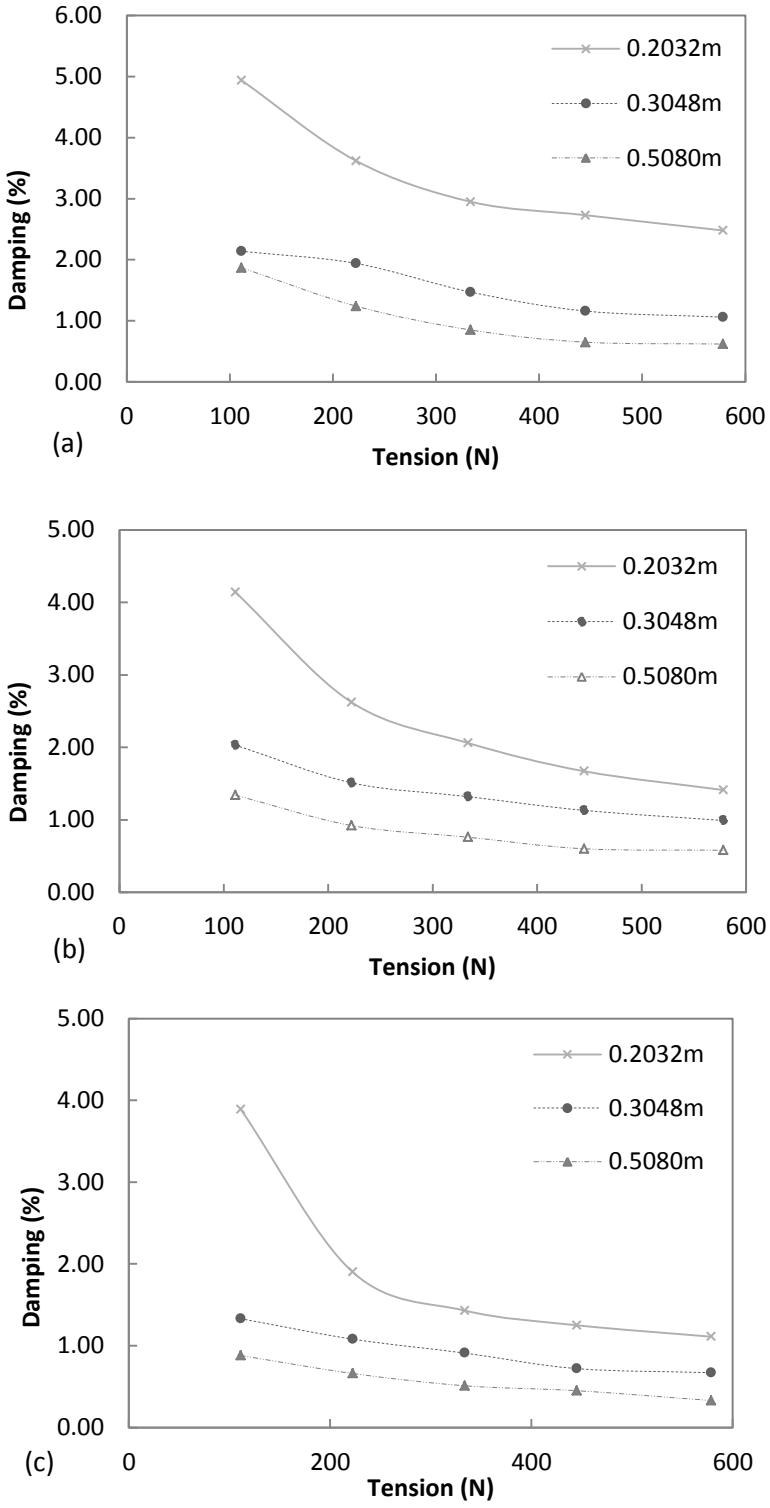

Figure 3.4.1.12 Damping versus tension for cables in a vacuum chamber (a) 20.71turns/m (b) 41.42turns/m (c) 62.13turns/m cables

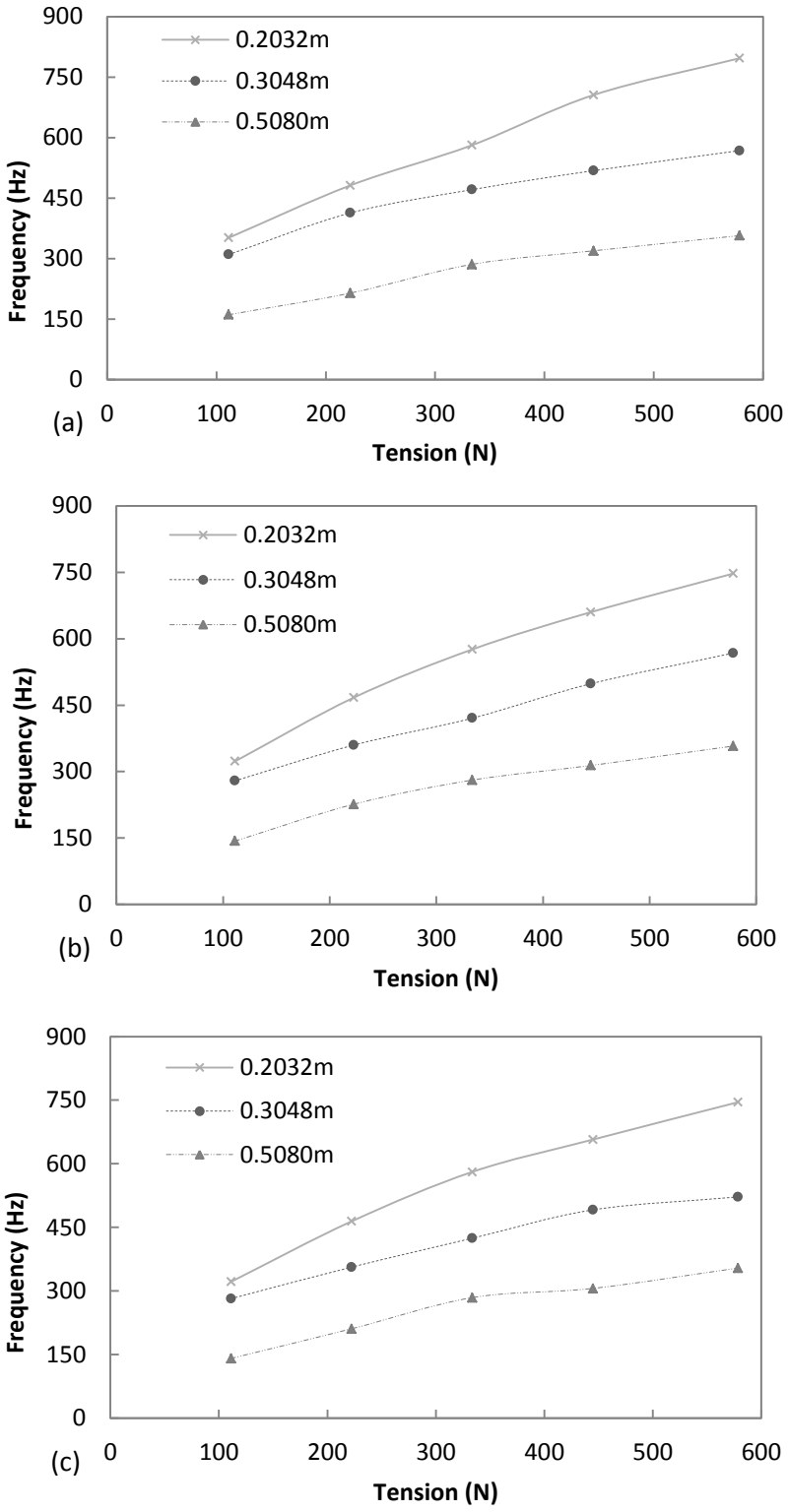

Figure 3.4.1.13 Vibration frequency versus tension for cables in vacuum chamber (a) 20.71turns/m (b) 41.42turns/m (c) 62.13turns/m cables

As shown in Fig. 3.4.1.12, for cables tested in vacuum chamber, the vibration damping varies in the same way as cables tested at normal atmosphere, the damping decreases as tension increases, and a significant decrease was noticed for cables in the length of 0.2032m when the tension is less than about 225.00N. Fig. 3.4.1.13 shows that the vibration frequency increases as cable tension increases and decreases as length increases.

3.4.1.4 Stainless Steel Cable Tested at Room Temperature

Stainless steel cables in the length of 0.3048m and in the diameter of 0.003175m were tested under different tensile force to investigate the variation of stainless steel cable damping with tension.

Fig. 3.4.1.14 presents the variation of stainless steel cable damping with tension. The results showed that for the stainless steel cable, higher tension results in lower damping, which is similar to that observed by Seppa (1971), Ramberg and Griffin (1977), Raoof (1993b), Xu et al., (1998, 1999), Kim and Jeong (2005), Zheng et al., (2003), and Barbieri et al., (2004a, 2004b), and demonstrates the same trend as the carbon fiber cables.

In addition, the modal damping ratios evaluated by the ‘half-power bandwidth’ method and the ‘logarithmic decrement’ method are shown in Fig. 3.4.1.14. From the figures, the modal damping ratios obtained in time domain agrees well with those evaluated in frequency domain, the difference is about 1-3%.

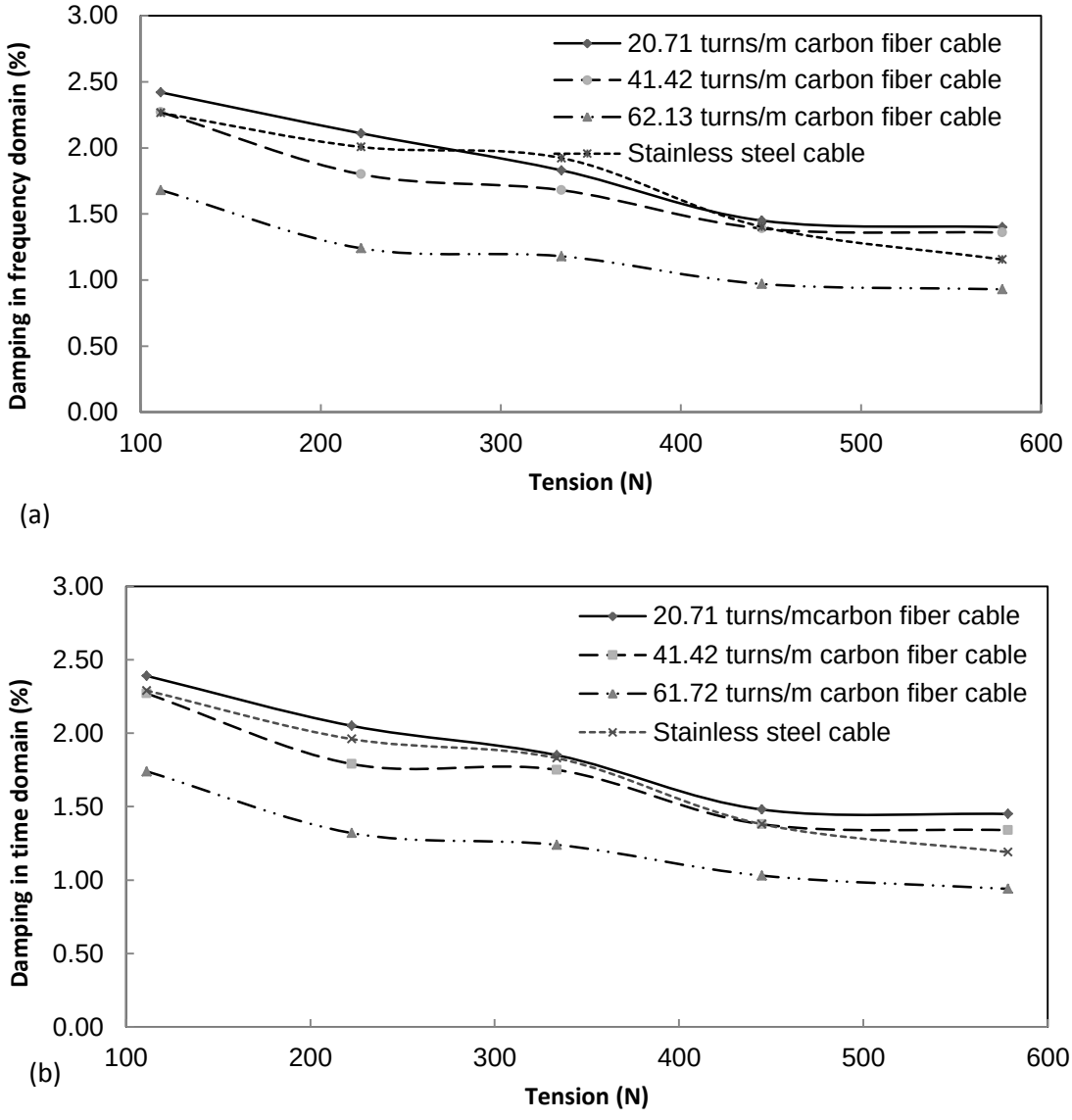

Figure 3.4.1.14 Variation of damping with applied tension

3.4.1.5 Evaluation of Rayleigh Damping Constants

Zhu and Meguid (2007) et al. concluded that Rayleigh damping is suitable to model the cable damping. In order to evaluate the dependence of damping on the vibration mode, the Rayleigh damping theory is introduced. For the Rayleigh damping theory, it is

assumed that the damping matrix is proportional to the combination of mass and stiffness matrices as given by the expression of Eq. (3-4) (Chopra 2001):

$$[c] = \alpha[M] + \beta[K] \tag{3-4}$$

Where:

[c] = damping matrix of the vibration system

[M] = mass matrix of the vibration system

[K] = stiffness matrix of the vibration system

α and β = the Rayleigh damping constants

After orthogonal transformation and reduction to n-uncoupled equation, we can obtain the following:

$$\begin{cases} 2\zeta_1\omega_1 = \alpha + \beta\omega_1^2 \\ 2\zeta_2\omega_2 = \alpha + \beta\omega_2^2 \end{cases} \tag{3-5}$$

From Eq. (3-5), the following is obtained:

$$\begin{cases} \alpha = \frac{2\omega_1\omega_2(\zeta_1\omega_2 - \zeta_2\omega_1)}{\omega_2^2 - \omega_1^2} \\ \beta = \frac{2(\zeta_2\omega_1 - \zeta_1\omega_2)}{\omega_2^2 - \omega_1^2} \end{cases} \tag{3-6}$$

Where:

ω_1, ω_2 = the first and the second circular vibration frequency of the tested cable

ζ_1, ζ_2 = the first and the second modal damping ratio of the tested cable

ω_1 and ω_2 can be determined from the spectrum analysis of cable vibration. ζ_1 and ζ_2 can be determined using the 'half-power bandwidth' method. Before applying those values to Eq. (3-6), the values are smoothed by quadratic curve fitting. The values of α and β for 0.3048m (20.71turns/m, 41.42turns/m and 62.13 turns/m) carbon fiber cables, and stainless steel cable were obtained by Eq. (3-6), the results are listed in Table 3.4.1.8 and plotted in Fig. 3.4.1.15 and Fig. 3.4.1.16, respectively. From the plots, it can be observed that α initially increases as tension increases, and then decreases. In addition, Fig.3.4.1.16 shows that β decreases as tension increases for both carbon-fiber cables and the stainless steel cable.

Table 3.4.1.8 Alpha and beta for the tested 0.3048m cables

Tension (N)	20.71turns/m carbon fiber cable		41.42 turns/m carbon fiber cable		62.13 turns/m carbon fiber cable		Stainless steel cable	
	Alpha	Beta	Alpha	Beta	Alpha	Beta	Alpha	Beta
111.25	-5.239	0.000027	-10.330	0.000029	-22.559	0.000028	24.252	0.000021
222.50	1.734	0.000017	1.130	0.000016	-18.438	0.000015	28.452	0.000015
333.75	5.337	0.000012	17.990	0.000009	-11.638	0.000010	29.676	0.000011
445.00	0.834	0.000009	27.292	0.000006	-6.238	0.000007	27.023	0.000008
578.50	18.208	0.000009	25.973	0.000006	-6.141	0.000007	18.784	0.000007

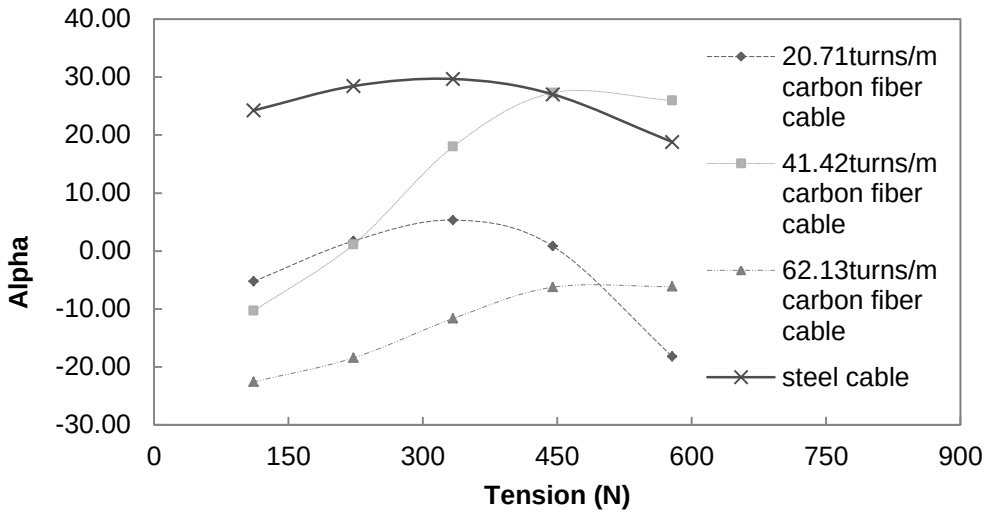

Figure 3.4.1.15 Relation curves of alpha with tension

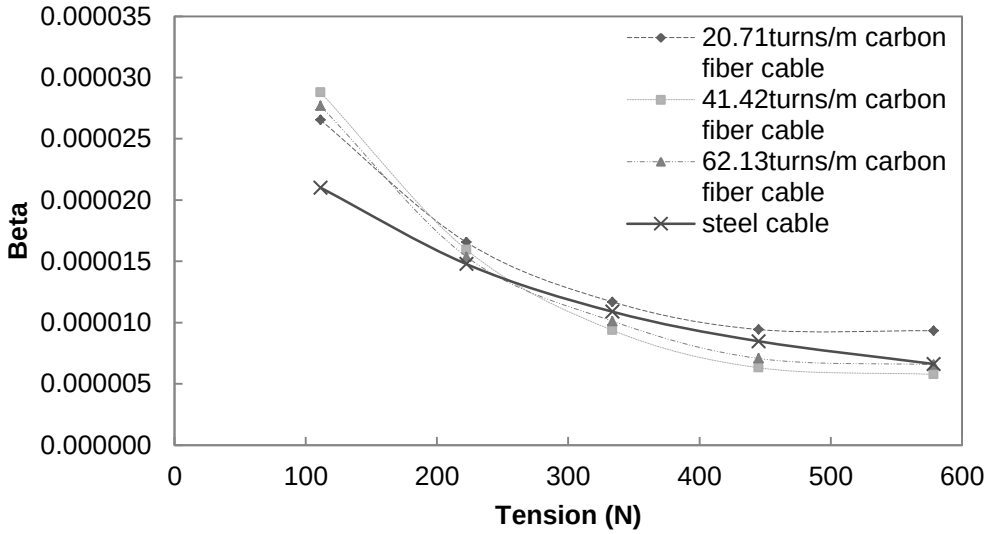

Figure 3.4.1.16 Relation curves of beta with tension

In summary, cable damping decreases as tension increases for the range of tension forces considered in this research. The same conclusion was derived by Seppa (1971), Ramberg and Griffin (1977) et al. The decrease in cable damping is caused by the increased interwire contact force, which reduces the occurrence of interwire slippage and causes

lower energy dissipation. The initial decrease in damping for short cable lengths could be due to greater end (boundary induced) effects for short cables. Concerning with the vibration frequency, as expected, a higher tension leads to a higher vibration frequency.

3.4.2 Effect of Cable Length

Some previously reported tests showed that damping decreases as cable length increases (Yu 1949, 1952, Barbieri et al., 2004a, 2004b); while others indicated that length has no significant effect on damping (Hard and Holben, 1967). This disparity may due to the difference of cable configuration and test apparatus. It is worthwhile to conduct some vibration tests on cables with different lengths to study the dependence of damping on length. Tests were performed using the experimental setup shown in Fig. 3.2.1 by modifying the location of the wooden components where the steel plates clamped. Cables in length of 0.2032m, 0.3048m, and 0.5080m with three different configurations (20.71turns/m, 41.42turns/m and 62.13turns/m) were tested at room temperature of 20℃ and 4℃, and in a vacuum chamber.

3.4.2.1 Carbon Fiber Cables Tested at Room Temperature

For carbon fiber cables tested at room temperature, the damping is plotted against cable length in Fig. 3.4.2.1. From Fig. 3.4.2.1, it is observed that damping has a significant decrement as length increases for cables shorter than 0.3m. Beyond this length, the decrement is small or negligible. In addition, for short cables (<0.3m), the decrement ratio of damping for cables under a tensile force less than 111.25N is about 2-3 times the decrement ratio for cables loading with a tensile force more than 111.25N .

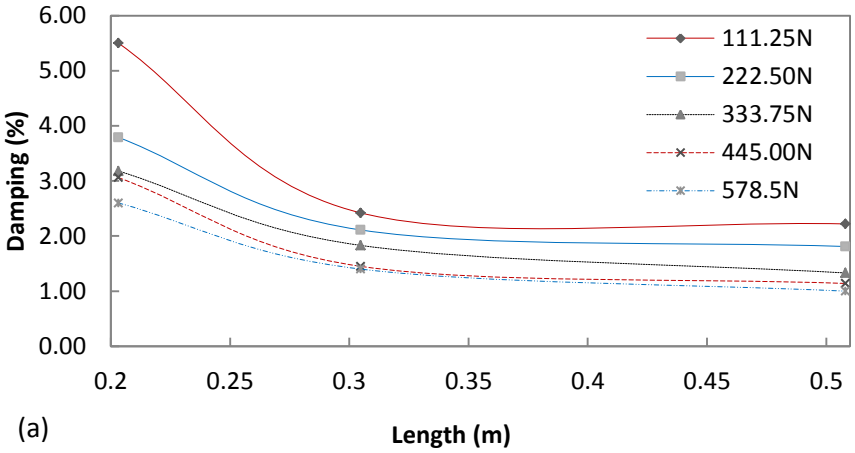

(a)

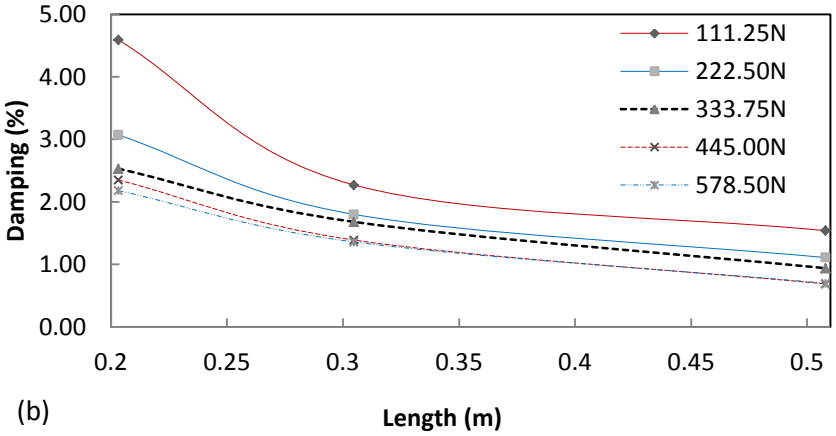

(b)

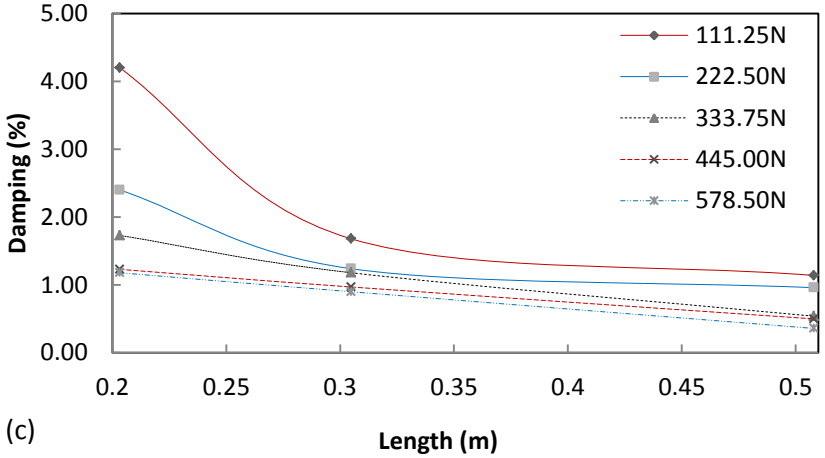

(c)

Figure 3.4.2.1 Cable damping versus length for cables at room temperature (a) 20.71turns/m (b) 41.42turns/m (c) 62.13turns/m cables

3.4.2.2 Carbon Fiber Cables Tested at a Temperature of 4℃

For carbon fiber cables tested in a cold room with temperature set at 4℃, the damping of cables with different length and construction are plotted in Fig. 3.4.2.2. It is clear from Fig. 3.4.2.2 that damping initially decreases as length increases, and is unaffected by length for a longer cable. A significant decrement of cable damping is noticed for the short cable with length less than about 0.3m.

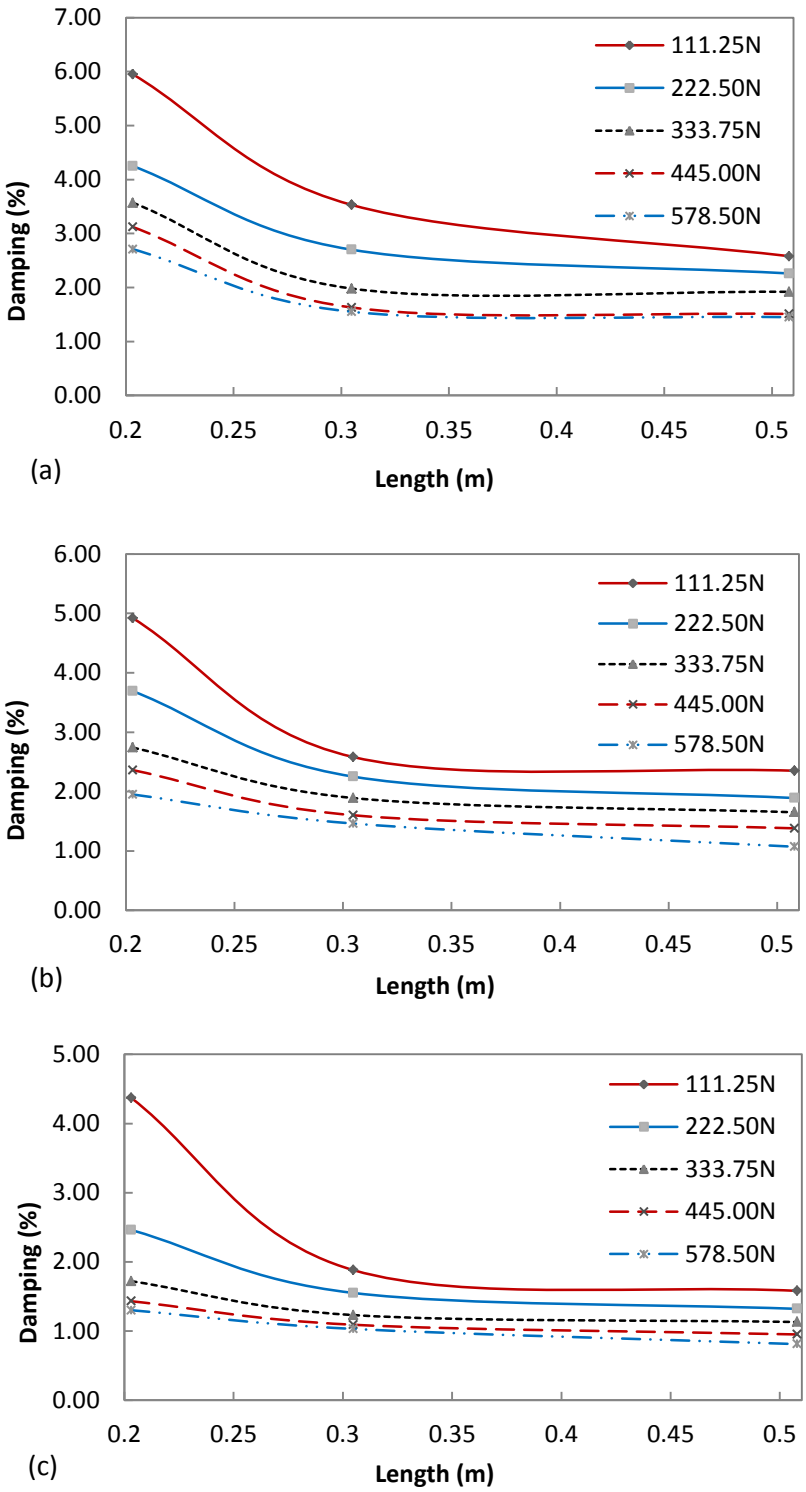

Figure 3.4.2.2 Cable damping versus length for cables at 4℃ (a) 20.71turns/m (b) 41.42turns/m (c) 62.13turns/m cables

3.4.2.3 Carbon Fiber Cables Tested in a Vacuum Chamber

Fig. 3.4.2.3 presents the damping for cables tested in a vacuum chamber, with different length and construction. From Fig.3.4.2.3, the variation of damping with length shows the same trend as the cables tested at room temperature and at a temperature of 4℃. A longer cable has a lower damping, and a quicker decrement is presented for a shorter cables.

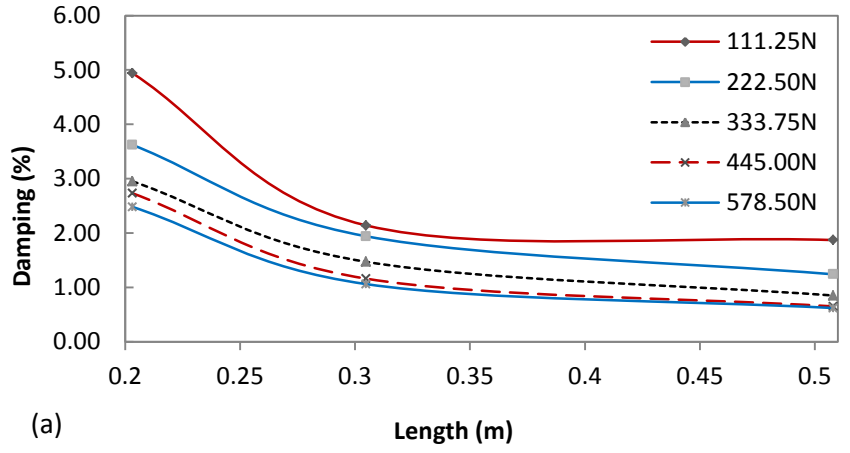

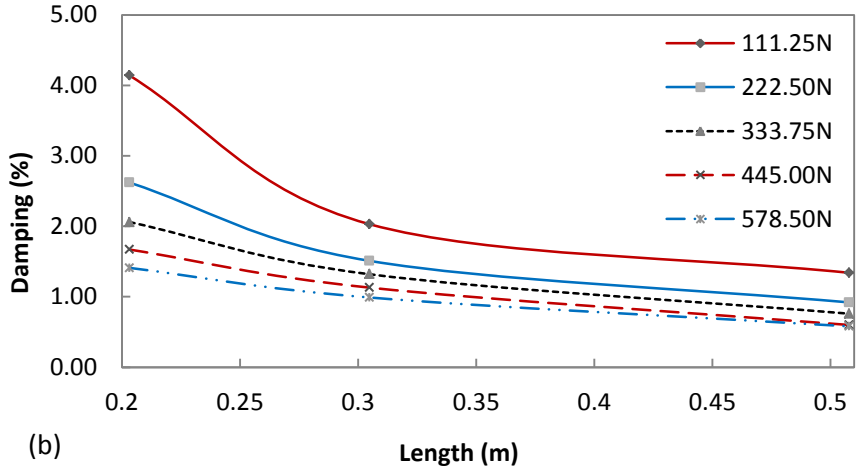

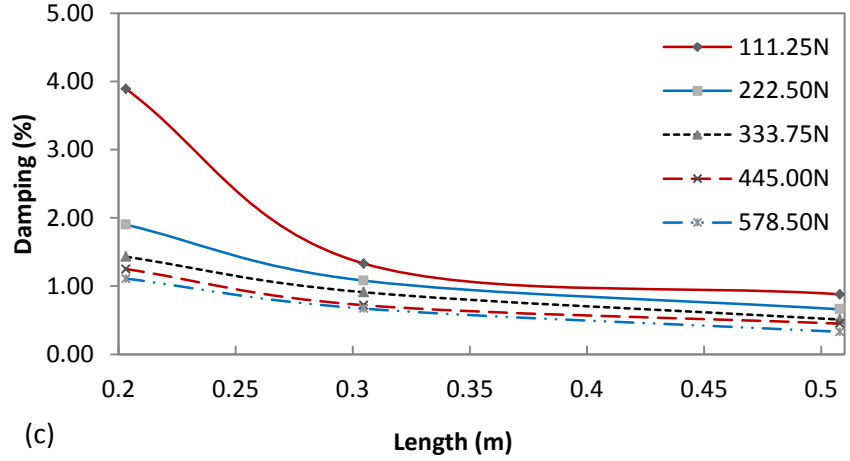

Figure 3.4.2.3 Cable damping versus length for cables in a vacuum chamber (a) 20.71turns/m (b) 41.42turns/m (c) 62.13turns/m cables

In summary, the cable vibration damping decreases as length increases up to a point (0.3m) beyond which it is unaffected by cable length.

3.4.3 Effect of Cable Lay Angle

Review of the literature reveals that cable lay angle can significantly affect cable behavior. Experimental and theoretical results, such as Hobbs and Raoof (1984), Labrosse and Conway (1999), Raoof and Davies (2006) showed that cable damping increases as lay angle decreases. (Raoof, 1997) demonstrated that most of the overall characteristics of large-diameter spiral strands are dominated by the magnitude of the lay angles in various layers. Thus, an optimum design of cable damping can be achieved by controlling the magnitude of lay angle. However, such changes will inevitably affect other cable characteristics.

The lay angle of a cable represented the construction of the cable. Here, we defined that the construction of a cable as the number of turns per meter. Three constructions of cables, 20.71turns/m, 41.42turns/m and 62.13turns/m, were considered in the tests. Untwisted strands were first fixed at one end, and then twisted the other end of the strands to form cables with different constructions.

3.4.3.1 Carbon Fiber Cables Tested at Room Temperature

The cable damping versus cable construction (turns/m) is plotted in Fig. 3.4.3.1. From Fig. 3.4.3.1, it is noticed that as the number of twists in the cable increases, damping decreases. In other words, damping decreases as the lay angle increases, which agrees with the conclusions by Hobbs and Raoof (1984), Labrosse and Conway (1999), Raoof

and Davies (2006). This could be because as the number of twist increases, the cable becomes tighter, hence reducing the movement and friction internal to the cable.

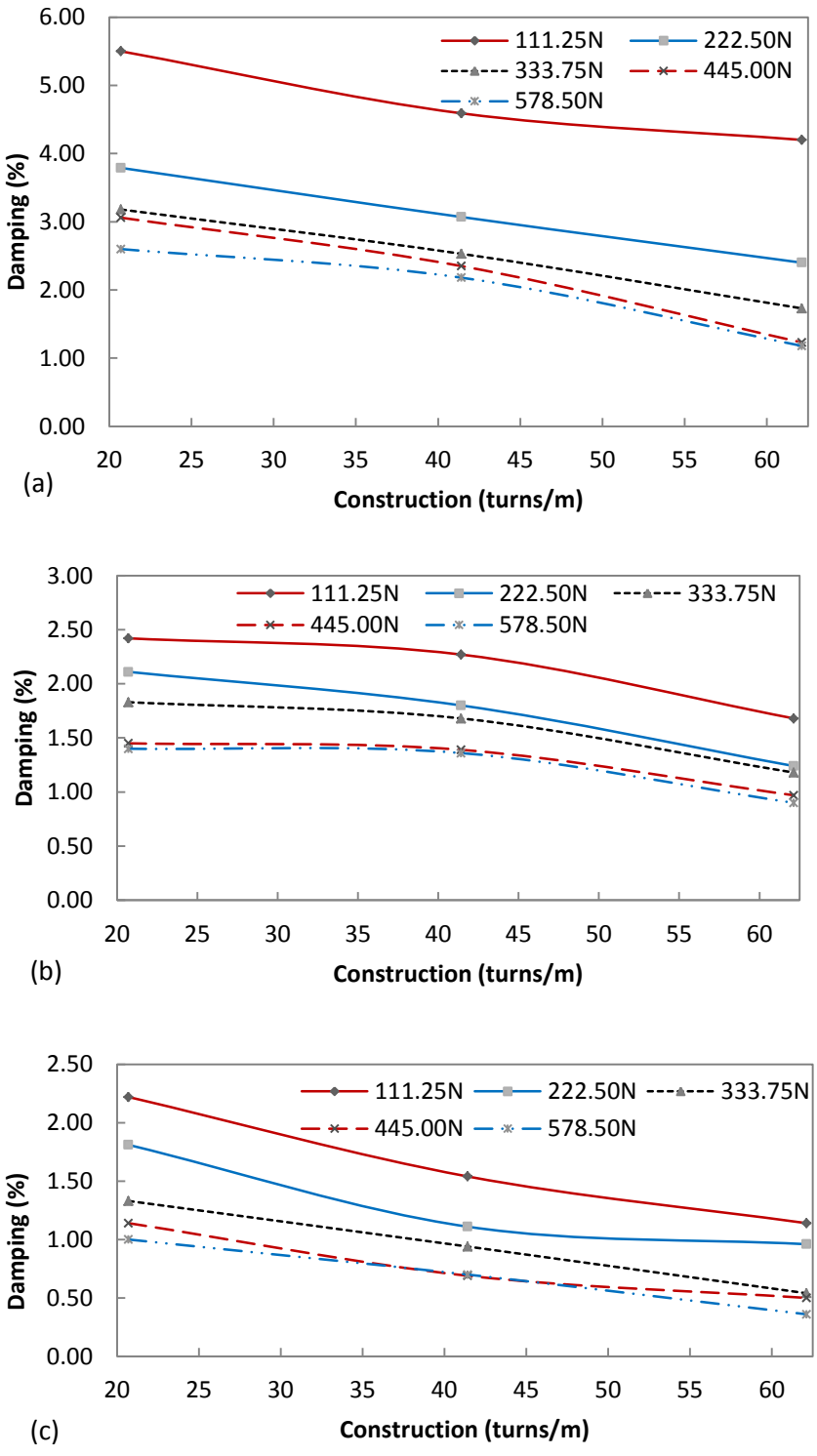

Figure 3.4.3.1 Cable damping versus cable construction for cables at room temperature (a) 0.2032m (b) 0.3048m (c) 0.5080m cables

3.4.3.2 Carbon Fiber Cables Tested at a Temperature of 4℃

Fig. 3.4.3.2 presents the damping versus construction for cables tested at a temperature of 4℃. The plots show that the damping decreases as the number of twists in the cable increases. The cables with greater lay angle exhibit lower damping.

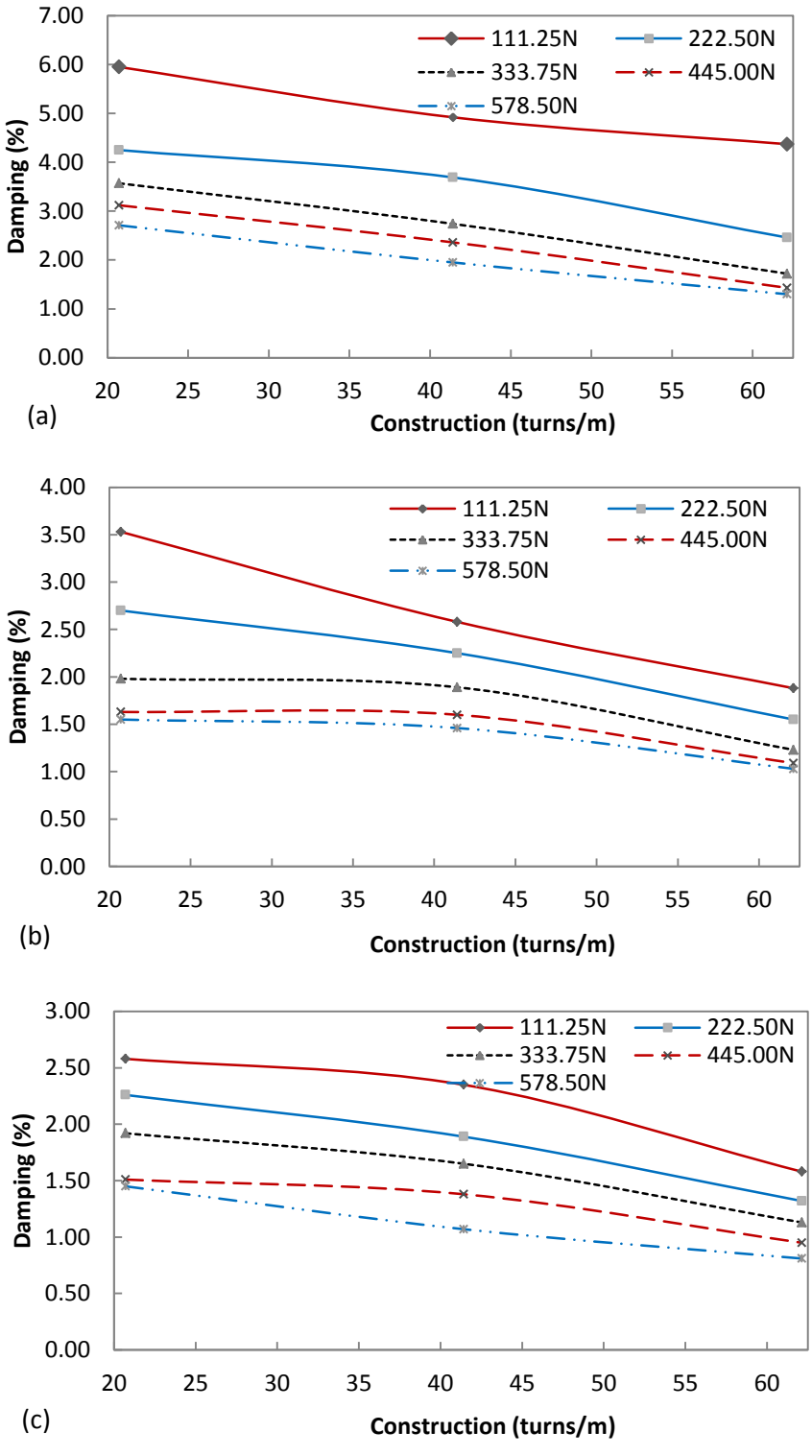

Figure 3.4.3.2 Cable damping versus cable construction for cables at a temperature of 4℃ (a) 0.2032m (b) 0.3048m (c) 0.5080m cables

3.4.3.3 Carbon Fiber Cables Tested in a Vacuum Chamber

Fig. 3.4.3.3 plots the damping versus cable configuration for cables tested in a vacuum chamber. According to the results, the variation of cable damping with lay angle is similar to that of cables tested at temperature of 20℃ and 4℃, the damping decreases as the number of twists in the cable increases.

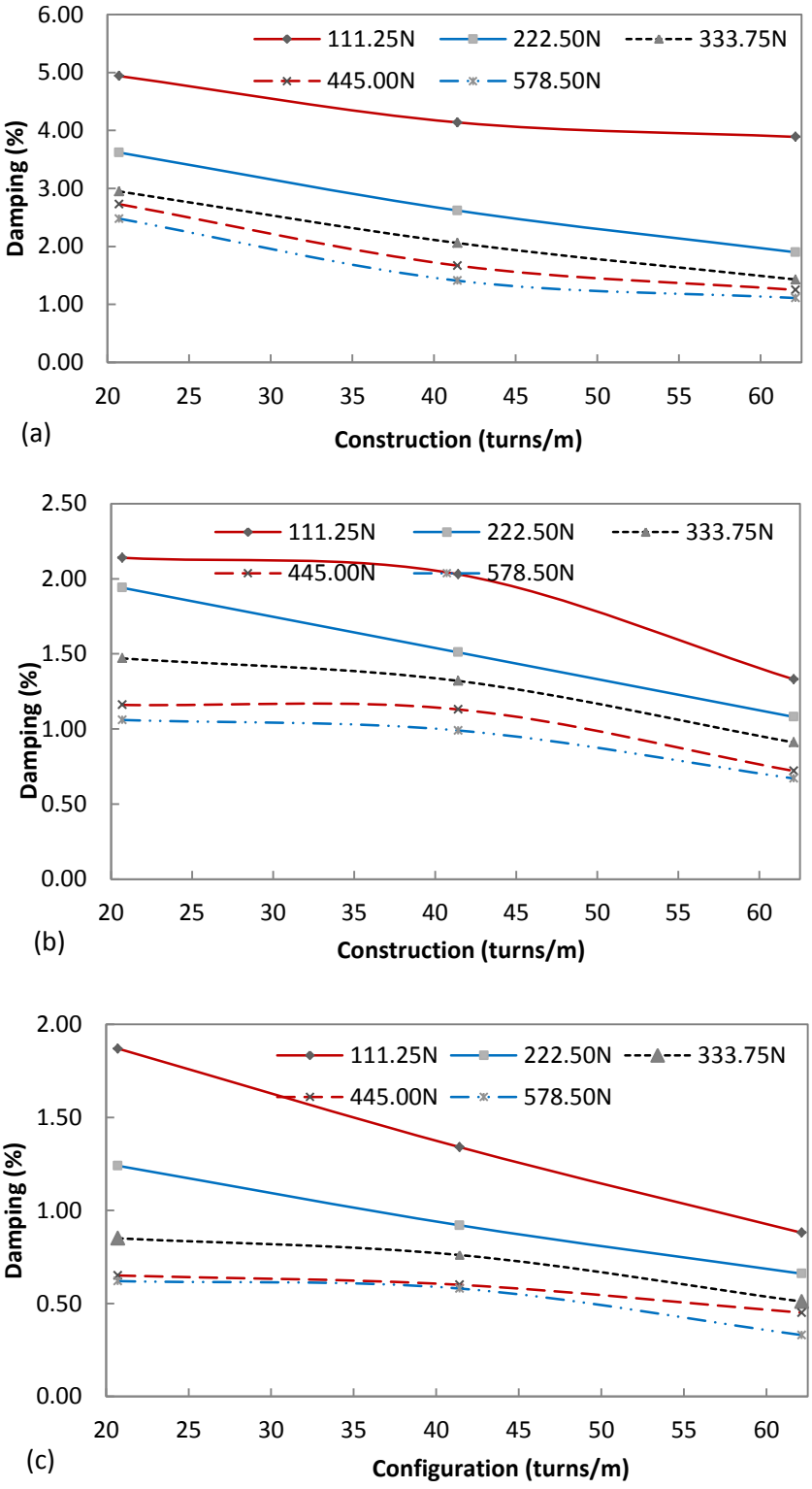

Figure 3.4.3.3 Cable damping versus cable construction for cables in a vacuum chamber (a) 0.2032m (b) 0.3048m (c) 0.5080m cables

In summary, from the tests, it is observed that cable damping increases as lay angle of the cable increases. This could be because as the number of twist increases, the cable becomes tighter, hence reducing the movement and friction internal to the cable.

3.4.4 Effect of Air Pressure

The fluid in which a structure is immersed can provide other damping mechanism. To investigate the effect of air pressure on cable damping, the experimental setup shown in Fig. 3.2.1 was modified to test the carbon fiber cable damping by excluding air from the chamber in the test. The wooden frame in Fig. 3.2.1 was sealed using plastic plates at the top and the bottom (Fig. 3.4.4.3). The foam tape (Fig. 3.4.4.6) was used between the plastic plates and the wooden frame to reduce leakage. A pressure gauge (Fig. 3.4.4.1) was connected to the chamber at the side of the chamber to measure the air pressure, shown as Fig. 3.4.4.4. The vacuum of the chamber (-20 in Hg), was achieved by pumping the air out of the chamber using the pump shown in Fig. 3.4.4.2.

There is a tiny hole at the bottom of the chamber which allows the finishing line (Fig. 3.4.4.5) to pass through. A weight (one pound) was connected to the cable using the fishing line, and the cable vibration was excited by cutting off the fishing line using a scissor and releasing the weight. The test results were compared to the modal damping ratios of cables tested in air to analyze what is the effect of air pressure on damping.

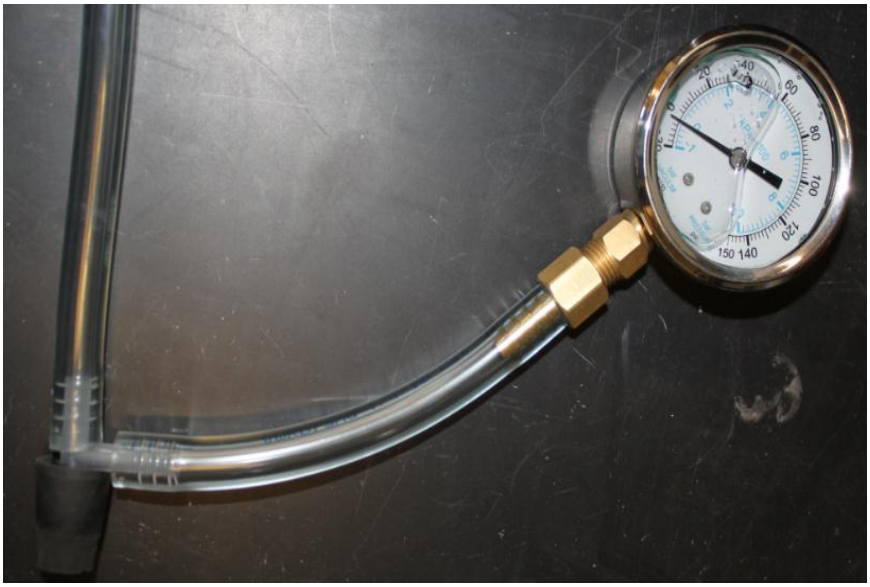

Figure 3.4.4.1 Pressure gauge

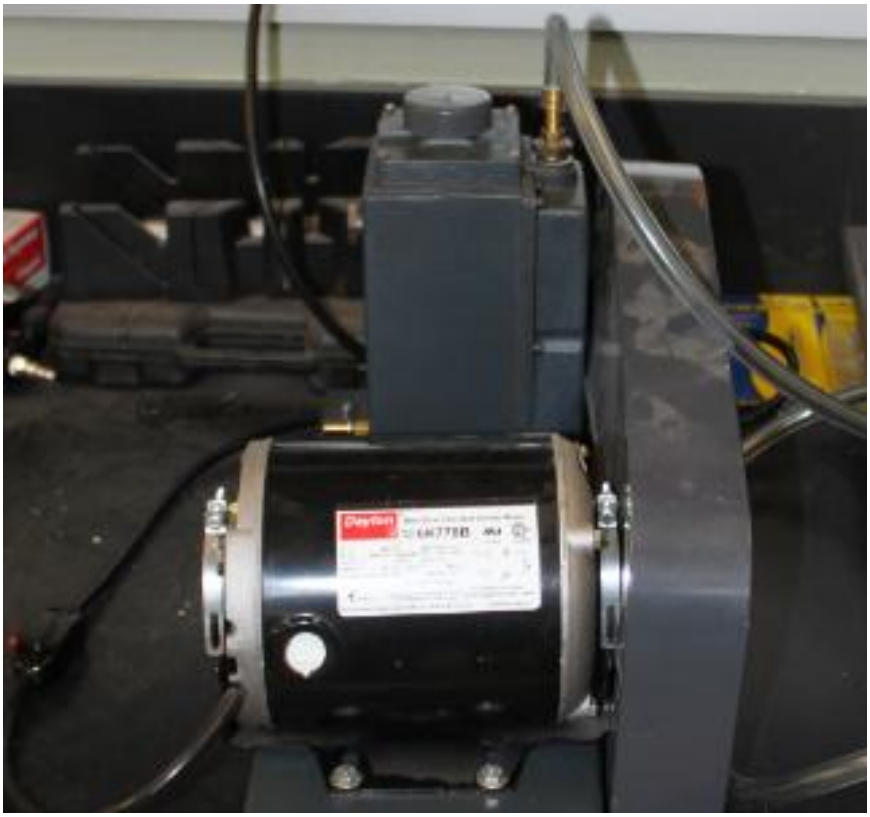

Figure 3.4.4.2 Air pumper

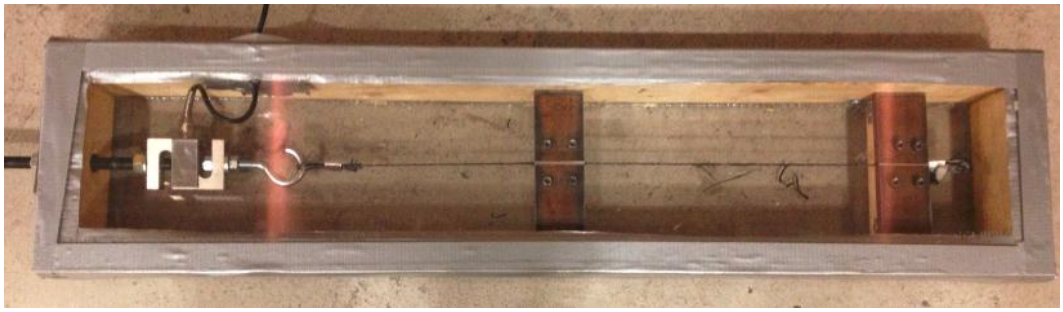

Figure 3.4.4.3 Vacuum chamber

Figure 3.4.4.4 Connection between pressure gauge and chamber

Figure 3.4.4.5 Fishing line

Figure 3.4.4.6 Foam tape

Table 3.4.4.1 lists the damping of a 0.3048m, 20.71turns/m carbon fiber cable tested in the vacuum chamber. The variance of the results is 6.79×10^{-3}, which shows a good repetition of the tests. The comparison of damping in air and in vacuum is shown in Table 3.4.4.2, Table 3.4.4.3 and Table 3.4.4, for 0.2032m, 0.3048m and 0.5080m carbon fiber cables, respectively.

Table 3.4.4.1 Damping in vacuum chamber (0.3048m, 20.71turns/m with 333.75N pretension)

Data No	1	2	3	4	5	6	7
Damping estimated with data recorded by accelerometer at 3/4 of cable length (%)	2.12	2.12	1.99	2.17	2.11	2.23	2.25
Damping estimated with data recorded by accelerometer at 1/5 of cable length (%)	2.10	2.09	1.96	2.1	2.18	2.22	2.20
Damping value of the tested cable	2.14						
Variance	6.79×10^{-3}						

Table 3.4.4.2 Comparison of damping (0.2032m carbon fiber cables)

Tension (N)	Damping for 20.71turns/m cables (%)			Damping for 41.42turns/m cables (%)			Damping for 62.13turns/m cables (%)		
	Normal	Vacuum	Decrement rate (%)	Normal	Vacuum	Decrement rate (%)	Normal	Vacuum	Decrement rate (%)
111.25	5.50	4.94	-10.24	4.59	4.14	-9.85	4.20	3.89	-7.43
222.50	3.79	3.62	-4.38	3.07	2.62	-14.56	2.40	1.90	-20.78
333.75	3.18	2.95	-7.23	2.53	2.06	-18.77	1.73	1.43	-17.51
445.00	3.06	2.73	-10.85	2.35	1.67	-29.02	1.23	1.25	1.46
578.50	2.60	2.48	-4.81	2.18	1.41	-35.46	1.18	1.11	-5.59

Table 3.4.4.3 Comparison of damping (0.3408m carbon fiber cables)

Tension (N)	Damping for 20.71turns/m cables (%)			Damping for 41.42turns/m cables (%)			Damping for 62.13turns/m cables (%)		
	Normal	Vacuum	Decrement rate (%)	Normal	Vacuum	Decrement rate (%)	Normal	Vacuum	Decrement rate (%)
111.25	2.42	2.14	-11.40	2.27	2.03	-10.40	1.68	1.33	-20.71
222.50	2.11	1.94	-7.87	1.80	1.51	-16.06	1.24	1.08	-13.00
333.75	1.83	1.47	-19.51	1.68	1.32	-21.37	1.08	0.91	-15.56
445.00	1.45	1.16	-20.07	1.39	1.13	-18.88	0.97	0.72	-25.46
578.50	1.40	1.06	-24.43	1.36	0.99	-27.11	0.90	0.67	-25.14

Table 3.4.4.4 Comparison of damping (0.5080m carbon fiber cables)

Tension (N)	Damping for 20.71turns/m cables (%)			Damping for 41.42turns/m cables (%)			Damping for 62.13turns/m cables (%)		
	Normal	Vacuum	Decrement rate (%)	Normal	Vacuum	Decrement rate (%)	Normal	Vacuum	Decrement rate (%)
111.25	2.22	1.87	-15.81	1.54	1.34	-12.79	1.14	0.88	-22.46
222.50	1.81	1.24	-31.77	1.11	0.92	-17.57	0.96	0.66	-31.35
333.75	1.38	0.85	-38.26	0.94	0.76	-19.26	0.54	0.51	-6.11
445.00	1.14	0.65	-42.87	0.69	0.60	-12.46	0.50	0.45	-9.20
578.50	1.00	0.62	-37.60	0.70	0.58	-17.29	0.36	0.33	-7.78

Fig. 3.4.4.7 to Fig. 3.4.4.9 showed the comparison of cable vibration damping tested in the vacuum chamber and in air (normal) for 0.2032m, 0.3048m, 05080m carbon fiber cables, respectively. It demonstrated that cable vibration damping decreased as air pressure decreased. Typically, the decrement rate is about 20%, with the maximum of 75%. The damping has a greater decrement when tension is small. This is because the void of the cable is larger when tension is smaller. In addition, the cables with small number of turns/m have greater decrement in damping.

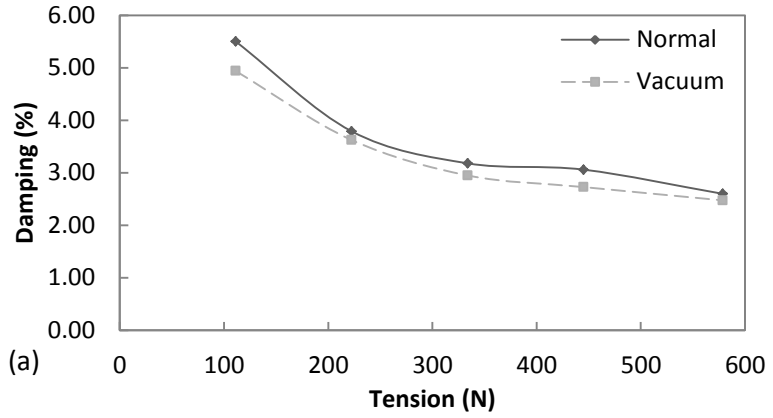

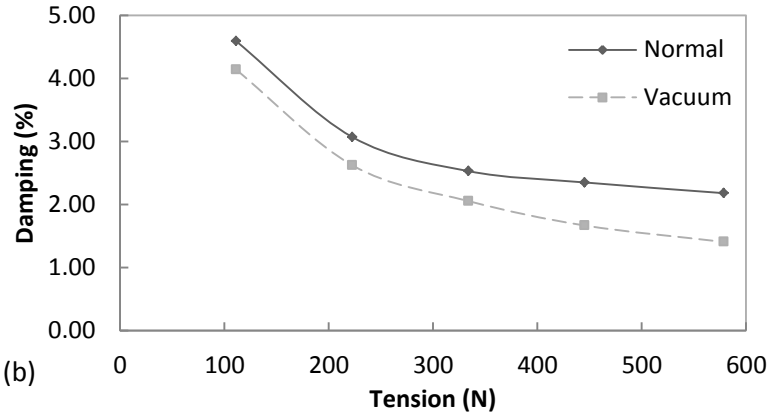

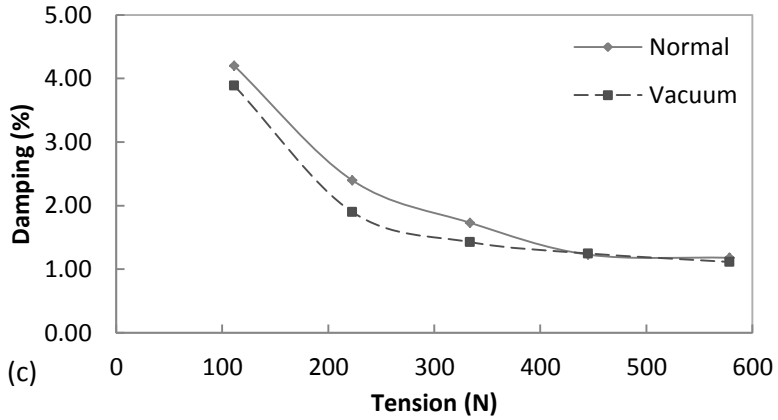

Figure 3.4.4.7 Comparison of damping for 0.2032m carbon fiber cables in air and in vacuum (a) 20.71turns/m (b) 41.42turns/m (c) 62.13turns/m cables

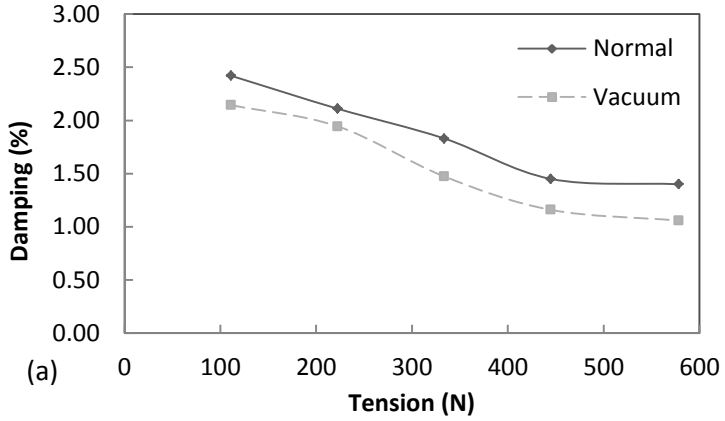

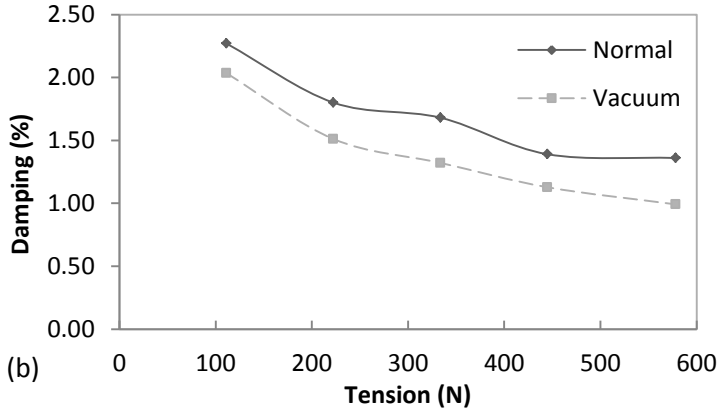

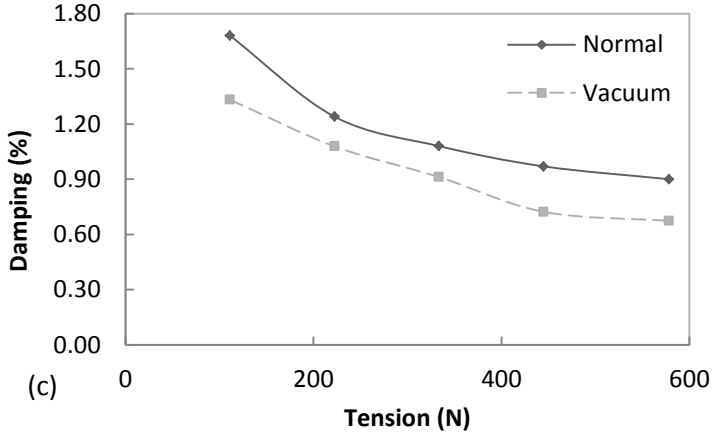

Figure 3.4.4.8 Comparison of damping for 0.3048m carbon fiber cables in air and in vacuum (a) 20.71turns/m (b) 41.42turns/m (c) 62.13turns/m cables

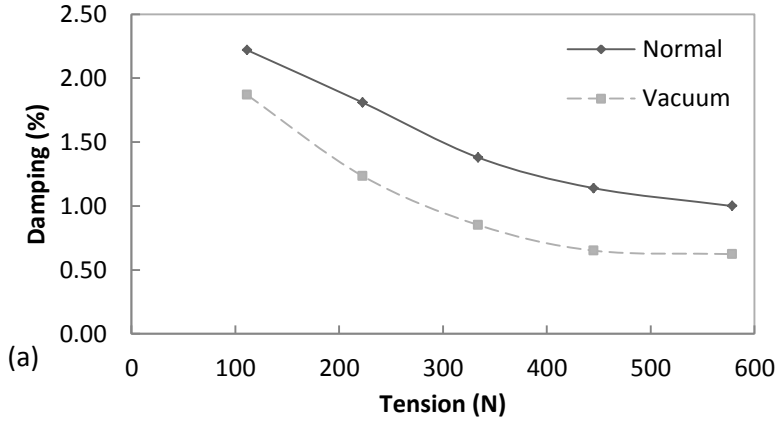

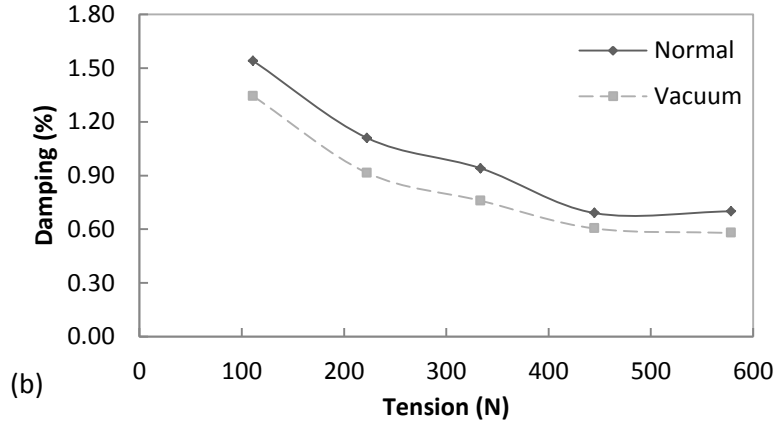

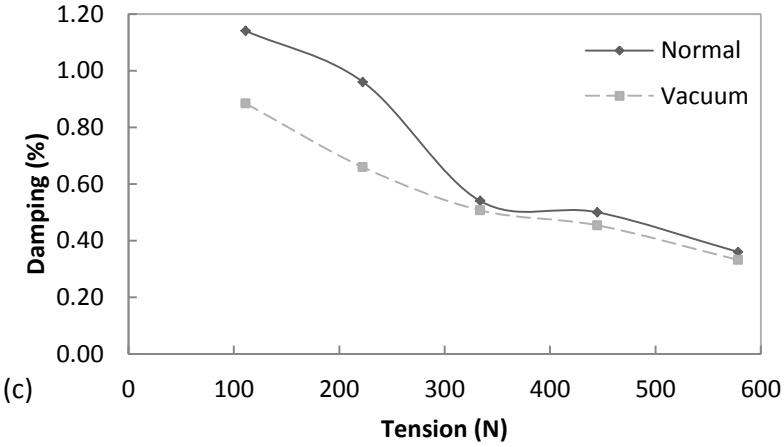

Figure 3.4.4.9 Comparison of damping for 0.5080m carbon fiber cables in air and in vacuum (a) 20.71turns/m (b) 41.42turns/m (c) 62.13turns/m cables

3.4.5 Effect of Support and Test Apparatus

Yamaguchi and Fujino (1988) investigated the effect of support flexibility on cable damping by the free-oscillation of suspended cables under various support conditions. The results showed that damping decreases as the support flexibility increases.

To investigate the effect of the test apparatus, including the support and the clamping system on cable damping, the experimental setup (Fig. 3.2.1) was modified by bracing the cable supports and the corners of the wooden frame, as shown in Fig. 3.4.5.1 and Fig. 3.4.5.2, respectively.

Figure 3.4.5.1 Details of the stiffened support

Figure 3.4.5.2 Details of the stiffened frame corners

A 0.3048m carbon fiber was tested with the new experimental set-up, and the damping was compared to the damping tested using the old experimental set-up (before stiffening). The results were compared in Fig. 3.4.5.3, which indicated that the effect of the test apparatus and fixtures is minimal, and the difference is within 1.5% percent.

Table 3.4.5.1 Vibration damping comparison

Tension (N)	Damping for 41.42 turns/m cables (%)		
	Previous test	After stiffening	Before stiffening
111.25	2.27	2.23	2.30
222.50	1.80	1.74	1.77
333.75	1.68	1.62	1.64
445.00	1.39	1.45	1.42
578.50	1.36	1.34	1.38

Table 3.4.5.2 Vibration frequency comparison

Tension (N)	Frequency for 41.42 turns/m cables (Hz)		
	Previous test	After stiffening	Before stiffening
111.25	280.96	279.30	272.99
222.50	369.40	364.72	360.37
333.75	430.00	415.42	426.55
445.00	500.49	489.86	484.61
578.50	534.65	543.76	545.42

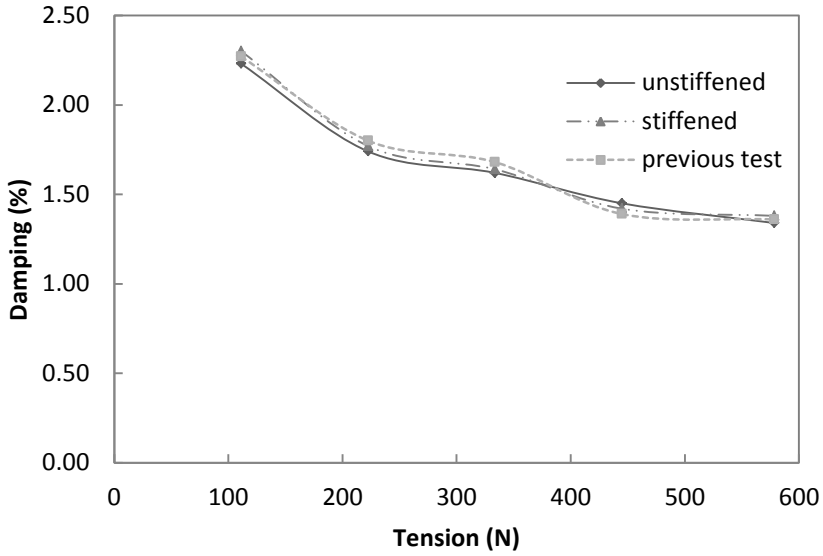

Figure 3.4.5.3 Comparison of damping for cable tested with stiffened and unstiffened setup

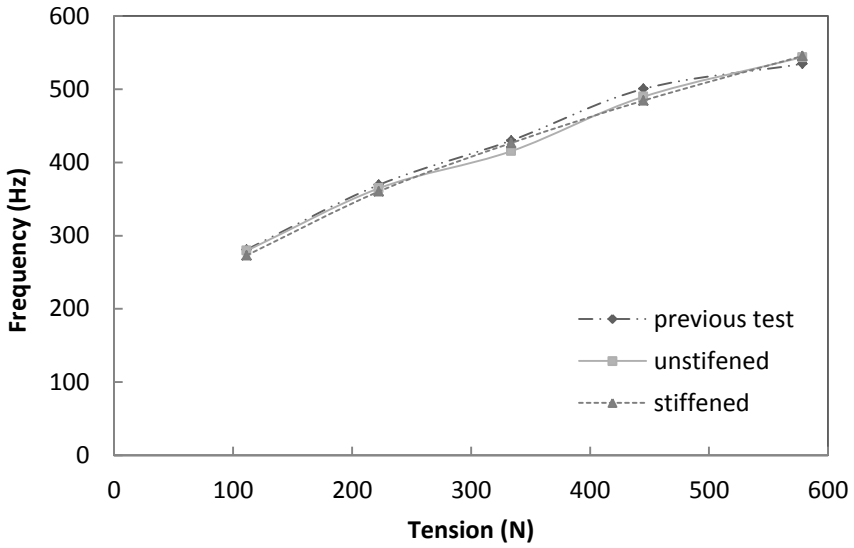

Figure 3.4.5.4 Vibration frequency with tension

In addition, to investigate if the test is repeatable, a 0.3048m, 41.42 turns/m carbon fiber cable was tested using the old experimental setup (before stiffening), and the results were compared to the previous test (test done about one year ago). From the plots in Fig. 3.4.5.3 and Fig. 3.4.5.4, the results indicated that the difference is within 1.5%, which showed that the test is repeatable, and the results are reliable.

3.4.6 Effect of Temperature

Temperature is usually considered as one of the most important environmental factors affecting mechanical properties of composite materials. Due to the motion of the space structure and sun, the cable structures will be subjected to a large variation of temperature in space. Thus, it is necessary to investigate the effect of temperature on cable damping. The available research is very scarce. The objective of these tests is to investigate the effect of temperature on damping and frequency properties of carbon fiber cables.

For our experiments carbon fiber cables of different length and different configuration were tested at room temperature (20℃) and in a freezer room at the University of New Mexico. The temperature of the freezer room was kept at 4℃. The control system for the room temperature is shown in Fig. 3.4.6.1.

Figure 3.4.6.1 Control system of the freezer room

Table 3.4.6.1, Table 3.4.6.2 and Table 3.4.6.3 list the cable modal damping ratios at room temperature and at a temperature of 4°C. Corresponding plots are shown in Fig. 3.4.6.2 to Fig. 3.4.6.3. It is observed that cable damping increases as the ambient temperature decreases, and the increment is more significant for a longer cable. Typically, for the 0.2032m long carbon fiber cables tested at 4℃, the damping increment is about 1-10% (maximum, 20.16%); and for cables in the length of 0.3048m, the damping increment is about 10%-15% (maximum, 45.87); while the cable in length of 0.5080m, the damping

increment is about 30-70% (maximum 124%). This increment could be due to the increase of moisture of the cable.

Table 3.4.6.1 Comparison of damping for 0.2032m cables at different temperatures

Tension (N)	Damping for 20.71turns/m cables (%)		Damping for 41.42turns/m cables (%)		Damping for 62.13turns/m cables (%)	
	20 ^{o}C	4 ^{o}C	20 ^{o}C	4 ^{o}C	20 ^{o}C	4 ^{o}C
111.25	5.50	5.95	4.57	4.92	4.20	4.37
222.50	3.79	4.25	3.07	3.69	2.40	2.46
333.75	3.18	3.57	2.53	2.74	1.63	1.72
445.00	3.06	3.12	2.35	2.36	1.36	1.43
578.50	2.60	2.71	1.94	1.95	1.18	1.30

Table.3.4.6.2 Comparison of damping for 0.3408m cables at different temperatures

Tension (N)	Damping for 20.71turns/m cables (%)		Damping for 41.42turns/m cables (%)		Damping for 62.13turns/m cables (%)	
	20 ^{o}C	4 ^{o}C	20 ^{o}C	4 ^{o}C	20 ^{o}C	4 ^{o}C
111.25	2.42	3.53	2.22	2.58	1.68	1.88
222.50	2.11	2.70	1.83	2.25	1.34	1.55
333.75	1.72	1.98	1.64	1.89	1.08	1.23
445.00	1.45	1.63	1.39	1.63	0.97	1.09
578.50	1.40	1.55	1.36	1.46	0.90	1.03

Table.3.4.6.3 Comparison of damping for 0.5080m cables at different temperatures

Tension (N)	Damping for 20.71turns/m cables (%)		Damping for 41.42turns/m cables (%)		Damping for 62.13turns/m cables (%)	
	20 ^{o}C	4 ^{o}C	20 ^{o}C	4 ^{o}C	20 ^{o}C	4 ^{o}C
111.25	2.22	2.58	1.54	2.35	1.14	1.58
222.50	1.81	2.26	1.11	1.89	0.96	1.32
333.75	1.38	1.92	0.94	1.65	0.55	1.13
445.00	1.14	1.51	0.68	1.38	0.50	0.85
578.50	1.00	1.15	0.70	1.07	0.36	0.81

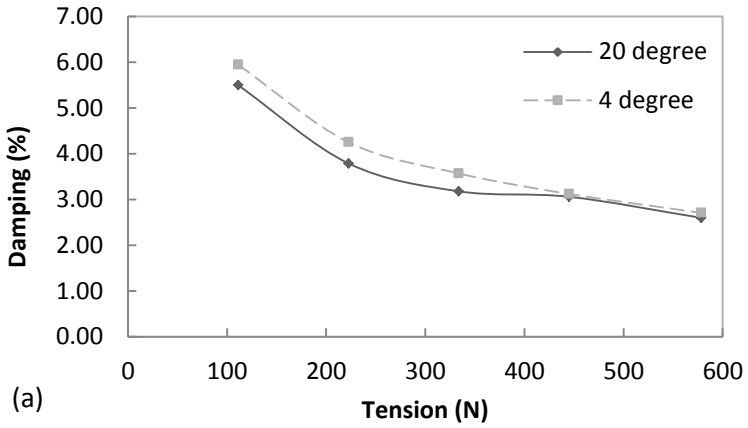

(a)

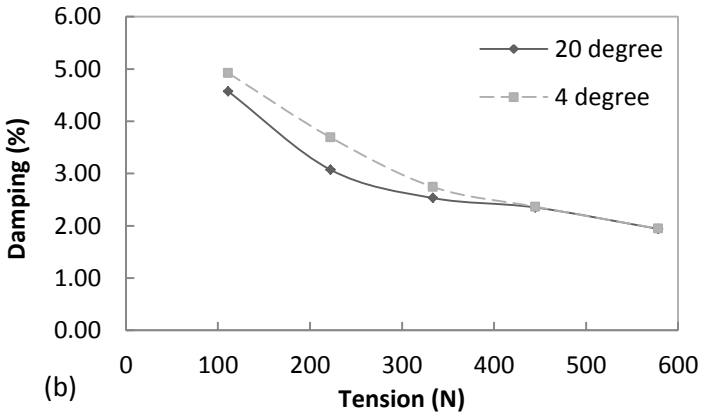

(b)

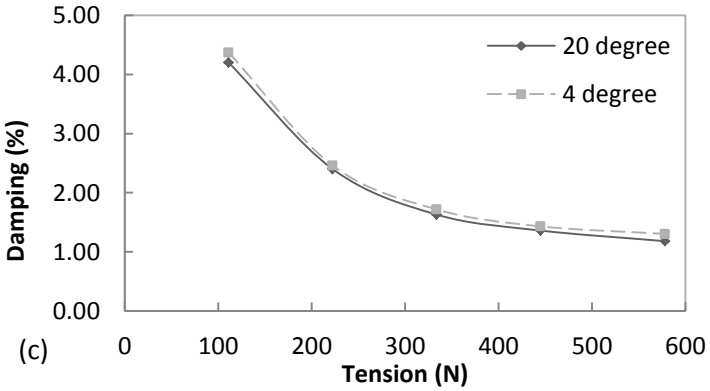

(c)

Figure 3.4.6.2 Comparison of damping for 0.2032m cables at different temperature (a) 20.71turns/m (b) 41.42turns/m (c) 62.13turns/m cables

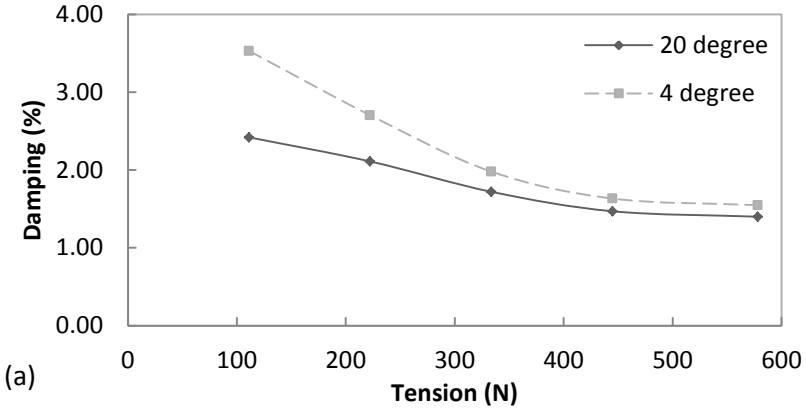

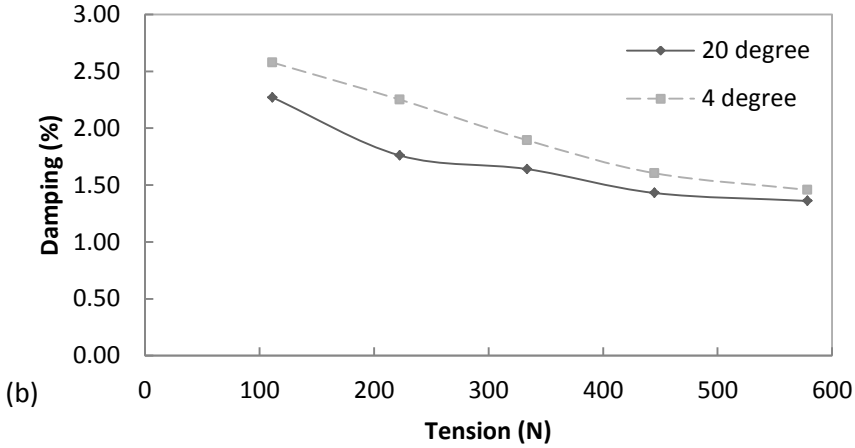

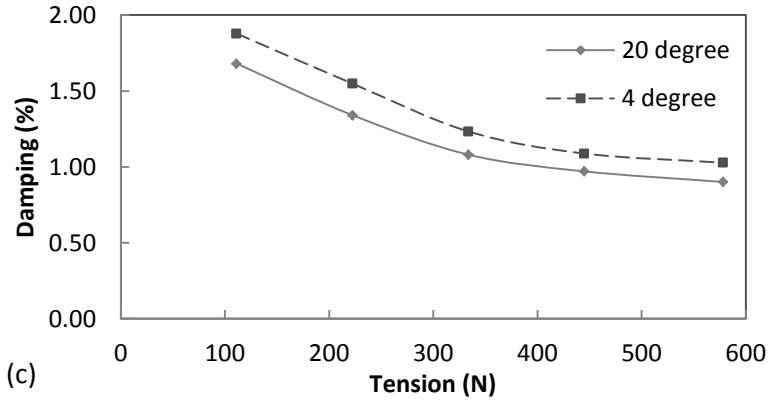

Figure 3.4.6.3 Comparison of damping for 0.3048m cables at different temperature (a) 20.71turns/m (b) 41.42turns/m (c) 62.13turns/m cables

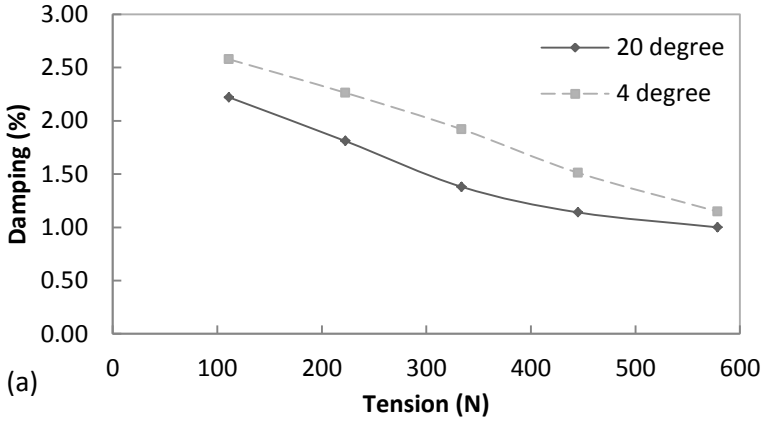

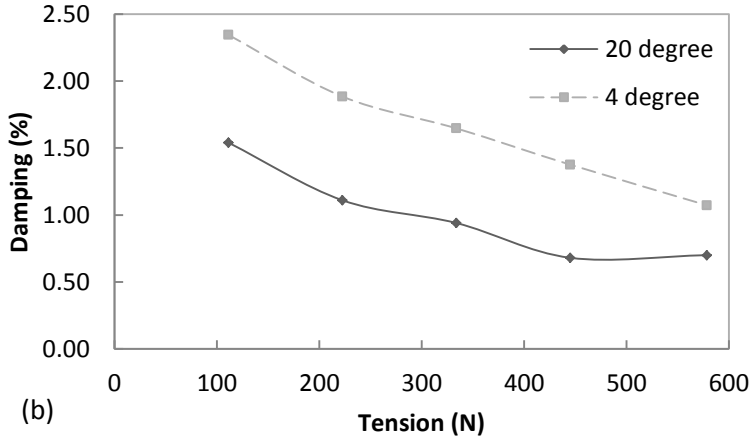

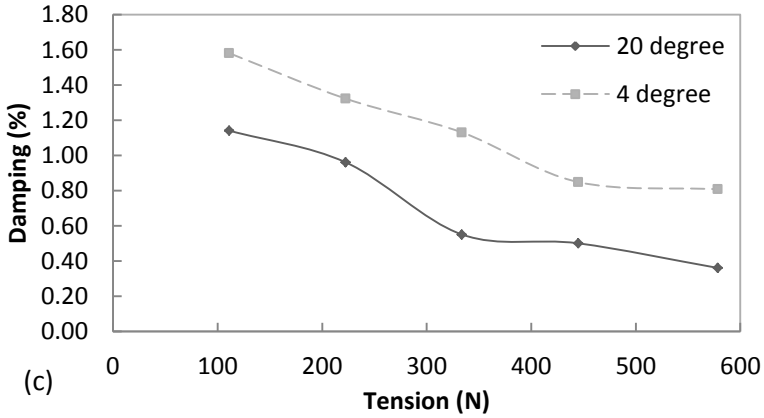

Figure 3.4.6.4 Comparison of damping for 0.5080 cables at different temperature (a) 20.71turns/m (b) 41.42turns/m (c) 62.13turns/m cables

3.4.7 Effect of Sensor Mass

The effect of sensor mass on cable damping was studied by testing cables of length 0.3048m in two different configurations, with or without the second accelerometer at 1/5 length.

The comparison of damping for cables tested in the two different configurations is presented in Table 3.4.7.1, and the comparison of vibration frequency is presented in Table 3.4.7.2. Fig. 3.4.7.1 shows that without the additional mass of the second accelerometer, the damping values are slightly lower; While there is a small increase in damping value when the second accelerometer is present, this difference (typically 1-4% range, with a maximum of 10%) is very small compared to the large (factor of 2-4) differences due to variation of tension, cable length, and # of turns shown in the previous sections, which is the focus of this work. The small increment of damping due to the additional mass could be explained as: the additional mass displays movements which are contrary to those of the cable, and the contrary movement causes inertial forces that compensate the cable movements by depriving the vibration energy from the system, and lead to the increment of damping.

Table 3.4.7.1 Comparison of damping for cables with one and two accelerometers

Tension (N)	Damping for 20.71turns/m cables (%)		Damping for 41.42turns/m cables (%)		Damping for 62.13turns/m cables (%)	
	two accelerometers	one accelerometer	two accelerometers	one accelerometer	two accelerometers	one accelerometer
111.25	2.42	2.45	2.27	2.24	1.68	1.74
222.50	2.11	1.92	1.80	1.65	1.34	1.41
333.75	1.80	1.76	1.68	1.55	1.08	1.09
445.00	1.47	1.38	1.39	1.38	0.97	0.99
578.50	1.40	1.24	1.36	1.19	0.90	0.88

Table 3.4.7.2 Comparison of vibration frequency for cables with one and two accelerometers

Tension (N)	Frequency for 20.71turns/m cables (Hz)		Frequency (Hz)- 41.42turns/m		Frequency(Hz)- 62.13turns/m	
	two accelerometers	one accelerometer	two accelerometers	one accelerometer	two accelerometers	one accelerometer
111.25	309.87	322.66	280.96	272.91	266.82	280.70
222.50	392.63	393.74	369.02	376.11	360.33	359.81
333.75	458.67	476.41	430.00	456.46	418.68	413.82
445.00	517.74	532.12	500.49	513.81	485.62	491.92
578.50	554.68	562.64	534.65	571.83	502.50	529.47

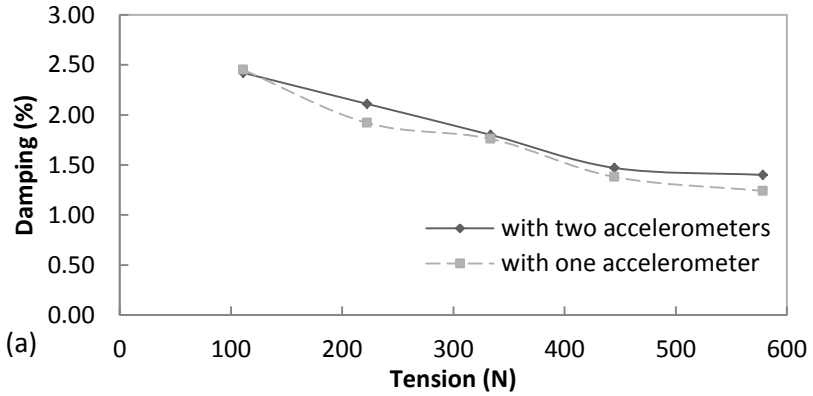

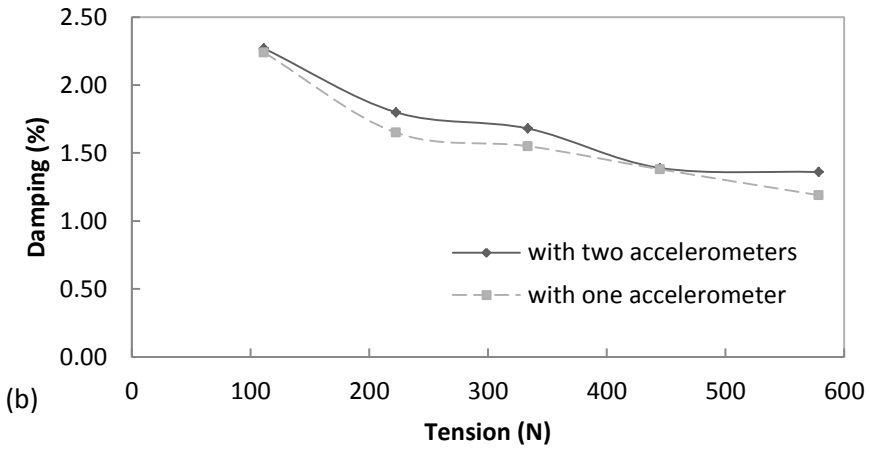

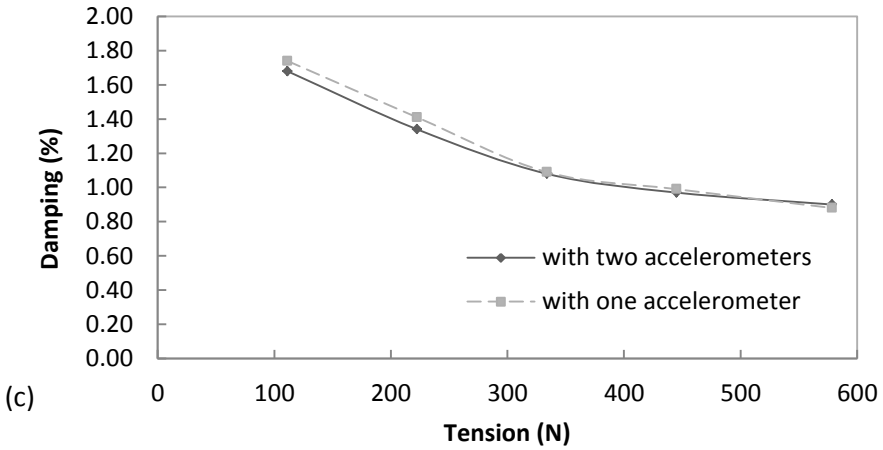

Figure 3.4.7.1 Comparison of damping for 0.3048m cables with one accelerometer and two accelerometers

(a) 20.71 turns/m (b) 41.42 turns/m (c) 62.13 turns/m cables

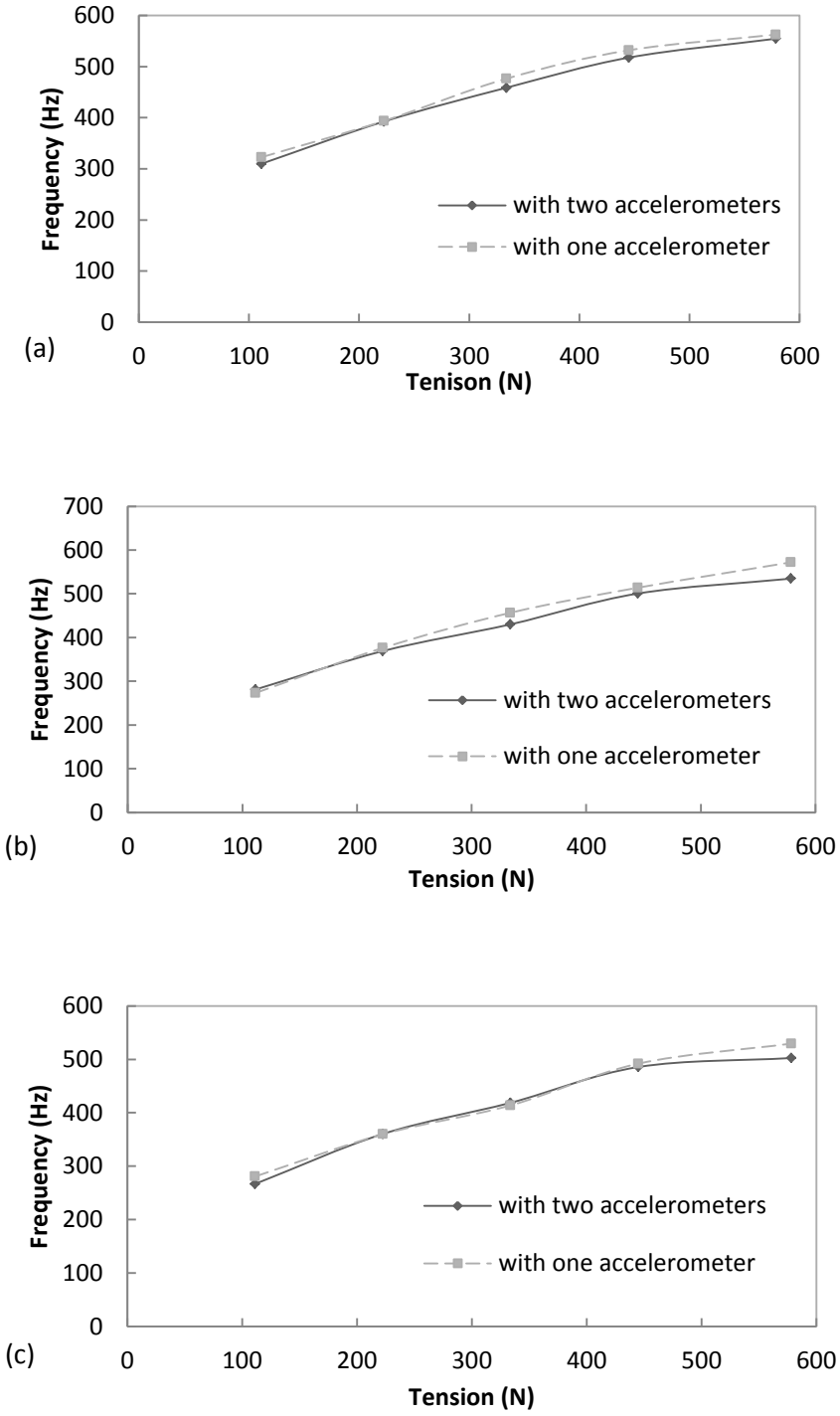

Figure 3.4.7.2 Comparison of vibration frequency for 0.3048m cables with one accelerometer and two accelerometers (a) 20.71 turns/m (b) 41.42 turns/m (c) 62.13 turns/m cables

In addition, damping for 0.3048m, 41.42 turns/m carbon fiber cables tested at room temperature (test 1), at temperature of 4℃ (test 2), in vacuum (test 3), with stiffened experimental apparatus (test 4), with one accelerometer (test 5) was compared in Fig. 3.4.7.3. Typically, it shows that the order of decreasing effect on cable damping is: the vacuum condition, the temperature, the additional sensor mass, and the stiffness of the experimental setup.

Table 3.4.7.3 Damping of a 41.42 turns/m, 0.3048m carbon fiber cable tested under different conditions

Tension (N)	Test 1	Test 2	Test 3	Test 4	Test 5	(2-1)/1 (%)	(3-1)/1 (%)	(4-1)/1	(5-1)/1 (%)
111.25	2.27	2.58	2.03	2.30	2.24	13.66	-10.57	1.32	-1.32
222.50	1.80	2.25	1.51	1.77	1.65	25.00	-16.11	-1.67	-8.33
333.75	1.68	1.89	1.32	1.64	1.55	12.50	-21.43	-2.38	-7.74
445.00	1.39	1.60	1.13	1.42	1.38	15.11	-18.71	2.16	-0.72
578.50	1.36	1.46	0.99	1.38	1.19	7.35	-27.21	1.47	-12.50

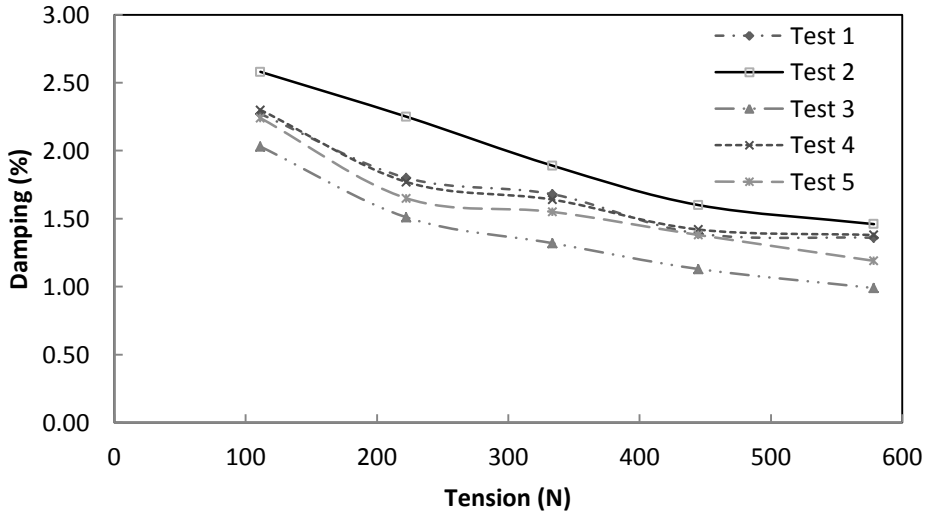

Figure 3.4.7.3 Damping for a 41.42 turns/m, 0.3048m carbon fiber cable under different conditions

3.5 Conclusions

In this chapter, an experimental setup was provided to measure the cable vibration damping. Cables in different length, different configuration, ambient temperature (20℃ and 4℃) and air pressure (normal and vacuum) were tested under five different cable tensile forces. The effects of different factors on damping were analyzed and discussed, and the following conclusions have been reached:

a) For carbon fiber and stainless steel cables tested under different tension forces (111.25N, 222.50N, 333.75N, 445.00N and 578.50N), damping decreases as tension increases within the tension force considered in this research. The same conclusion was obtained by Seppa (1971), Ramberg and Griffin (1977), Raoof (1993b), Xu et al., (1998, 1999), Kim and Jeong (2005), Zheng et al., (2003), and Barbieri et al., (2004a, 2004b) et al.; the decrease in damping is caused by the increased cable interwire contact force, which made the occurrence of interwire slippage getting harder, and causes lower energy dissipation. For carbon fiber cables in the length of 0.2032m, damping has a significant decrement as tension increases when tension is less than a certain value (say 222.50N). But this significant variation is not noticed for the 0.3048m and 0.5080m carbon fiber cables, which indicates that this is attributable to the end effect for short cables;

b) Cables in three different lengths (0.2032m, 0.3048m and 0.5080m) were tested, typically, damping decreases as length increases. A significant decrement in damping was observed initially as length increases when length is less than about

0.3m, subsequently the decrement is slow or the damping has a tendency to be unaffected by length;

c) Carbon fiber cables in three different configurations (20.71turns/m, 41.42turns/m and 61.23turns/m) were tested, as the number of turns/m increases, damping decreases, in other words, as lay angle of the cable increases, damping decreases. The conclusion is the same as that of steel cables tested by Hobbs and Raoof (1984), Labrosse and Conway (1999), Raoof and Davies (2006) et al., and this could be because as the number of twist increases, the cable becomes tighter, and reducing the movement and friction internal to the cable;

d) The carbon fiber cables tested in vacuum presented a typically 20% lower damping than the cables tested in air. For cables in the length of 0.2032m, a significant decrement of cable damping was noticed when the applied tension is less than a certain value (say 222.5N). Typically, greater decrement for cables with small tension and small number of turns/m was noticed;

e) The stiffness of the test apparatus and the supports were adequate and did not significant influence the test results;

f) A lower ambient temperature gives a higher cable damping, and the variation is more for a longer cable;

g) The additional sensor mass increases cable damping, but the effect is minimal, comparing with the effects of tension, configuration and temperature on damping.

h) Rayleigh damping factor α initially increases as tension increases, and then decreases, and damping factor β decreases as tension increases.

Chapter 4

Finite Element Simulation of Cable Vibration

In this chapter, first, previous research on cable analysis using the Finite Element Method (FEM) is reviewed. Then, vibration frequency and the time history response of carbon fiber cable are obtained using the FEM-based modal analysis and transient analysis in ANSYS13.0 using COMBIN14 and MSASS21 elements. The FEM analysis results are then compared with the theoretical and experimental ones.

4.1 Review of Literature in FEM Analysis of Cables

Carlson and Kasper (1973) built a simplified model for armored cables using the finite element method. Then, Cutchins et al. (1987) studied a cable damping isolator using the finite element method. Yamaguchi (1992) analyzed a cable–tie system using the finite element method. Chiang (1996) modeled a small length of single strand cable for geometric optimization purposes, however, a large number of elements were required for an accurate modeling, and the computational cost is too expensive. To decrease the computational cost, Jiang et al., (1999) provided a concise finite element model by considering the structural and loading symmetries. In this analysis, the contacts between the core and helical wires were simulated using surface contact elements. However, while the usage of the surface-to-surface contact can provide more accurate results, it is time consuming. Armin and Habib (1998) applied the finite difference method to consider the

effect of cable tension, bending stiffness and end conditions on cable vibration. Nawrocki and Labrosse (2000) established a finite element model of a simple straight wire rope strand to study the interwire motions. All the possible cases of interwire contacts were studied, and the results showed that rolling and sliding have no effect on the overall behavior of cables in axial loading, and the cable response was governed by the interwire pivoting. Wu et al., (2006) using cable finite elements and the Rayleigh element damping studied the parametric vibration of stay cables of cable-stayed bridges. Casciati and Ubertini (2007) established a nonlinear finite element model to simulate the vibration of shallow cables and demonstrated the capability to enforce semi-active control using tuned-mass dampers. Ghoreishi et al., (2007) determined the validity domain of analytical models of synthetic wire rope and steel strand using 3D finite element model. Sometimes, the accurate mechanical cable damping models which considered the flexural hysteresis between cable strands are not useful towards large-scale engineering applications because of the complex mathematical solution. Moreover, it is difficult to implement the theoretical model in the finite element simulation. To address these difficulties, Zhu and Meguid (2006) developed a framework and numerical tool using the curved beam element to predict the dynamic response of low tension cable systems. The term ‘low tension cable’ refers to a class of cable systems where the cable is subjected to small and/or dynamically fluctuating tension which may vanish anywhere along the cable. Zhu and Meguid (2007) modeled slack wire cables using curved beam element with large displacement and rotation, and simulated the damping as homogenized Rayleigh damping in the nonlinear finite element simulation. The finite element prediction of the cable motion agrees well with their experimental measurement.

In summary, though different finite element models have been established to investigate cable behavior, most of the available cable analysis using FEM focuses on the static behavior of steel cable, the investigation of cable dynamic behaviors and cable damping using FEM is very scarce. It is the objective of this work to provide a simple but effective method to simulate the cable vibration and damping, and to compare the results against our experiments.

4.2 Finite Element Analysis of Cable Vibration

In this dissertation, the modal analysis was implemented to compute the vibration frequency and the transient analysis was used to determine the time history responses of the carbon fiber cable.

In the modal analysis and the transient analysis, a simple straight carbon fiber cable was modeled using the COMBIN14 and the MASS21 elements, as shown in Fig. 4.2.1 and Fig. 4.2.2, respectively. The COMBIN14 element was chosen as a longitudinal spring damper, which is a uniaxial tension-compression element with up to three degrees of freedom at each node: translations in the nodal x, y, and z directions. No bending or torsion is considered. Because the spring damper element has no mass, additional mass elements are needed. The mass was added by using the MASS21 elements, which are point elements having up to six degrees of freedom: translations in the nodal x, y, and z directions and rotations about the nodal x, y and z axes.

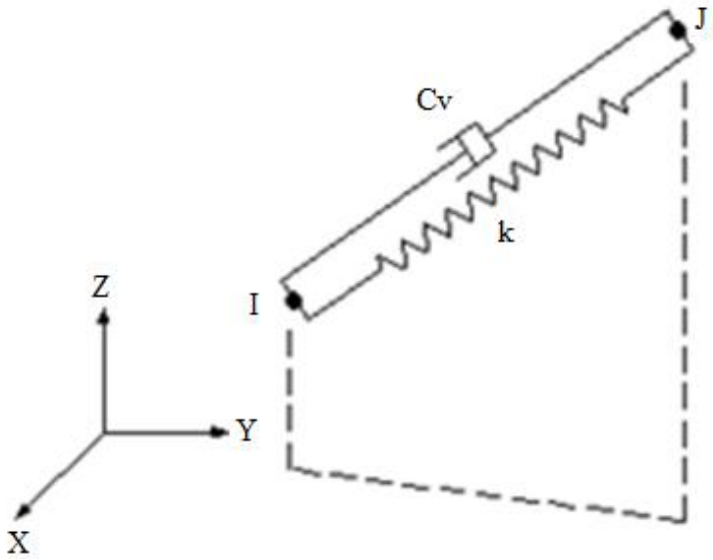

Figure 4.2.1 COMBIN14 Spring-Damper (ANSYS help)

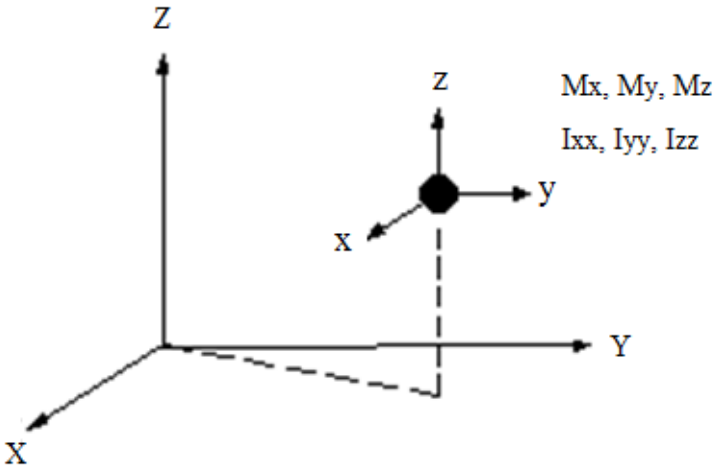

Figure 4.2.2 MASS21 Structural Mass (ANSYS help)

4.2.1 Modal Analysis

Modal analysis of cables was conducted to determine the natural vibration frequency. 20.71 turns/m carbon fiber cables in different length (0.2032m, 0.3048m, and 0.5080m)

were analyzed under different tensile force (111.25N, 222.50N, 333.75N, 445.00N and 578.50N), and the results were compared with the theoretical results and the experimental results.

The loads in the FEM analysis were defined and applied in the same order as in the experiments. First, the left end of the cable was constrained in all translation and rotation, and then a tension was applied at the left end of the cable. After applying tensile force, the right end of the cable was fixed. A 0.3048m carbon fiber cable was meshed with 60 COMBIN14 elements and 59 MASS21 elements. Fig. 4.2.3 gives a finite element representation of the cable.

Figure 4.2.3 Finite element representation of a carbon fiber cable

Table 4.2.1.1, Table 4.2.1.2 and Table 4.2.1.3 list the vibration frequencies from the finite element analysis, the theoretical analysis for a taut string and the tests for 0.2032m, 0.3048m and 0.580m carbon fiber cables, respectively. In the previous study (Irvine, 1981, Kashani, 1989), the first circular natural frequency of a taut string is given by Eq. (4-1):

$$\omega_1 = \frac{\pi}{l}\sqrt{\frac{H}{m}} \tag{4-1}$$

Where: l is the length of the cable, H is the tension, and m is the mass per unit length of the cable.

Table 4.2.1.1 Vibration frequency from different methods (0.2032m, 20.71 turns/m carbon fiber cable)

Tension (N)	Theoretical results (Hz)	Experimental results (Hz)	FEM Analysis results (Hz)
111.25	375.78	365.71	396.24
225.00	534.41	517.79	560.37
333.75	650.88	625.85	686.31
445.00	751.57	694.65	792.48
578.50	856.92	797.60	903.57

Table 4.2.1.2 Vibration frequency from different methods (0.3048m, 20.71 turns/m carbon fiber cable)

Tension (N)	Theoretical results (Hz)	Experimental results (Hz)	FEM Analysis results (Hz)
111.25	264.78	309.87	275.00
225.00	374.46	392.63	375.00
333.75	458.62	458.67	460.20
445.00	529.57	517.74	525.00
578.50	603.80	554.68	600.00

Table 4.2.1.3 Vibration frequency from different methods (0.5080m 20.71 turns/m carbon fiber cable)

Tension (N)	Theoretical results (Hz)	Experimental results (Hz)	FEM Analysis results (Hz)
111.25	158.86	159.62	158.50
225.00	224.67	225.82	224.15
333.75	275.17	263.45	274.52
445.00	317.74	308.86	316.99
578.50	362.27	355.53	361.43

Fig. 4.2.1.1 to Fig. 4.2.1.3 present the cable vibration frequency versus tension, the results show that the vibration frequency increases as tension increases, and the finite element solution closely matches the theoretical results, and the vibration frequency obtained from FEM analysis is about 2-4% higher than the test results. This difference

could come from the mass per unit length used in the FEM analysis is smaller than the exact mass per unit length. The results demonstrated that the modeling of cable with the COMBIN14 and MASS21 elements is applicable to obtain a good prediction of the cable's natural vibration frequency. For the cables with other configurations, this model can be easily modified by replacing the appropriate parameters (density, cross-sectional area etc.) of the model.

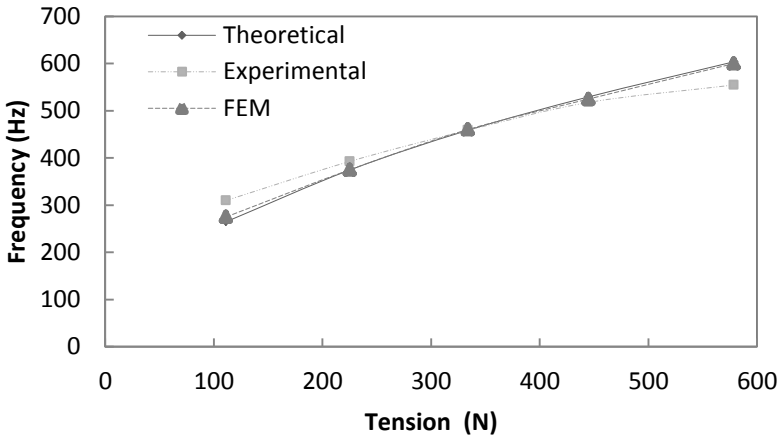

Figure 4.2.1.1 Vibration frequency from different methods (0.3048m, 20.71 turns/m carbon fiber cable)

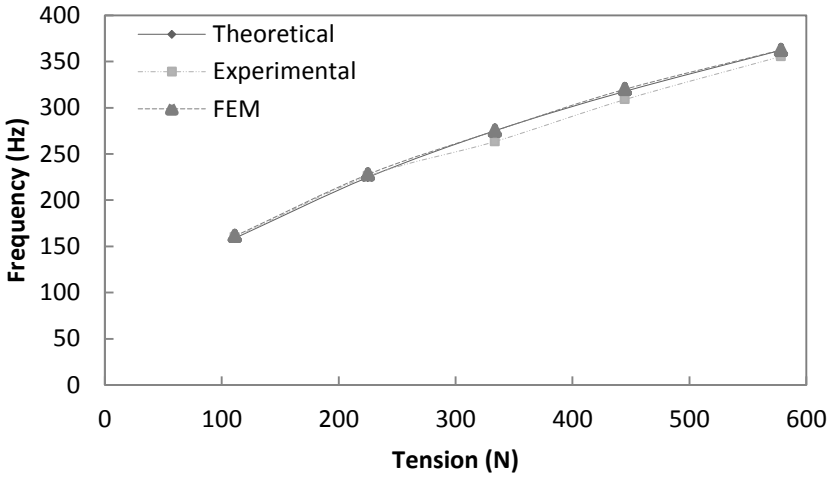

Figure 4.2.1.2 Vibration frequency from different methods (0.5080m, 20.71 turns/m carbon fiber cable)

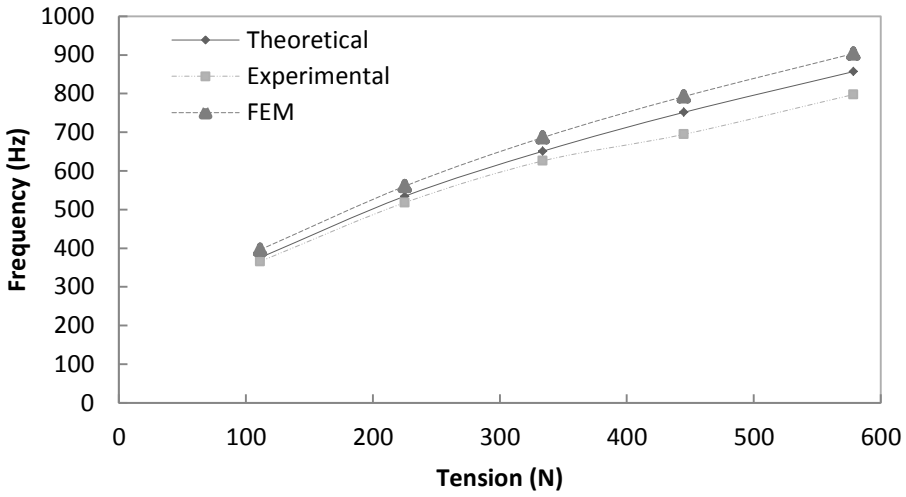

Figure 4.2.1.3 Vibration frequency from different methods (0.2032m, 20.71 turns/m carbon fiber cable)

4.2.2 Transient Dynamic Analysis

Transient dynamic analysis using the Finite Element Method (FEM) was used to explore the feasibility of using Rayleigh damping parameters to obtain the time history response of a vibrating cable. A 0.3048m, 20.71turns/m carbon fiber cable was investigated. The cable was modeled with COMBIN14 and MASS21 elements, as shown in Fig. 4.2.2.1.

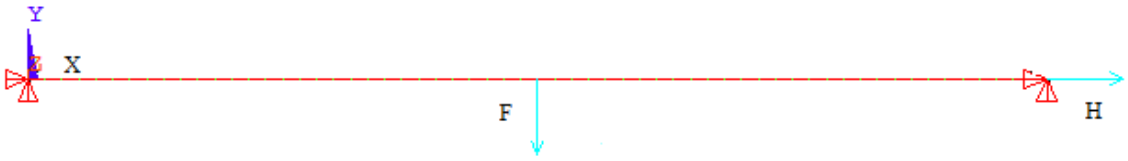

Figure 4.2.2.1 Finite element representation of a cable

The experimentally determined α and β Rayleigh damping constants were used to include cable damping in the finite element analysis. The integration time step was

carefully selected on the basis of ≈1/20 of the period to allow the initial step acceleration change to be followed reasonably well and to enhance the accuracy of analysis. The experimentally determined damping constants for this cable are α=5.377 and β=0.000012, as listed in Table 3.4.1.8. The loads in the finite element model were applied in the same order as the experiments. The cable was first fixed at the left end, and then a pretension force *H* was applied to the right end of the cable. After applying the pretension force *H*, the right end of the cable was fixed. Then an impulse load *F* was applied at the center of the cable for the transient analysis.

The FEM simulated time history response and the experimental recorded time history response of the nodes at one fifth and three quarters of the cable length are shown in Fig. 4.2.2.2 and Fig. 4.2.3, respectively, for the 0.3048m, 20.71 turns/m carbon fiber cable tested with 333.75N pretension. Comparing the time history responses from different methods, it can be seen that the finite element simulation and the experimental measurements are in good agreement (has close amplitude peak and elapsed in about 35 cycles). This demonstrates that the carbon fiber cable vibration damping can be modeled effectively with the selected elements and the Rayleigh damping.

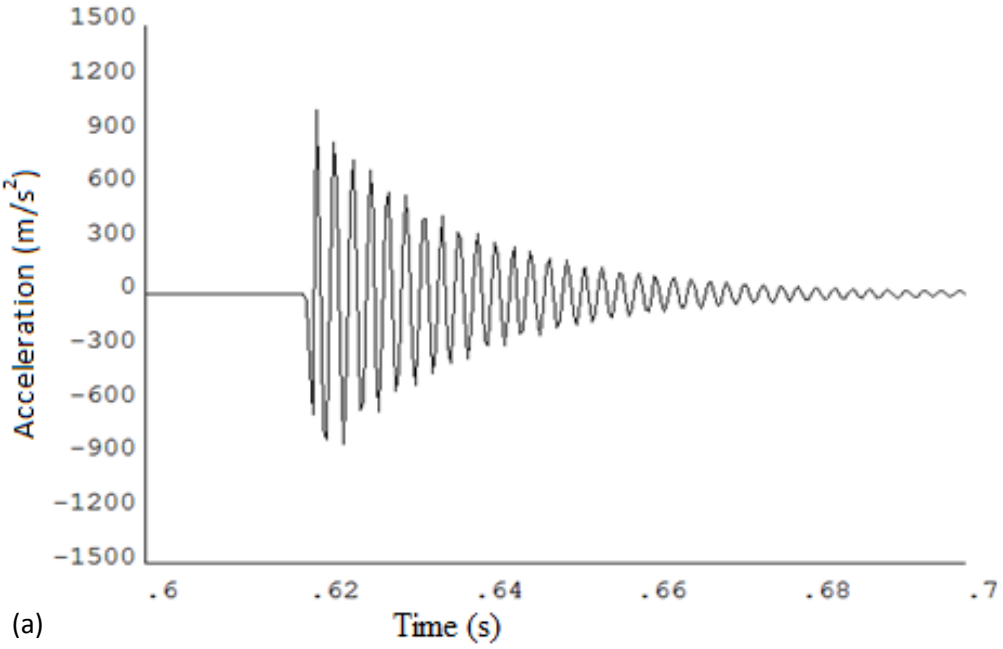

(a)

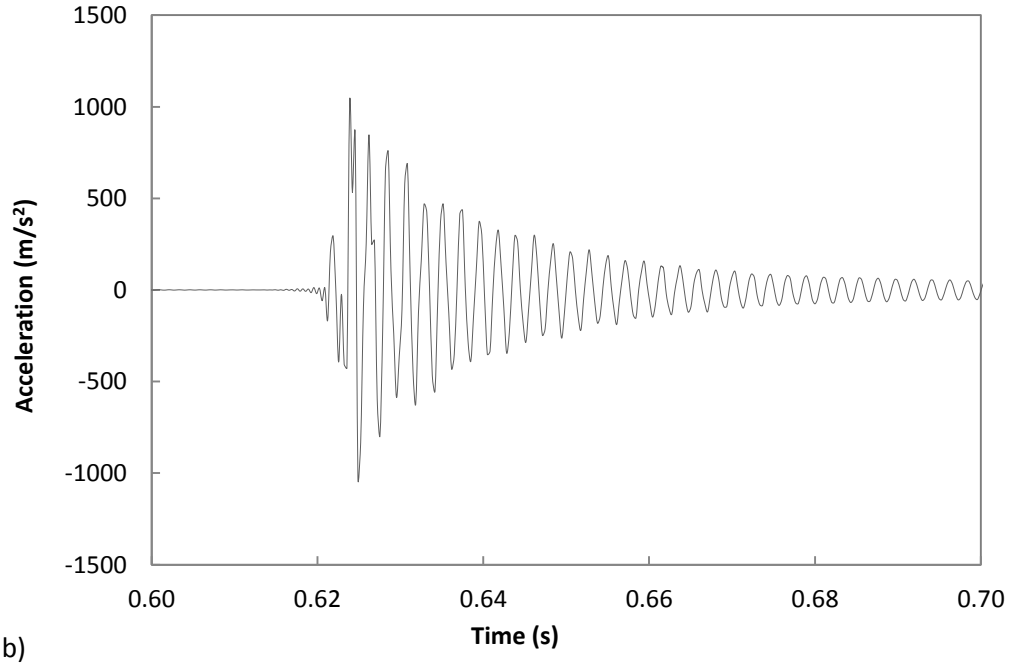

(b)

Figure 4.2.2.2 Comparison of time history response (a) FEM result of node at 1/5 of cable length (b) experimental result of node at 1/5 of cable length

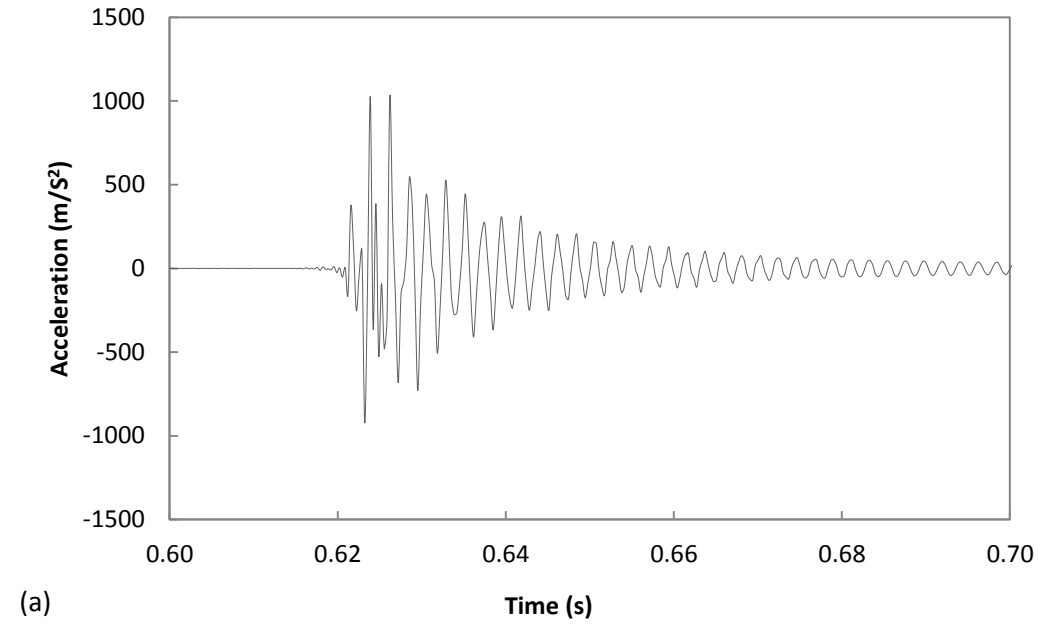

(a)

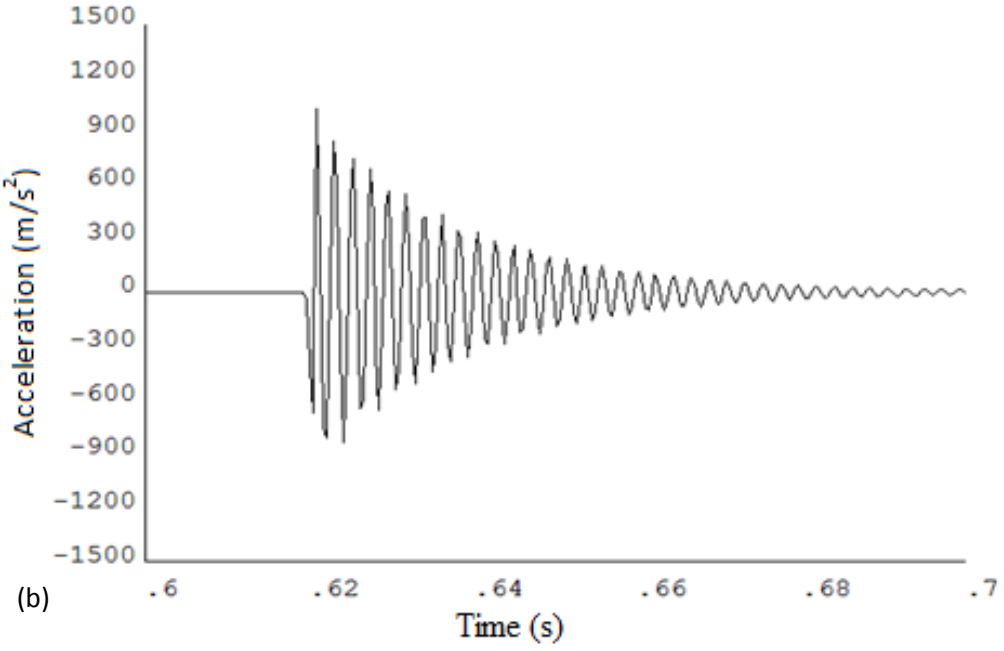

(b)

Figure 4.2.2.3 Comparison of time history response (a) FEM result of node at 3/4 of cable length (b) experimental result of node at 3/4 of cable length

4. 3 Conclusions

A simple finite element modeling of straight carbon fiber cable using the COMBIN14 and MASS21 elements is discussed. Modal analysis and transient dynamic analysis of carbon fiber cables show that the finite element simulation of cable vibration using the COMBIN14 and MASS21 elements provides good estimation of natural frequency and time history response, respectively. In addition, the Rayleigh damping is adequate for modeling carbon fiber cable damping.

Though, the simple finite model presented can simulate the time history responses of the carbon fiber cable adequately, the cable interwire behaviors cannot be taken into account. Therefore, further work on the modeling of cable by considering the cable's actual geometry and cable interwire behaviors is needed to give a more accurate estimation of cable vibration frequency and time history response. In addition, the effects of temperature and air pressure on damping needed to be considered in the FEM simulation.

Chapter 5

Analytical Model of Cable Vibration Damping

In this chapter, an analytical model of cable vibration damping is presented. The model is developed using simplified but physical realistic assumptions on material constitutive properties and geometric compatibility conditions. The proposed method and several related issues are discussed and compared with experimental data.

5.1 Introduction

Cables are commonly used as tension members in many engineering structures, such as the cable-stayed bridge, large span roofs, mooring systems, deployable space structures, etc. Existing analytical models appear to have concentrated on steel cables and much less attention has been paid to carbon fiber cables and their effects on the dynamic behavior of space structures. Recently, researchers attempted to include interwire friction and contact forces to their theoretical models. Some encouraging progress has been made by Claren and Diana (1996a, 1969b), who analyzed the internal damping of axially loaded stranded cables by introducing the slippage coefficient. However, no further work to formulate the cable internal damping and slippage coefficient was provided. Hobbs and Roof (1984) addressed the problem of energy dissipation in multilayered spiral strands, but simplified their model based on homogenization of the cable layers into orthotropic cylindrical sheets. The integration of friction forces and contact forces into the cable

damping mechanics remains a challenge. To simplify the problem, usually only one type of cable contact, cable core-wire contact or wire-wire contact, is considered, and interwire friction is neglected or assumed to be a constant. Sathikh (1989a, 1989b, 1989c), Labrosse and Conway (2000a, 2000b), Leech (1987, 2002) studied the interwire friction effects on seven-wire cables considering only the wire-core contact of the cable; Machida and Durelli (1973), Chi (1974a, 1974b), Knapp (1979), Kumar and Cochran (1987) investigated cable damping but neglected the effect of interwire friction. Huang and Vinogradov (1992) analyzed the dynamic behavior of a structural cable under cyclic tension using the 'thin rod model' and assuming constant friction. As a result, the friction-free models and constant friction models of cables are not appropriate to simulate the damping properties of cables. Moreover, if the strand does not have core or if the core radius were too small, the helical wires are in contact with each other along helical lines. Therefore, the wire-core contact or wire-wire contact model cannot correctly predict carbon fiber cable vibration damping.

The present work aims at removing some of these assumptions and establishing a model by including the cable interwire contact and interwire friction to predict the damping properties of carbon fiber cables. The section is organized as follows:

Step 1: Parameters related to the geometry of the cable and relevant assumptions are introduced.

Step 2: The relevant simplifying assumptions are identified.

Step 3: The axial strain of the helical wires due to cable elongation and rotation are derived.

Step 4: The consequent contact normal forces and the cable interwire frictional forces are thereafter included in the analytical model.

Step 5: Using the energy dissipation principle, the formula for cable internal vibration damping is derived for the axially loaded carbon fiber cable.

5. 2 Description of Cable Geometry

The carbon fiber cables are assemblies of millions of IM7 fibers and are fabricated by twisting. For simplification, let us consider a 1+6 cable structure, as shown in Fig. 5.2.1, in which the cable has 1 central straight fiber core and 6 helical wires. It should be noted that this geometry usually represents the metallic cables, and the tested carbon fiber cables can be approximately represented by this geometry. The geometry of each helical wire is characterized by the pitch length, P, which is the reciprocal of twist per unit length, and the lay angle, α, measured with respect to the axis of the cable (Z axis). The helical wire centerline is then a helical curve of radius of R_h. Let R_w be the radius of the helical wires, and R_c the radius of the cable fiber core, then we have:

$$R_h = R_c + R_w \tag{5-1}$$

The pitch length of the cable was determined by (Costello, 1997) as:

$$P = \frac{2\pi R_h}{\tan(\alpha)} \tag{5-2}$$

Where:

R_h = initial radius of helical wires centerline

R_c = radius of cable core

R_w = radius of helical wires

P = pitch length of helical wires

α = initial lay angle of helical wires

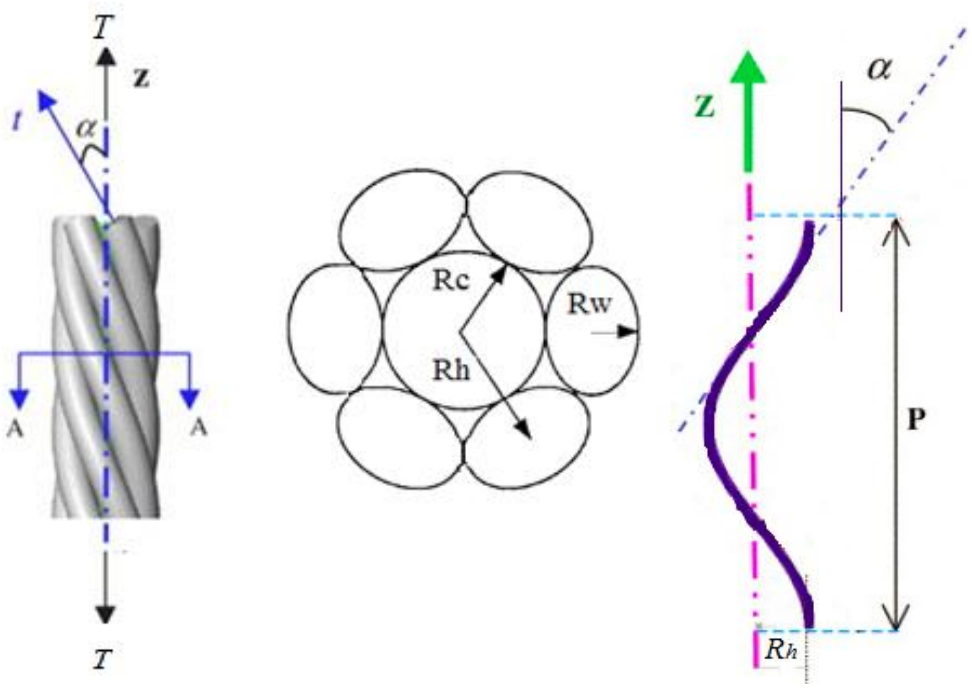

Figure 5.2.1 Cable geometry

5. 3 Relevant Assumptions

The following assumptions were made:

a) Displacements and strains are assumed to be small;

b) The cable wires have a coupling behavior between extension and twisting, and the helix angle variation is considered;

c) Although the carbon fiber cable was made with non-circular IM7 tows, the cable core is assumed to have a circular cross-section, and the helical wires are assumed to have elliptical cross-section due to the process of manufacture of the cables;

d) The cable is considered to be comprising of a core and six helical wires. Both core helical wire interaction and interaction among helical wires are considered in the analysis;

e) Effect of Poisson's ratio and the contact deformation are considered.

5. 4 Axial Strain of Helical wires

In axial loading, with traction and torsion, the axial strain of each cable wire is assumed to have two parts: the first part results from the elongation of the structure, whereas the second part is due to its rotation. For small deformation, the strain of the cable wires can be expressed as:

$$\varepsilon_t = \varepsilon_t^A + \varepsilon_t^R \tag{5-3}$$

Where:

ε_t = total strain of the helical wires along the tangent direction, *t* designates the tangent direction of the helical wires

ε_t^A = the tangential strain of the helical wires due to elongation

ε_t^R = the tangential strain of the helical wires due to rotation

5.4.1 Axial Strain due to Elongation

Let γ_z be the extension ratio of the deformed structure length to the initial structure length measured along the cable's axis (z-axis), and γ_t be the corresponding extension ratio for a helical wire whose initial and final radii are R_h and R_{h1}, respectively, as shown in Fig. 5.4.1.1, we have:

$$\gamma_z = \frac{L_1}{L} \tag{5-4}$$

$$\gamma_t = \frac{S_1}{S} = 1 + \varepsilon_t^A \tag{5-5}$$

Where:

L = initial length of the cable structure

L_1 = length of the deformed cable structure

S = initial length of the helical wires

S_1= length of the deformed helical wires

θ, θ_1 = the initial and final angle that a helical wire sweeps out in a plane perpendicular to the axis of the cable.

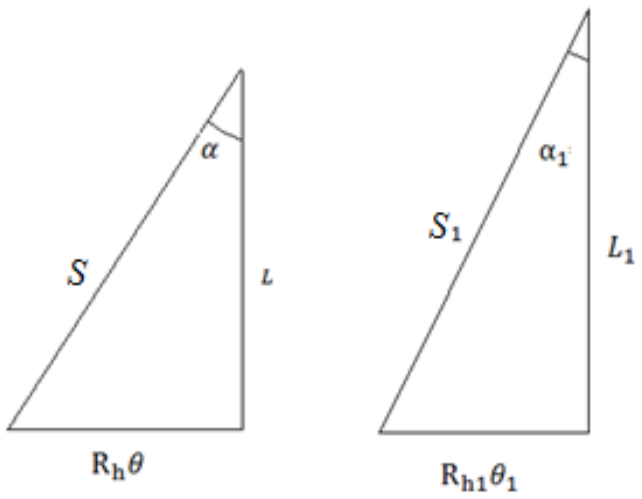

Figure 5.4.1.1 Developed view of helical wire centerline

As the helical wires are extended, the cable strands undergo a compaction of volume. The ratio of the deformed and un-deformed volume of the cable is defined as the compaction factor (CF), we have:

$$\gamma_z = \frac{L_1}{L} = \frac{\frac{V_1}{\pi R_{h1}^2}}{\frac{V}{\pi R_h^2}} = CF\,\frac{R_h^2}{R_{h1}^2} \tag{5-6}$$

Where:

V, V_1= the volume of the un-deformed and deformed cable

CF= compaction factor of the cable

R_h, R_{h1}= radius of the un-deformed and deformed helical wires

From Eq. (5-2), we have:

$$tan\,\alpha = \frac{2\pi R_h}{P} \tag{5-7}$$

Therefore, the pitch length in the deformed state can be determined by:

$$P_1 = P\gamma_z \tag{5-8}$$

From Eq. (5-7) and Eq. (5-8), the lay angle of the deformed state can be determined as:

$$\tan\alpha_1 = \frac{\tan\alpha}{\gamma_z^{3/2}} \tag{5-9}$$

The initial length of a cable helical wire with lay angle α is:

$$S = \frac{L}{\cos\alpha} \tag{5-10}$$

From Eq. (5-4), the axial length L_1 corresponding to the deformed state is:

$$L_1 = L\gamma_z \tag{5-11}$$

Hence, the corresponding helical wire length in the deformed state is:

$$S_1 = \frac{L_1}{\cos\alpha_1} = \frac{L*\gamma_z}{\cos\alpha_1} \tag{5-12}$$

Where:

α_1=lay angle of the deformed helical wires

Using Eq. (5-5), Eq. (5-9), Eq. (5-10) and Eq. (5-12), the helical wire extension ratio can be expressed as:

$$\gamma_t = \gamma_z \frac{\cos\alpha}{\cos\alpha_1} \tag{5-13}$$

$$\gamma_t^2 = \gamma_z^2 cos^2\alpha + \frac{sin^2\alpha}{\gamma_z} \tag{5-14}$$

From Eq. (5-5) and Eq. (5-14), the axial strain of the cable wires due to tension can be obtained as:

$$\varepsilon_t^A = \sqrt{\gamma_z^2 cos^2\alpha + \frac{sin^2\alpha}{\gamma_z}} - 1 \tag{5-15}$$

From Eq. (5-15), the axial strain of helical wires is a function of the initial lay angle, initial radius of helical wires centerline and the radius of deformed cable helical wires centerline. The lay angle can be determined from the cable construction defined in Chapter 3 (turns/m) using Eq. (5-7). The radius of the deformed cable helical wires centerline will be discussed in Section 5.5 by considering the contact deformation and Poisson's ratio.

5.4.2 Axial Strain due to Rotation

A relative rotation θ_z, exists between the undeformed and deformed cable end section. The axial strain of the helical wires due to this rotation can be expressed as:

$$\varepsilon_t^R = \frac{\Delta S}{s} \tag{5-16}$$

Where:

$$\Delta S = \mathrm{R_h} * \theta_z * sin\alpha_1 \tag{5-17}$$

Substituting Eq. (5-6), Eq. (5-10) and Eq. (5-17) into Eq. (5-16), the axial strain of the helical wires due to rotation can be expressed as:

$$\varepsilon_t^R = \sqrt{CF}\frac{\mathrm{R_h}}{\sqrt{\gamma_z}}\frac{\theta_z}{L}sin\alpha_1\cos\alpha \tag{5-18}$$

$$\frac{\mathrm{R_h}\theta_z}{L} = \frac{\mathrm{R_h}(1+\varepsilon_c)}{\mathrm{R_{h1}}cot\alpha_1} - \frac{1}{cot\alpha} \tag{5-19}$$

Where:

$\theta_z = \theta_1 - \theta$ = the relative rotation of the helical wires

Substituting Eq. (5-19) into Eq. (5-18), the axial strain due to rotation can be rewritten as:

$$\varepsilon_t^R = \frac{\sqrt{CF}}{\sqrt{\gamma_z}}\left[\frac{\mathrm{R_h}(1+\varepsilon_c)}{\mathrm{R_{h1}}cot\alpha_1} - \frac{1}{cot\alpha}\right] sin\alpha_1\cos\alpha \tag{5-20}$$

Where:

ε_c = the axial strain in the cable core

Assuming small deformation:

$$\Delta\alpha = |\alpha_1 - \alpha| \ll 1 \tag{5-21}$$

Hence $cos\alpha_1$ can be expressed as:

$$cos\alpha_1 = \cos(\alpha + \Delta\alpha) = cos\alpha - \Delta\alpha sin\alpha \tag{5-22}$$

The axial strain of a straight cable core ε_c in Eq. (5-20) is therefore:

$$\varepsilon_c = \frac{L_1 - L}{L} = (1 + \varepsilon_t)\frac{cos\alpha_1}{cos\alpha} - 1 \tag{5-23}$$

Substituting Eq. (5-22) into Eq. (5-23), and neglected the higher order terms, Eq. (5-22) can now be written as:

$$\varepsilon_c = \varepsilon_t - \Delta\alpha tan\alpha \tag{5-24}$$

From Eq. (5-9), we have:

$$cot\alpha_1 = \frac{\gamma_z^{3/2}}{\tan\alpha} \tag{5-25}$$

$$sin\alpha_1 = \sqrt{\frac{tan^2\alpha}{\gamma_z^3 + tan^2\alpha}} \tag{5-26}$$

Substituting Eq. (5-15), Eq. (5-20), Eq. (5-24) and Eq. (5-26) into Eq. (5-3), the total strain of the helical wires along the tangent direction can be written as:

$$\varepsilon_t = \sqrt{\gamma_z^2 cos^2\alpha + \frac{sin^2\alpha}{\gamma_z}} - 1 + \sqrt{\frac{CF}{\gamma_z}}\left[\frac{\left(\sqrt{\gamma_z^3 cos^2\alpha + sin^2\alpha} * (1 - \Delta\alpha tan\alpha)\right.}{\sqrt{CF}\frac{\gamma_z^{3/2}}{\tan\alpha}} - \frac{1}{cot\alpha}\right]\sqrt{\frac{tan^2\alpha}{\gamma_z^3 + tan^2\alpha}}\cos\alpha \tag{5-27}$$

From Eq. (5-27), the total strain of the helical wires along the tangent direction can be determined as a function of the initial lay angle α, initial radius of helical wires centerline R_h, radius of the helical wires centerline of the deformed cable $\mathrm{R_{h1}}$, the compaction factor (CF) and the change of the lay angle $\Delta\alpha$. Determination of $\mathrm{R_{h1}}$ and $\Delta\alpha$ are presented in the following section.

5. 5 Modeling Contact and Friction Forces

5. 5.1 Radius of Deformed Helical Wires Centerline

If Poisson's ratio effects in the individual wires are considered, the radius of the deformed helical wire centerline becomes:

$$\mathrm{R_{h1}} = R_c(1 - \nu\varepsilon_c) + R_w(1 - \nu\varepsilon_t) \tag{5-28}$$

Where:

ν=Poisson's ratio of the material

Contact forces between cable wires result in deformation that reduces the radius of the helical wires and consequently reduces the equilibrium contact force per unit length and tension resulting in the wires corresponding to specific strand strains. If the contact deformation in the cable core and helical wires is considered, the final helical radius can now be written as:

$$\mathrm{R_{h1}} = R_c(1 - \nu\varepsilon_c) + R_w(1 - \nu\varepsilon_t) - \delta_a \tag{5-29}$$

Where δ_a is the mutual approach of the cable core and cable helical wires, which can be determined from contact theory. The mutual approach between two parallel cylinders is given by Roark and Young (1975) as:

$$\delta_a = \frac{2P_{nch}(1-\nu^2)}{\pi E_t}\left(\frac{2}{3} + ln\frac{4R_c}{a} + ln\frac{4R_w}{a}\right) \tag{5-30}$$

Therefore the final helical wire centerline radius R_{h1} is:

$$R_{h1} = R_c(1 - \nu\varepsilon_c) + R_w(1 - \nu\varepsilon_t) - \frac{2P_{nch}(1-\nu^2)}{\pi E_t}\left(\frac{2}{3} + ln\frac{4R_c}{a_c} + ln\frac{4R_w}{a_c}\right) \quad (5\text{-}31)$$

Where:

E_t = transverse modulus

5. 5.2 Interwire Contact and Friction

Strands in cables may subject to core-wire, wire-wire or coupled core-wire and wire-wire contacts depending on the construction of the strand and the type of loading. The contact models may change from one model to the other depending on the loads and the deformation of the core and wires. Most of the literature on vibration damping analyzes the cable strand with either the core-wire contact or wire-wire contact. In this research a coupled core-wire and wire-wire contact is considered to understand the effect of interfacial forces on the cable vibration damping. Furthermore, the consideration of friction at the interface was also included in this model. In the portion where slip occurs the helix angle will change. This increase in helix angle under loads is determined from Eq. (5-22) to Eq. (5-24) by considering the small deformation:

$$\Delta\alpha = (2 - \varepsilon_t)tan\alpha \quad (5\text{-}32)$$

In a simple cable, the contact zone between a helical wire and the core forms a narrow strip whose central line is a helix. This contact can be locally approximated as the contact between two parallel straight cylinders. Because the contact width is very small

compared with the wire radius, the Hertzian contact theory is applicable. The contact half-width between a core and a helix, a_{ch} was determined by Labrosse and Conway (2000a, 2000b) as follows:

$$a_{ch} = 2\sqrt{\frac{2(1-\nu^2)R_w R_c P_{nch}}{\pi E(R_w+R_c)}} \tag{5-33}$$

Similarly, the contact half width between two helical wires a_{hh} is:

$$a_{hh} = 2\sqrt{\frac{2(1-\nu^2)R_w R_c P_{nhh}}{\pi E(R_w+R_c)}} \tag{5-34}$$

Where:

P_{nch} = the normal load per unit length between cable core and helical wires

a_{ch} = the contact half-width of cable core and helical wires contact

P_{nhh} = the normal load per unit length between helical wires

a_{hh} = the contact half-width of helical wires contact

E = Young's modulus of the cable material

5. 5.2.1 Contact Normal Load per Unit Length

Along the contact line between the helical wires, the normal distributed force P_{nhh} and the tangential distributed force W_1 and W exist, as shown in Fig. 5.5.2.1. Furthermore, along the line of contact between the cable core and a helical wire, the normal distributed force P_{nch} and the tangential distributed force Q_1 and Q act as shown in Fig. 5.5.2.1.

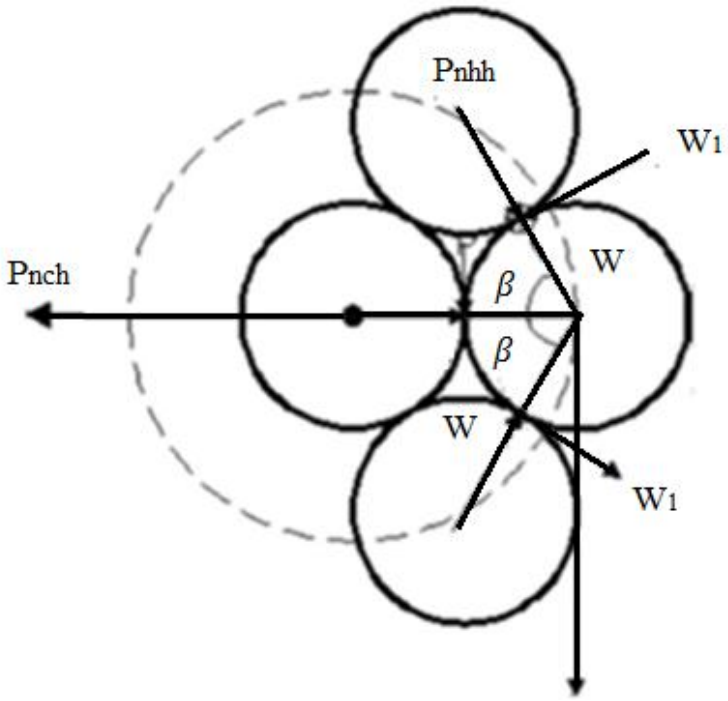

Figure 5.5.2.1 Distributed loads on a helical wire

Where β is the contact angle, which defines the direction of the distributed contact load P_{nch}, and is given by Costello and Phillips (1974) as the following:

$$cos\beta = \frac{1}{cos^2\alpha}\left\{\sqrt{1+\frac{tan^2\left(\frac{\pi}{2}-\frac{\pi}{m}\right)}{sin^2\alpha}}-\sqrt{tan^2\left(\frac{\pi}{2}-\frac{\pi}{m}\right)\left\{1+\frac{1}{tan^2\alpha*cos^2\left(\frac{\pi}{2}-\frac{\pi}{m}\right)\left[sin^2\alpha+tan^2\left(\frac{\pi}{2}-\frac{\pi}{m}\right)\right]}\right\}+sin^4\alpha}\right. \quad (5\text{-}35)$$

Where:

m = the number of helical wires, equal to six for a 1+6 strand

When slip between helical wires during the extension of the cable is considered, the tangential distributed forces between the core-wire and the wire-wire can be given by:

$$W_1 = \mu P_{nhh}; W = \mu P_{nhh}; Q_1 = \mu P_{nnhh}; Q = \mu P_{nhh} \quad (5\text{-}36)$$

Where:

μ = friction coefficient of the material

As showed by Hobbs and Roof (1982), when the changes in helix angle and radius are small, the interwire distributed forces in the normal direction can be represented approximately as:

$$P_{nch} = -\mathrm{H}\sin^2\alpha/\mathrm{R_h} \quad (5\text{-}37)$$

Where:

$$H = \pi R_w^2 E \varepsilon_t \quad (5\text{-}38)$$

Substituting Eq. (5-38) into Eq. (5-37), the distributed contact force between the cable core and helical wires, denoted by P_{nch}, (Fig. 5.5.2.2) can be rewritten as:

$$P_{nch} = -\pi R_w^2 E \varepsilon_t \sin^2\alpha/\mathrm{R_h} \quad (5\text{-}39)$$

The contact force between the helical wires can be determined to be:

$$P_{nhh} = -\frac{P_{nch}}{2cos\beta} = \frac{\pi R_w^2 E \varepsilon_t \sin^2\alpha}{2\mathrm{R_h} cos\beta} \quad (5\text{-}40)$$

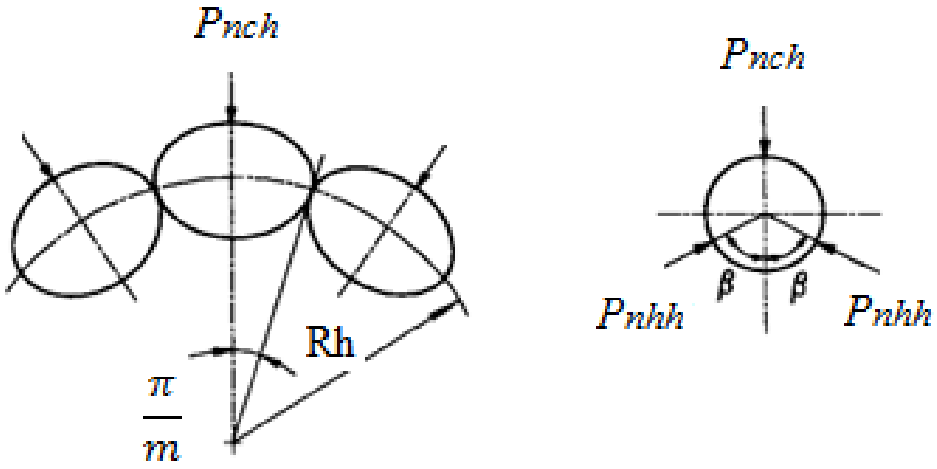

Figure 5.5.2.2 Contact force in cable

5. 6 Determination of Vibration Damping

An energy based method is used to evaluate the cable vibration damping. For low damping, the energy stored at two successive peak amplitudes, a_n and a_{n+1}, of a freely decay vibration is related to the loss factor by (Raoof and Huang, 1991):

$$\eta = \frac{\Delta U}{U} \approx \frac{a_n^2 - a_{n+1}^2}{a_n^2} \approx \frac{2(a_n - a_{n+1})}{a_{n+1}} \tag{5-41}$$

Where:

η = loss factor of the system

ΔU = the energy dissipation per cycle

U = the stored energy

a_n, a_{n+1}= two successive vibration amplitudes

The logarithmic decrement δ of the cable system is given as (Chopra, 2001):

$$\delta = \ln(\frac{a_n}{a_{n+1}}) \tag{5-42}$$

For low damping, the following expression can be obtained:

$$\delta = \frac{\eta}{2} \approx \frac{(a_n - a_{n+1})}{a_{n+1}} = \frac{1}{2}\frac{\Delta U}{U} \tag{5-43}$$

Then damping ratio of the cable system ξ is determined by:

$$\xi = \frac{\delta}{\sqrt{4\pi^2+\delta^2}} = \frac{\frac{\Delta U}{U}}{\sqrt{16\pi^2+(\frac{\Delta U}{U})^2}} \tag{5-44}$$

Considering two adjacent helical wires of an axially preloaded carbon fiber cable, sliding takes places while the tangential friction forces remains at μf_s. The tangential relative displacement between central wires is estimated by Raoof (1991a), based on the parametric studies, and is given as:

$$\Delta_1 = 4R_w S_{6T} \tag{5-45}$$

$$S_{6T} = \varepsilon_t(0.00196\alpha - 0.000394\alpha^2 + 0.0000247\alpha^3), \alpha \leq 25° \tag{5-46}$$

Where:

Δ_1=tangential relative displacement

S_{6T}= shear strain between cable wires associated with wire axial strain

Then friction energy dissipation of helical wires is determined as:

$$\Delta U = m\mu f_s(\varepsilon_t + \Delta_1) \tag{5-47}$$

Where f_s is the contact normal force determined by Eq. (5-39), Eq. (5-40) and the associated contact half width, and *m* is the number of helical wires.

The stored strain energy can be determined as:

$$U_\varepsilon = \int_0^l \frac{1}{2} EA\varepsilon_t^2 ds \tag{5-48}$$

Assuming that the sinusoidal vibration profile is:

$$y = b\sin\frac{\pi x}{l} \tag{5-49}$$

For small amplitude of vibration, axial tension can be approximated to be a constant, and the strain energy due to the tension can be expresses as:

$$U_T = \frac{1}{2}\int_0^l y'T(x)\,dx = \frac{b^2}{2}\frac{\pi^2}{l^2}T\int_0^l(\cos\frac{\pi x}{l})^2\,dx \tag{5-50}$$

Where:

U_T = initial stored energy due to the applied tension force

y = the assumed sinusoidal cable vibration profile

b = vibration amplitude

The stored energy of the cable is then expressed as:

$$U = U_T + U_\varepsilon \tag{5-51}$$

Then the damping can be determined using Eq. (5-44)-Eq. (5-51).

The above mentioned procedure is further described in the form of a flow chart (Fig. 5.6.1), the procedure was implemented using an iterative MatLab code.

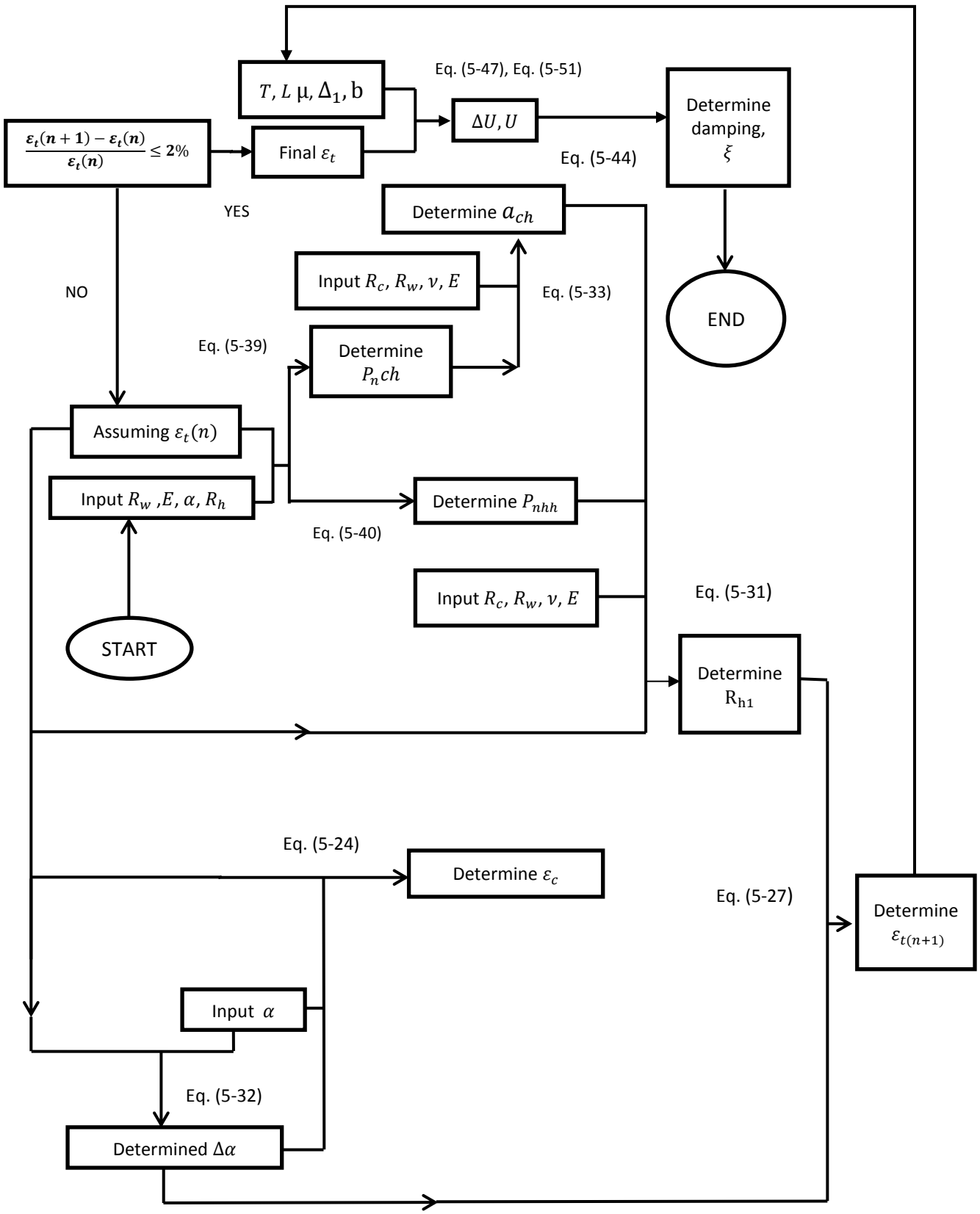

Figure 5.6.1 Analysis flow chart

5. 7 Results and Discussion

The carbon fiber cables tested in the laboratory were analyzed using the proposed approach. Table 5.7.1 shows the data pertinent to these cables. The length of cable is 0.2032m, 0.3048m, and 0.5080m, respectively, and the transverse modulus of the cable is assumed as 6% of the longitudinal tensile modulus. The results of this analytical cable damping model is shown in Table. 5.7.2.

Table 5.7.1 Cable properties

Cable No	Lay angle (rad)	Poisson's ratio	Young's Modulus (Gpa)	Helical centerline radius (m)	Friction coefficient
1	0.1207	0.3	2.76E+11	0.0004658	0.4
2	0.2332	0.3	2.76E+11	0.0004562	0.4
3	0.3328	0.3	2.76E+11	0.0004425	0.4

Table 5.7.2 Theoretical analysis results of cable vibration damping

Tension (N)	Damping for 20.71turns/m cables (%)			Damping for 41.42turns/m cables (%)			Damping for 62.13turns/m cables (%)		
	0.2032m	0.3048m	0.508m	0.2032m	0.3048m	0.508m	0.2032m	0.3048m	0.508m
111.25	6.09	4.11	2.81	5.02	3.19	1.92	4.67	3.11	1.87
222.50	3.72	2.52	1.77	2.89	1.82	1.09	2.62	1.75	1.05
333.75	2.67	1.82	1.30	2.02	1.27	0.76	1.83	1.22	0.73
445.00	2.09	1.42	1.02	1.56	0.98	0.59	1.40	0.93	0.56
578.50	1.65	1.13	0.81	1.22	0.76	0.46	1.09	0.73	0.44

Fig. 5.7.1 shows how the analytical results compare with the experimental data. The three Figures (Fig. 5.7.1 a-c) correspond to the three different cable construction (# of turns). In each Figure the variation of damping with applied tension and length of the cable is presented. From the figures, the analytical model is capable of capturing the trends on the variation of damping corresponding to each of the three independent variables (length, applied tension and construction/lay angle).

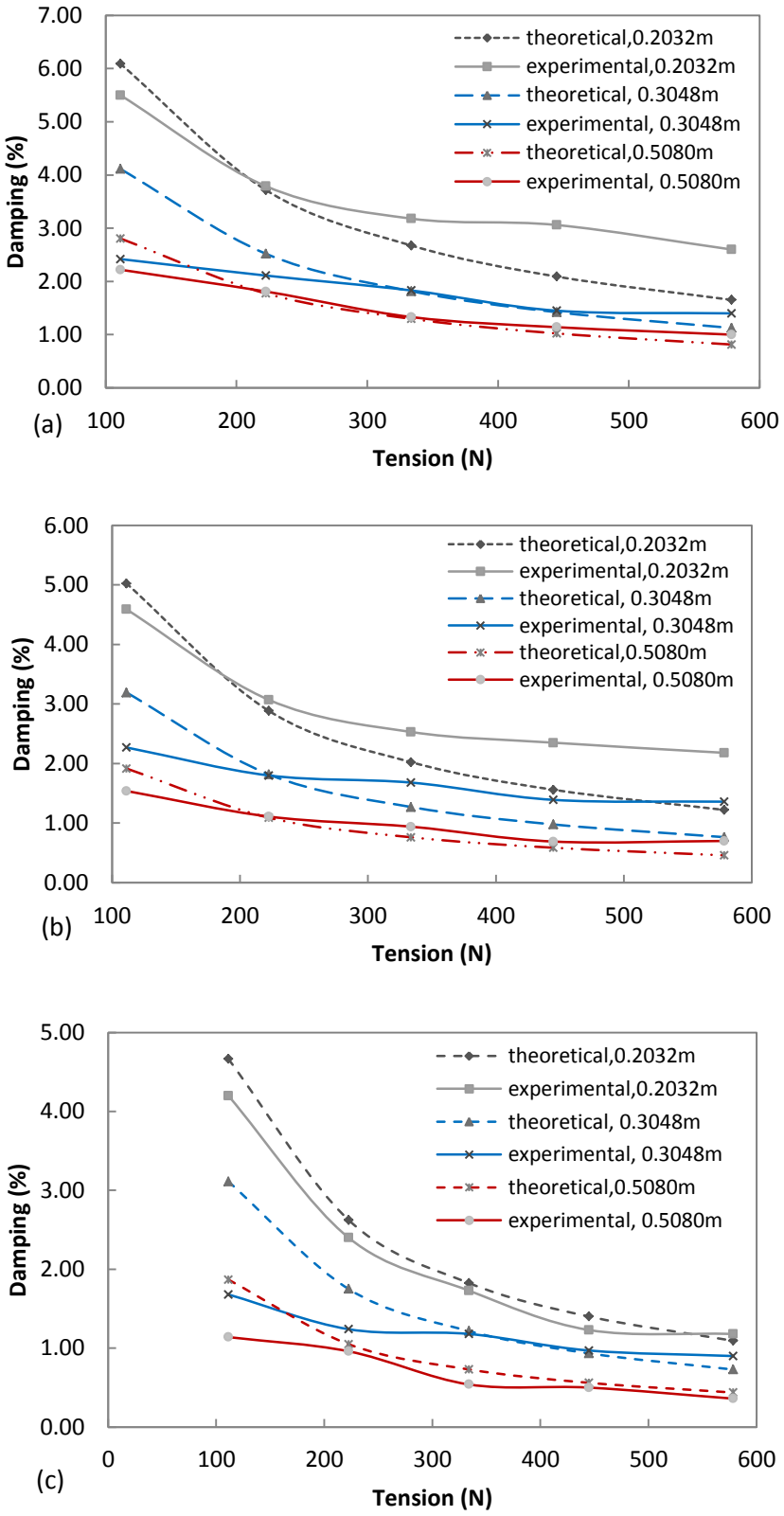

Figure 5.7.1 Comparison of cable damping (a) 20.71 turns/m (b) 41.42 turns/m, (c) 62.13turns/m cables

Fig. 5.7.1 shows that the analytical model captures the decrease in damping as tension increases. Typically, the cable damping is higher in the present model compared with the experimental results for a low tension, whereas smaller damping is presented under high tension. This could be attributed to the transverse property of the cable wires. The modulus in the transverse direction is likely to increase as more tension is applied, which was not included in the analyses.

The analytical damping results provided in Table 5.7.2 are presented in graphical form in Figures 5.7.2 and 5.7.3 against with cable construction and length, respectively. The trends compare very well with the test data presented earlier in Chapter 3.

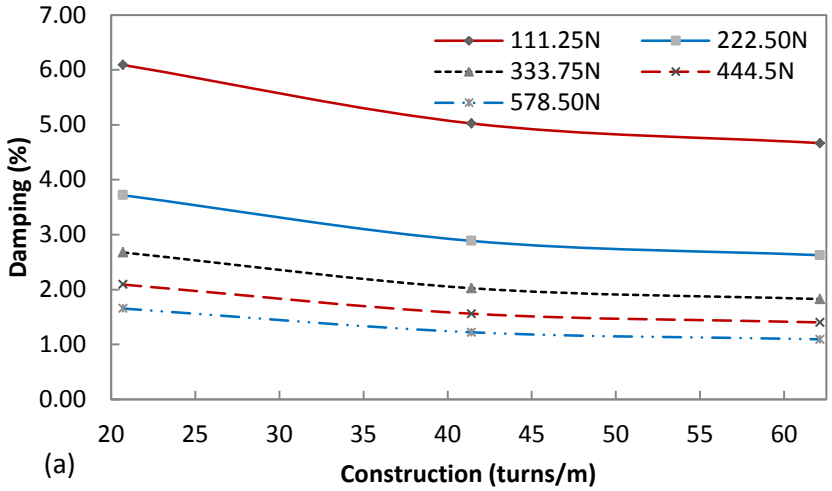

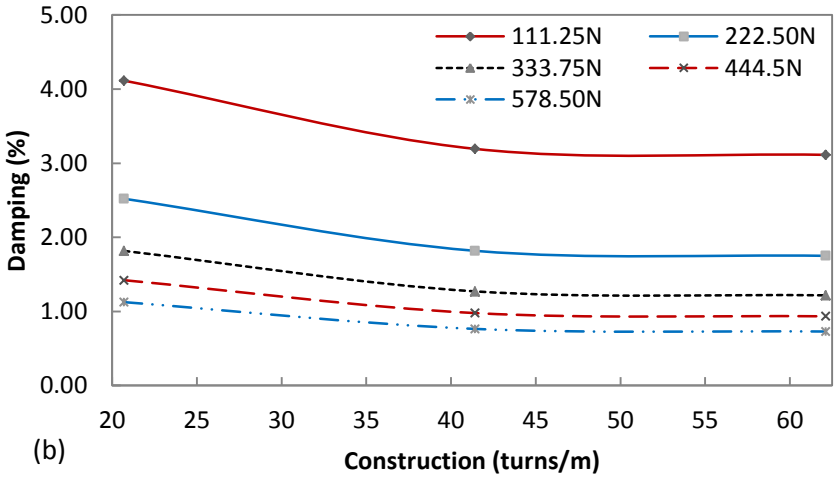

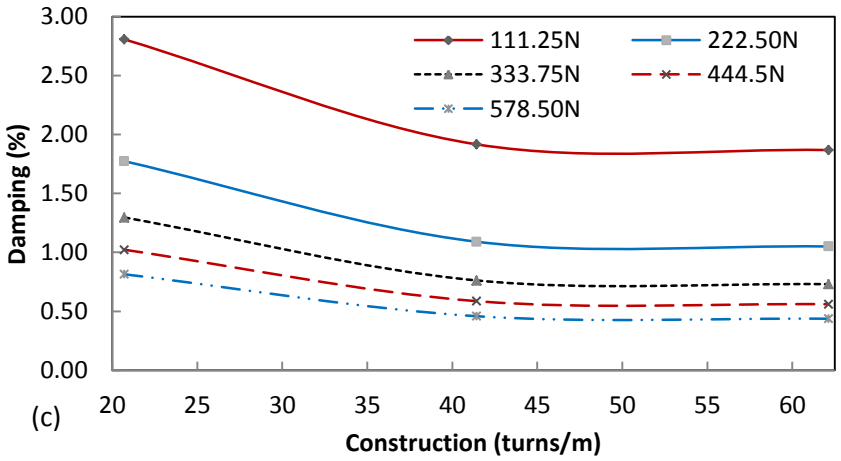

Figure 5.7.2 Cable damping versus cable construction (a) 0.2032m (b) 0.3048m (c) 0.5080m cables

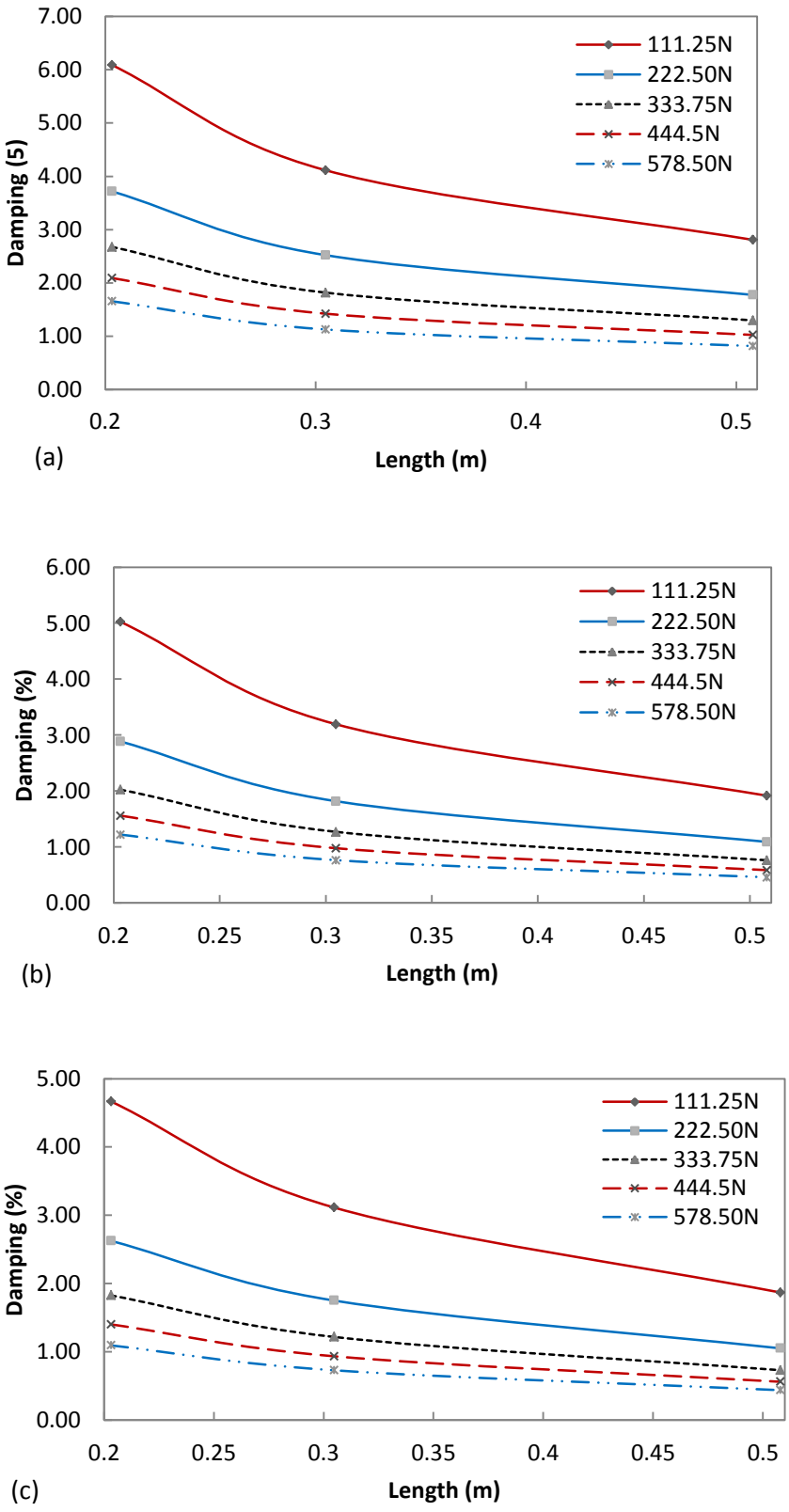

Figure 5.7.3 Cable damping versus length (a) 20.71 turns/m (b) 41.42turns/m (c) 62.13turns/m cables

To investigate if it is necessary to include the change of lay angle in the model, Fig. 5.7.4 presents the theoretical identified damping with ($\Delta\alpha \neq 0$) and without ($\Delta\alpha = 0$) consideration of the change of lay angle, and are compared with the test results. It shows that without taking into account of the change of lay angle, the analytical model underestimate cable damping (around 50% decrement ratio).

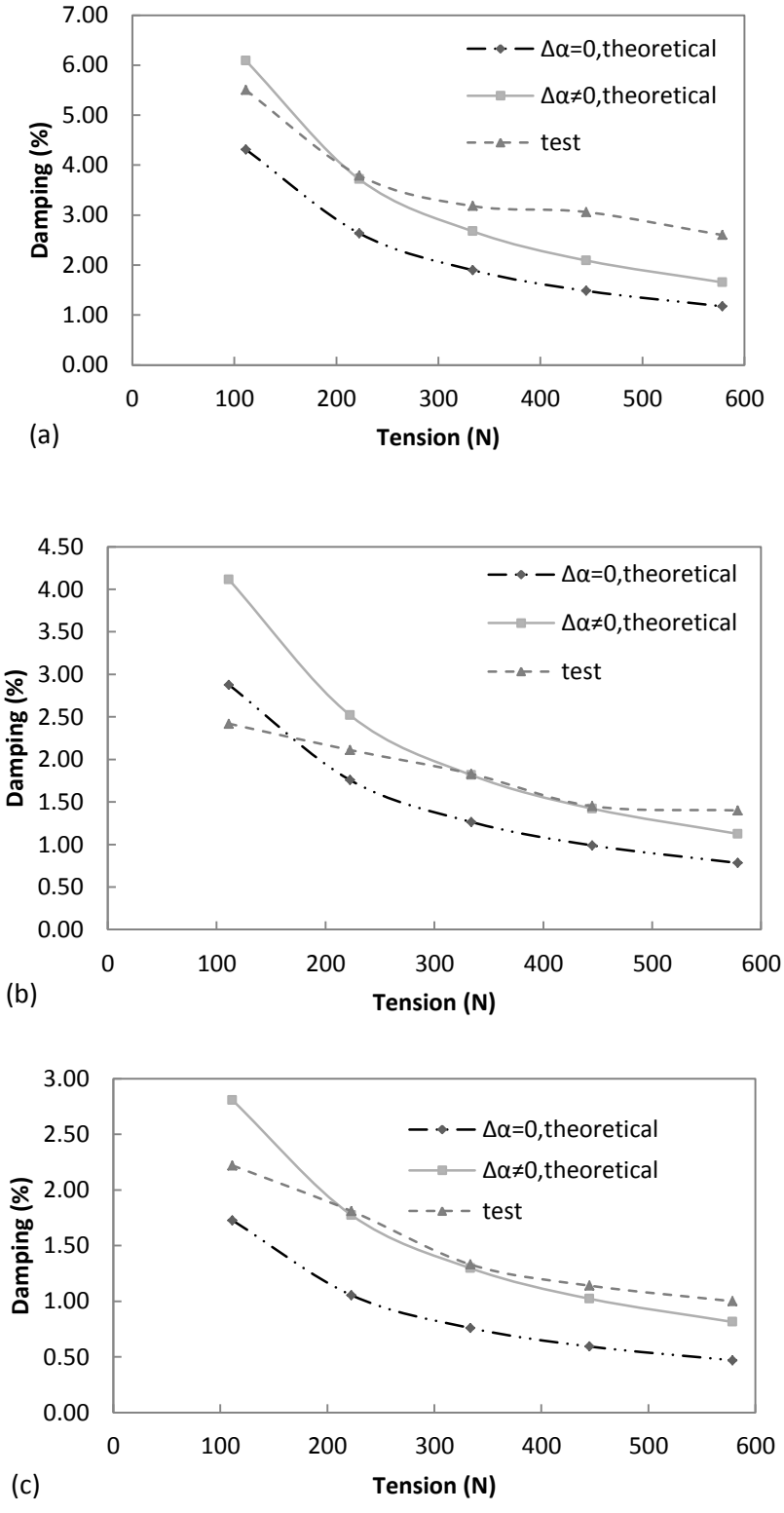

Figure 5.7.4 Comparison of damping (with and without consideration of change of lay angle) (a) 20.71 turns/m, 0.2032m (b) 20.71turns/m, 0.3048m (c) 20.71turns/m, 0.5080m cables

Fig. 5.7.5 shows the sensitivity of the analytical value of cable damping to the Poisson's ratio. It is notable that the damping values are not very sensitive to the Poisson's ratio for small and reasonable assumptions (0.3 used in this analysis, typical of carbon fibers). With a higher Poisson's ratio, the flattening of the cable causes more contact and friction between cable wires which leads to higher energy dissipation, as shown in Eq. (5-31).

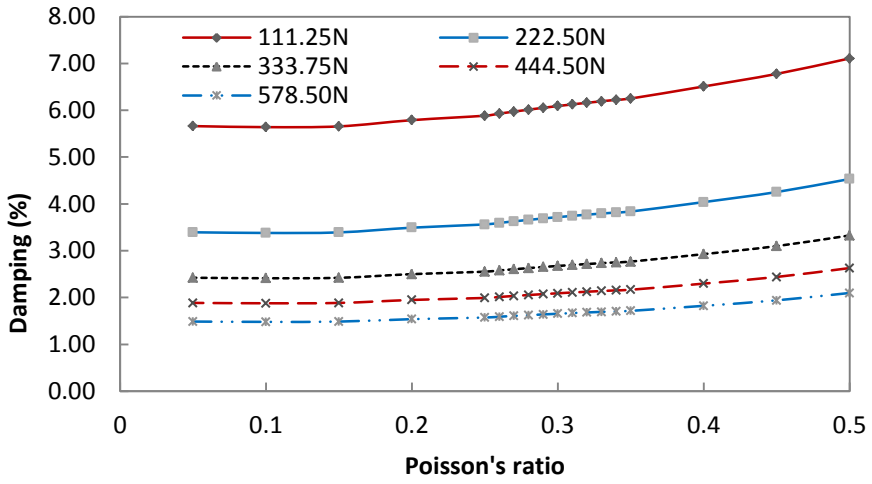

Figure 5.7.5 Cable damping versus Poisson's ratio (20.71 turns/m, 0.2032m carbon fiber cable)

5. 8 Conclusions

An analytical model has been developed which allows the damping of an axially loaded carbon fiber cable to be predicted with reasonable accuracy, based on the properties of the cable. The frictional energy dissipation is considered to be the main source of cable damping. Information has also been provided for estimating the extensional-torsional axial strain, the wire flattening and the contact behavior. In particular, the coupled wire-wire contact and wire-core contact, the change of lay angle were considered in the model.

The analytical model captured the trends on the variation of damping corresponding to each of the three independent variables (length, applied tension and construction/lay angle).

To this end, some straightforward formulations were presented which should prove useful in predicting cable vibration damping. However, the accuracy and appropriateness of the model is affected by the simplifying assumptions and is also affected by the manufacturing process is not as controlled as the analytical derivation.

Chapter 6

Summary and Conclusions

The studies taken up in this dissertation have developed an experimental setup to test cable vibration damping, and a theoretical approach for the analysis of cable damping. Summary and detailed discussions were presented at the end of each relevant chapter. The purpose of this chapter is to recapitulate the main findings and unify them to suggest some further research directions.

6.1 Summary of the Contributions Made

a) Cable damping in a vibrating structure has long been an active research area, and it is still considered as somewhat of an unknown area. Especially for the carbon fiber cables in the space structural application, the available data is scarce. This dissertation provides test data on the carbon fiber cable damping under different length, tension and configuration. In particularly, a vacuum chamber was designed to test damping of carbon fiber cables in the absence of atmosphere. Also, the effect of temperature on damping was investigated. Some conclusions are derived from the test results, which enrich the understanding of carbon fiber cable damping properties;

b) The finite element simulation of carbon fiber cable vibration using the COMBIN14 and MASS21 elements provides a simple but good estimation of cable vibration natural frequency and time history response; Also, it shows that the Rayleigh damping is adequate and effective for the modeling of cable damping;

c) A tensile load provokes not only extension, but also torque or rotation in cables due to their helical geometry. This coupling extensional-torsional behavior is quite important in the damping prediction of carbon fiber and steel cables. The strain caused by the extension and torsion is considered in the analytical model in this dissertation;
d) The Poisson's ratio effect, the mutual approach of cable wires and friction are considered in the determination of cable damping in the analytical model;
e) The analytical model captured the trends on the variation of damping corresponding to each of the three independent variables (length, applied tension and construction/lay angle).

6.2 Suggestions for Future Work

The following recommendations are made for future work in order to improve the accuracy of damping estimation:

a) The cable damping should be tested under a wider range of length, tension, configuration, ambient temperature and air pressure in order to obtain more data to analyze the effect of different factors on damping;
b) To get a better understanding of the characterizations of cable contact and interwire slippage and their effects on damping, it is important to measure the interwire pressure and slippage with sensors;
c) The effects of temperature and air pressure could be considered in the FEM simulation;

d) The effect of the microstructure of the cable could provide a better understanding of the frictional damping mechanism;

e) The proposed analytical solution is based on the small displacement and deformation assumption. In order to get a better prediction of cable damping, large deformation theory could be applied;

f) Different types of cables are applied in engineering field, therefore it is necessary to extend the research to multilayer cables and damping treated cables, etc.;

g) The shape of wire strand section in a cable or wire rope cross-section is usually assumed as elliptical, and the analysis of contact between strands is based upon this assumption. This assumption is valid when the helical angle is large, and errors can result when the helix angle is small. Thus, it is necessary to investigate the true geometry and shape of the strand section, and understand its effect on damping;

h) Damping of carbon fiber cables in air and in vacuum shows a maximum difference of 40%, but the full contribution of air damping to the overall damping has not been addressed. Considering the changes to void ratio could provide a way to improve the theoretical prediction.

References

Achkire, Y. (1997), "Active tendon control of cable-stayed bridges", Ph. D. thesis, University of Brussels

Achkire, Y., and Preumont, A. (1996), "Active damping of cable structures" Proc. Conferences on Spacecraft Structures, Material and Mechanical Testing, Grand Hotel Huis ter Duin, Noordwijk, The Netherlands, 27-29, March, pp. 207-216

Achkire, Y., and Preumont, A. (1998), "Optical measurement of cable and string vibration", Shock and vibration, 5, pp.171-179

Ahid D. Nashif., David I. G. Jones., and John P. Henderson. (1985), "Vibration damping", John Wiley & Sons, Inc., ISBN 0-471-86772-1

Armin B. Mehrabi., and Habib Tabatabai. (1998), "Unified finite difference formulation for free vibration of cables", Journal of Structural Engineering, Vol. 124, No. 11, November, pp. 1313-1322

Burgess, J. J., and Triantafyllou, M. S. (1988) "The elastic frequencies of cable", Journal of Sound and Vibration, 120 (1), pp. 153-165

Blouin, F., and Cardou, A. (1989), "A study of helically reinforced cylinders under axially symmetric loads mathematical modeling", International Journal of Solids and Structures, 25 (2), pp. 189-200

Barbieri Nilson., Paulo Rogerio Novak., and Barbieri Renato. (2004), "Experimental identification of damping", International Journal of Solids and Structural, 41, pp. 3585-3594

Barbieri Nilson., Oswaldo Honorato de Souza Junior., Barbieri Renato. (2004a), "Dynamical analysis of transmission line cables. Part 2-daming estimation", Mechanical System and Signal Processing, (18), pp. 671-681

Barbieri Nilson., Oswaldo Honorato de Souza Junior., and Barbieri Renato. (2004b), "Dynamical analysis of transmission line cables Part 1-linear theory", Mechanical System and Signal Processing, (18) , pp. 659-669

Babuska. V. (2010), "Modeling and experimental validation of space structures with wiring harness", Journal of Spacecraft and Rockets, Vol. 47, No. 6, November-December, pp. 1038-1052

Claren Rodolfo., and Diana Giorgio. (1969a), "Mathematical Analysis of Transmission Line Vibration", IEEE Transactions on Power Apparatus and Systems, Vol. PAS-88, No. 12, December, pp. 1741-1771

Claren Rodolfo., and Diana Giorgio. (1969b), "Dynamic strain distribution on loaded stranded cables", IEEE Transactions on Power Apparatus and Systems, Vol. PAS-88, No. 11, November, pp. 1678-1690

Carlson A. D., and Kasper R. G. (1973), "A structural analysis of multi-conductor cable" Report No. AD-767 963, Naval underwater systems center, distributed by National Technical Information Service

Chi M. (1974), "Analysis of multi-wire strands in tension and combined tension and Torsion", Proc. of The seventh south-eastern conference on theoretical and applied Mechanics. Vol.7, pp.599-639

Chi M. (1974), "Analysis of Multi-Wire strands in Tension and Combined Tension and Torsion", Proc. of VII SECTAN, Vol.7, pp.559-639

Costello G.A. and Phillips J.W. (1974), "A more exact theory for twisted wire cable", ASCE, J. Eng. Mech. Div., 102(EM5), pp.1096-1099

Cutchins MA., Cochran JE., Guest S., Fitz-Coy NG., and Tinker ML. (1987), "An investigation of the damping phenomena in wire rope isolators". Proceedings of the 1987 ASME Design Technology Conference, vol. 5, Boston, Massachusetts, pp. 197-204

Chopra, A.K. (2001). "Dynamics of Structures: Theory and Applications to Earthquake Engineering, Second Edition," Prentice-Hall, Upper Saddle River, New Jersey

Chiang YJ. (1996), "Characterizing simple stranded wire cables under axial loading", Finite Elements in Analysis and Design, 24, pp. 49-66

Costello, G. A. (1997), "Theory of wire rope", 2nd edition, Springer: New York, N.Y,

Cardou, A, and Jolicoeur, C. (1997), "Mechanical models of helical strands", Applied Mechanics Reviews, Vol. 50, No. 1, pp.1-14

Cluni, F., Gusella, V., and Ubertini, F. (2007), "A parametric investigation of wind-induced cable fatigue", Engineering Structures, 29(11), pp. 3094-3105

Coombs, M. Douglas., Glaese, Roger., Vit Babuska., and Robertson, M. Lawrence. (2008), "Structural dynamic effects of cables on a sparse aperture deployable optical telescope", 49th AIAA/ASME/ASCE/AHS/ASC Structures, Structural Dynamics, and Materials Conference , 07-10 April 2008, Schaumburg, IL, AIAA , pp.2008-2266

Casciati, F., and Ubertini, F. (2007), "Nonlinear vibration of shallow cables with semi-active tuned mass damper", Nonlinear Dynamics Vol. 53, Issue 1-2, pp. 89-106

Casciati, F. Faravelli,L., and Fuggini. C. (2008), "Cable vibration mitigation by added SMA wires", Acta Mech 195, DOI 10.1007/s00707-007-0541-x, printed in The Netherlands, pp. 141-155

Charles B. Rawlins., "Flexural self-damping in overhead electrical transmission conductors", Journal of Sound and Vibration, 323 (2009), pp. 232 -256

Duan, Y. F. , Ni, Y. Q., J. M. KO., and Chen, Z. Q. (2003), "Amplitude-dependent frequency and damping identification of bridge cables with MR dampers in different setups", Smart Structures and Materials 2003; Smart System and Nondestructive Evaluation for Civil Infrastructures, Shih-Chi Liu, Editor, Proceedings of SPIE Vol. 5057, pp. 218-228

Du, Yanliang., Li, Jianzhi., and Sun, Baochen. (2011), "Study on Damping Properties of Fiber Reinforced Composite for Stayed cable", Advanced Materials Research, Vols. 163-167, pp. 288-292.

EL Kady, H. M., Arockiasamy, M., and Samaan, S. (2000), "Damping characteristics of carbon fiber composite cable for application in cable-stayed bridges", Cable-stayed bridges, past, present and future, IABSE Conference. Malmo, IABSE Reports (No. 82), pp.551-558

Filipe Magalhaes., Alvaro Cunha., Elsa Caetano., and Rune Brincker. (2010), "Damping estimation using free decay and ambient vibration tests", Mechanical Systems and Signal Processing, 24, pp. 1274-1290

Gutzer, Ulrich., Seemann, Wolfgang., and Hegedorn Peter. (1995), "Nonlinear structural damping described by the Masing model and the method of slowly varying amplitude and phase",

Proceeding of the 1995 Design Engineering Technical Conferences, DE-Vol. 84-1, Volume 3-Part A ASME, pp. 773-779

Ghoreishi. S. R., Messager Tanguy., Cartraud Patrice., and Davies Peter (2007). "Validity and limitation of linear analytical models for steel wire strands under axial loading, using a 3D FE model", International Journal of Mechanical Science 49, pp. 1251-1261

G. Masing (1923), "Zur Heynschen Theorie der Verfestigung der Metalle durch verborgene elastiche Spannungen" (= On Heyn's Theory of Stiffening of Metals by Hidden Elastic Stress), Wissenschaftliche Veroffentlichungen asu dem Siemens-Konzern, 3

Hard, A. R., and Holben, R. D. (1967), "Application of the vibration decay test to transmission line conductors", IEEE Transactions on Power Application and Systems, Paper 31, TP, 65-654, pp.189-195

Huang, N. C. (1978), "Finite extension of an elastic strand with a center core", Journal of Applied Mechanics ASME, Vol. 45, pp. 852-858

Hobbs, R. E., and Raoof, M (1982), "Interwire slippage and fatigue prediction in stranded cables for TLP tethers", Behavior of Offshore Structures, Hemisphere publishing/McGraw-Hill, New York, Vol. 2, pp. 77-99.

Hobbs, R. E., and Raoof, M (1984), "Hysteresis in bridge strand", Proc. Instn Civ. Engrs, Part 2, 77, Dec., pp.445-464

He, Xiaohua., and Powell, J. David. (1990), "Tether damping in space", Journal of guidance, control, and dynamics, Vol. 13, No. 1, pp. 104-112

Hobbs, R. E., and Raoof, M. (1994), "Mechanism of fretting fatigue in steel cables", International Journal of Fatigue, Vol. 16, No. 4, June, pp. 273-280

Hosaka. H., Itao, K., and Kuroda, S. (1995), "Damping characteristics of beam-shaped micro-oscillators," Sensors and Actuators, Vol. 49, pp. 87–95

Huang Xiaolun., Vinogradov, G. O. (1992) "Interwire slip and its influence on the dynamic properties of tension cables", Proceedings of the Second (1992) International Offshore and Polar Engineering Conference, San Francisco, USA, 14-19 June, pp.392-396

Huang Xiaolun., Vinogradov, G. O. (1994), "Analysis of dry friction hysteresis in a cable under uniform bending", Structural Engineering and Mechanics, Vol. 2, No. 1, pp. 63-80

Huang Xiaolun., Vinogradov, G. O. (1996a), "Dry friction losses in axially loaded cables", Structural Engineering and Mechanics, Vol. 4, No. 3, pp. 330-344

Huang Xiaolun., Vinogradov, G. O. (1996b), "Extension of a cable in the presence of dry friction", Structural Engineering and Mechanics, Vol.4, No. 3, pp. 313-329

Irvine H. Max (1981). "Cable Structures". MIT ISBN 0-262-09023-6

Jolicoeur, C., and Cardou, A. (1994), "An analytical solution for bending of coaxial orthotropic cylinders", Journal of Engineering Mechanics, 120 (12), pp. 2556-2574

Jiang. W. G., Yao. M. S., Walton. J. M. (1999), "A concise finite element model for simple straight wire rope strand", International Journal of Mechanical Sciences, 41, pp. 143-161

Knapp R.H. (1979), "Derivations of a new stiffness matrix for helically armored cables considering tension and torsion", Int. J. Numer. Methods Eng., 14, pp.515-529

Kunoh, T., and Leech, C. M. (1985) “Curvature effects on contact position of wire strands”, Int. J. Mech. Sci. Vol. 27, No. 7/8, pp. 465-470

Kumar K., and Cochran J. E. (1987) “Closed form analysis of elastic deformations of multilayered strands”, J. Appl. Mech., 54, pp.898-903

Kashani K. A. (1989), “Vibration of Hanning Cables”, Computers & Structures. Vol.31, No.5, pp. 699-715

Kwan, A. S. K., You, Z., and Pellegrino, S. (1993), “Active and passive cable elements in deployable/retractable masts”, International Journal of Space Structures, Vol. 8, No. 1, Jan, pp. 29-40

KO, J. M., Zheng, G., Chen, Z. Q., and Ni, Y. Q. (2002), “Field vibration tests of bridge stay cables incorporated with magneto-rheological (MR) dampers”, Smart Structures and Materials 2002; Smart System for Bridges, Structures, and Highways, S.–C. Liu, Darryii J. Pines, Editors, Proceedings of SPIE Vol. 4696, pp. 30-40

Knapp, R. H., and Xin Liu. (2005), “Cable Vibration Considering Interlayer Coulomb Friction”, International Journal of Offshore and Polar Engineering, Vol. 15, No. 3, September, pp. 229-234

Kim Nan-Sik and Jeong Woon. (2005), “Development of cable-exciting system for evaluating modal damping of stay cables”, Journal of Vibration and Control, 11, pp. 481-498

Leech, C. M. (1987) “Theory and numerical methods for the modeling of synthetic ropes”, Communications in Applied Numerical Methods, Vol. 3, pp. 407-413

Leech, C. M. (2002) "The modeling of friction in polymer fiber ropes", International Journal of Mechanical Science, 44 pp. 621-643

LeClair, R. A. (1989), "Upper bound to mechanical power transmission loss in wire rope", Journal of Engineering Mechanics, ASCE, Vol. 115, No. 9, pp. 2011-2019

Lanteigne, J. (1985), "Theoretical estimation of the response of helically armored cables to tension, torsion, and bending", Journal of Applied Mechanics. ASME, Vol. 52, pp. 423-432

Labrosse. M., Nawrocki. A., and Conway. T. (2000a), "Influence of friction on the cyclic response of simple straight wire rope strands under axial loads", Tire Science & Technology, TSTCA, Vol. 28, No. 4, October-December, 2000, pp.233-247

Labrosse. M., Nawrocki. A., and Conway. T. (2000b) "Frictional dissipation in axially loaded simple straight strands", Journal of Engineering Mechanics, Vol. 126, No. 6, June, 2000, pp. 641-646

Liu Xin. (2004), "Cable vibration considering internal friction", M. S. Thesis, University of Hawaii, August

Liu Xin., and Knapp, R. H. (2005), "Cable vibration considering internal friction", Proceedings of the Fifth (2005) International Offshore and Polar Engineering Conference, Seoul, Korea, June 19-24, pp. 213-219

Machida S., and Durelli A. J. (1973) "Response of a strand to axial and torsional displacements", J. Mech. Eng. Sci., 15(4), pp. 241-251

Marcel Migdalovici., Tudor Sireteanu., and Emil Matei Videa. (2010), "Rigidity influence of suspended cable on free vibration modes", Analele University, Eftime Murgu Resita, ANUL, XVII, NR. 1, pp. 1453-7397

Mankowski, R. R. (1988), "Internal damping characteristics of a mine hoist cable undergoing non-planar transverse vibration", J. S. Afr. Inst. Min. Metall., Vol. 88. No.12. Dec, pp. 401-410

Nawrocki . A., and Labrosse. M. (2000), "A finite element model for simple straight wire rope strands", Computers and Structures, 77, pp. 345-359

Novak, P. R., Barbieri, Nilson., and Barbieri, Renato (2004), "Damping identification through of non-contact sensors, Sixth International Conference on Vibration Measurement by Laser Techniques; Advances and Application; 22-25 June, Ancona, Italy, 5503 Issue, 2004, pp. 310-319

Owada S. (1952), "Calculation of tensile and torsional stiffnesses of single lay cables". In: Proceedings of the 2nd Japan national congress for applied mechanics,. pp. 159-164

Pivovarov, I., and Vinogradov O. G. (1985)"The phenomenon of damping in stranded cables", A Collection of Technical Papers-AIAA/ASME/ASCE/AHS, 85-0660, 2, pp. 232-237

Preumont, Y. Achkire. (1996) "Active damping of cable structures", Proc. Conference on Spacecraft Structures, Materials & Mechanical Testing, Grand Hotel Huis ter Duin, Noordwijk, The Netherlands, 27-29 March 1996 (ESA SP-386, June, pp. 207-216

Ramberg, E. Steven., and Griffin, M. Owen. (1969), "Free vibration of taut and slack marine cables", Journal of the Structures Division, Proceedings of the American Society of Civil Engineers, 09, pp. 1968-1981

Ramberg, E. Steven., and Griffin, M. Owen. (1977), "Free vibration of taut can slack marine cables", Journal of the Structure Division, Vol. 103, No. 11, November, pp. 2072-2092

Roark, Raymond J., and Young, Warren C. (1975), "Formulas for stress and strain", 5th edition, ISBN 0070530319

Ramsey, H. (1990), "Analysis of interwire friction in multilayered cables under uniform extensions and twisting", International Journal of Mechanical Sciences, Vol. 32, No. 8, pp.709-716

Raoof, M. (1989), "Torsional stiffness and hysteresis in spiral strands", Proc. Instn CIV. Engrs, Part 2, 87, Dec, pp. 501-515

Raoof, M. (1990), "Comparison between the performance of newly manufactured and well-used spiral strands", Proc. Instn Civ. Engrs, Part 2, Design and construction, 89, Mar, pp.103-120

Raoof, M. (1991a), "Methods for analyzing large spiral strands", The Journal of Strain analysis for engineering design, Vol. 26, No. 3, 1991, pp. 165-174

Raoof, M. (1991b) "The prediction of axial damping in spiral strands", Journal of Strain Analysis for engineering design, Vol. 26, No. 4, pp.221-229

Raoof, M. (1996) "Behavior of large diameter wire ropes", International Journal of Offshore and Polar Engineering, Vol. 6, No. 3, March, pp. 119-226

Roof, M. (1997), "Effect of lay angle on various characteristic of spiral strands", International Journal of Offshore and Polar Engineering, Vol. 7, No. 1, March 1997, pp. 54-62

Raoof, M., and Huang, Y. P. (1991a), "Upper bound prediction of cable damping under cyclic bending", ASCE, J. Eng. Mech., 117 (12), pp. 2729-2747

Raoof, M., and Huang, Y. P. (1991b) "Free bending characteristics of sheathed spiral strands under cyclic loading", Journal of Strain Analysis, Vol. 27, No. 4, pp.219-226

Raoof, M., and Huang, Y. P. (1993a), "Lateral vibrations of steel cables including structural damping", Proc. Instn Civ. Engrs Structs & Bldgs, 99, May, pp.123-133

Raoof, M., and Huang, Y. P. (1993b), "Effect of Non-linear Structural damping on cable lateral vibrations", The proceedings of the Third (1993) International Offshore and Polar Engineering Conference, 1993b, pp.435-444

Roof, M., and Kraincanic, I. (1995), "Analysis of large diameter steel ropes", Journal of Engineering Mechanics, Vol. 121, No.6, June, pp. 667-675

Raoof, M., and Hobbs, R. E. (1988), "Analysis of multilayered structural strands", Journal of Engineering Mechanics, Vol. 114, No.7, July, pp. 1166-1182

Raoof, M., and Davis, J. Timothy. (2006), "Simple determination of the maximum axial and torsional energy dissipation in large diameter spiral strands", Computers and Structures, 84, pp.676-689

Robertson M. Lawrence et al. (2007), "Cable effects on the dynamics of large precision structures", 48th AIAA/ASME/ASCE/AHS/ASC Structures, Structural Dynamics, and Materials Conference, 23-26 April 2007, Honolulu, Hawaii, AIAA 2007-2389, pp. 1-5

Renato Barbieri., Nilson Barbieri., and Oswaldo Honorato de Souza Junior. (2008), "Dynamical analysis of transmission line cables. Part 3-nonlinear theory", Mechanical System and Signal Processing, 22, pp. 992-1007

SEPPA, T. O. (1971), "Self damping measurements and energy balance of ACSR Drake", Institute of Electrical and Electronics Engineers, Winter Power Meeting Conference Paper 71, CP 161 PWR

Sathikh, S., and Parthasarathy, N. S. (1989), "Effect of friction on bending stiffness and slip damping of stranded cables", Proceedings of National Conference on Industrial Tribology-89, Jan 19-20, 1989, India Space Research Organization (ISRO), Trivandrum, India

Sathikh, S. (1989a), "Nonlinear effect of interwire friction on natural frequency and structural damping of wire rope and cables", Proc. of International Conference-Noise and Vibration, 89, Nanyang Technological Institute, Singapore, Aug 16-18

Sathikh, S. (1989b), "Bending of Helically Stranded Cable with Friction", a paper communicate to J. Offshore Mech. Arctic Engrg

Sathikh, S. (1989c), "Effect of interwire friction on transverse vibration of helically stranded cable", Structural vibration and acoustics: AMSE design technical conference-12 Biennial Conference on Mechanical Vibration and Noise, Montreal, Quebec, Canada, September 17-21, pp.147-153

Sathikh, S., Rajasekaran, Jayakumar andJebaraj, C. (2000), "General thin rod model for preslip bending response of strand", Journal of Engineering Mechanics, Vol. 126, No. 2, Feb, pp. 132-139

Sauter. D., and Hagedorn, P (2002), "On the Hysteresis of Wire Cables in STOCKBRIDGE Dampers," Int J Non-linear Mech, Vol 37, Issue 8 ,pp. 1453-1459

Thomas G. Carne. (1981), "Guy cable design and damping for vertical axis wind turbines", SAND 80-2669, Jun22

Tan, G. E. B., and Pellegrino, S. (2008). "Nonlinear vibration of cable-stiffened pantographic deployable structures", Journal of Sound and Vibration, 314, pp. 783-802

Vanderveldt, H. H., Chung, B. S., and Reader, W. T. (1973), "Some dynamic properties of axially loaded wire ropes", Experimental Mechanics, 13(1), pp. 24-30

Vinogradov, O. G., and Atatekin. I. S. (1986), "Internal friction due to twist in bent cables", Journal of engineering Mechanics, ASCE, 112(9), pp. 859-873

Wei, C. Y., and Kukureka, S. N. (2000), "Evaluation of damping and elastic properties of composites and composite structures by the resonance technique", Journal of Materials Science, 35 pp. 3785-3792

Wei, C. Y., and Kukureka, S. N. (2004), "Temperature dependence of dynamic modulus and damping in composites and optical telecommunication cables tested by the vibration resonance technique", Materials Evaluation, 62(3), 2004, pp. 376-381

Wu. Q., Takahashi. K., and Nakaumura. S. (2003), "Non-linear vibrations of cables considering loosening", Journal of Sound and Vibration, 2 (61), pp. 385-402

Wu. Q., Takahashi. K., and Chen. B. (2006), "Using cable finite elements to analyze parametric vibraitons of stay cables in cable-stayed bridges", Structural Engineering and Mechanics, Vol. 23, No. 6pp. 691-711

Wang Xin., and Wu Zhishen. (2011), "Modal damping evaluation of hybrid FRP cable with smart damper for long span cable-stayed bridges", Composite Structures, 93 , pp. 1231-1238

Xie Xu., Zhang He., and Shen Yong-gang. (2008), "Study on characteristics of modal damping of steel and CFRP stay cables", Engineering Mechanics, Vol. 25 No.3, pp.151-157, (In Chinese)

Xie Xu., Zhang He., and Shen Yong-gang. (2010), "Theoretical analysis and experimental test on damping characteristics of CFRP stay cables", Engineering Mechanics, Vol. 27 No.3, pp.205-211, (In Chinese)

Xu Y. L., and Yu, Z. (1998), "Vibration of inclined sag cables with oil dampers in cable-stayed bridges", Journal of Bridge Engineering, Vol. 3, No. 4, November, PP. 194-203

Xu, Y. L et al. (1999), "Experimental study of vibration mitigation of bridge stay cables", Journal of Structural Engineering, Vol. 125, No. 9, September, pp. 977-986

Yu Ai-Ting (1949), "Vibration damping of stranded cable", Dissertation for Degree of Philosophy, Leigh University

Yu Ai-Ting (1952), "Vibration damping of stranded cable", Proceedings of the Society for Experimental Stress Analysis, Vol. IX, No. 2, June, pp.141-158

Yamaguchi, H., and Fujino, Yozo. (1987), "Modal damping of flexural oscillation in suspended cables", Structural Eng. / Earthquake Eng. Vol. 4. No.2. October pp.413s-421s

Yamaguchi, H., and Fujino, Yozo. (1988), "Effects of support flexibility on modal damping of cables", Structural Eng. / Earthquake Eng. Vol. 5. No.2. October , pp.303s-311s

Yamaguchi Hiroki., and Jayawardena Loranjana. (1992), "Analytical estimation of structural damping in cable structures", Journal of Wind Engineering and Industrial Aerodynamics, 41-44, pp. 1961-1972

Yamaguchi, H., and Adhikari, R. (1994), "Loss factor of damping treated structural cables", Journal of Sound and Vibration, 176 (4), pp. 487-495

Yamaguchi, H., Alauddin, M., and Poovarodom, N. (2001), "Dynamic characteristics and vibration control of a cable system with sub-structural interactions", Engineering Structures, 23, pp. 1348-1358

Zhong, M. (2003), "Dynamic analysis of cables with variable flexural rigidity", M. S. Thesis, University of Hawaii, May

Zheng, G. Ni., Y. Q., KO, J. M., and Xu.(2003), "Tension-Dependent Internal damping of a Cable Model", Key Engineering Materials, Vols. 24.3-244 , pp. 415-420

Zhu Z. H., and Meguid S. A. (2006) 'Elastodynamic Analysis of Low Tension Cables Using a New Curved Beam Element', Int. J. of Solids and Structures, Vol.43, No. 6, pp.1490-1504

Zhu Z. H., and Meguid S. A. (2007), "Nonlinear FE-based investigation of flexural damping of slacking cables" International Journal of Solids and Structure, 44, pp.5122-5132